DYNAMIC SIMULATION OF AC/DC SYSTEMS WITH REFERENCE TO CONVERTOR CONTROL AND UNIT CONNECTION

A thesis
presented for the degree of
Doctor of Philosophy in Electrical Engineering
in the
University of Canterbury,
New Zealand

by

S. Sankar, B.E., M.Tech

1991

Abstract

This thesis investigates the limitations of conventional steady state formulation when applied to the unit connected generator-HVdc convertor systems and justifies the need for dynamic simulation.

The merits of available dynamic simulation algorithms, namely the state variable and EMTP techniques are discussed with reference to generator-convertor modelling. The state variable is selected and an existing algorithm (TCS) is improved to permit flexible controller modelling. The TCS algorithm is verified by comparison with another dynamic simulation program, EMTDC, which is based on EMTP algorithm. Both TCS and EMTDC are shown capable of predicting the same dynamic performance following disturbances.

The limitations of steady state formulation for unit connected HVdc systems are demonstrated with the help of TCS and it is shown that the characteristics must be derived using a dynamic simulation program.

Comparative operational capability charts are developed using TCS for conventional and unit connected HVdc schemes, showing the limitations of the latter to provide temporary overloads. Harmonic current and voltage ratings spectra for the region of operational capability of the unit connection are also derived.

The operating characteristics and harmonic problems of variable speed unit connected generator-HVdc convertor systems are later analysed. With reference to a typical hydro electric test system, it is shown that it is possible to operate the turbine generator units within a wide range of frequencies at high efficiencies and with good voltage controllability.

Contents

List of Figures

List of Tables

List of Principal Symbols

e - machine open circuit voltage (instantaneous)

E - machine open circuit voltage (rms)

E_c - commutating voltage

f - frequency

f_n - nominal frequency

G - conductance matrix

h - harmonic order

i - instantaneous current

I - current vector

I_d - direct axis current

I_{dc} - dc current

I_{en} - negative sequence equivalent current

I_g - machine stator current

I_h - h^{th} harmonic current

I_q - quadrature axis current

L_g - generator inductance matrix

L_{rr} - rotor-rotor sub-matrix of L_g

L_{rs} - rotor-stator sub-matrix of L_g

L_{sr} - stator-rotor sub-matrix of L_g

L_{ss} - stator-stator sub-matrix of L_g

N - machine speed

P_{dc} - dc power

R_g - machine resistance vector

t - time

u - commutation angle

U - control variable vector

V - voltage vector

V_{dc} - dc voltage

V_h - h^{th} harmonic voltage

V_t - terminal voltage

X - state variable vector

X_c - commutation reactance

X_d - direct axis reactance

X_i - quadrature component of commutation reactance

X_q - quadrature axis reactance

X_t - transformer reactance

X_r - real component of commutation reactance

X'' - machine sub-transient reactance

X''_d - direct axis sub-transient reactance

X''_q - quadrature axis sub-transient reactance

Y - output variable vector

Z - dependent variable vector

α - convertor firing angle

α_{min} - minimum firing angle

α_{max} - maximum firing angle

α_{ord} - firing angle order

α_{ref} - firing angle reference

γ - invertor extinction angle

γ_{low} - lowest extinction angle

γ_{ref} - extinction angle reference

δ_i - angle between generator stator current and internal emf

Δt - time step

θ_0 - switching instant

ϵ - synchronising error

ϕ - power factor angle

Acknowledgements

I would like to thank my supervisor Prof. Jos Arrillaga, for his advice, assistance, friendship and patience during the course of this work. Also, my sincere thanks are due to Dr. Chris Arnold and Dr. Neville Watson for their valuable suggestions and help.

The financial support of Transpower New Zealand Ltd. is gratefully acknowledged.

I would also like to thank Dr.C.Callaghan, Dr.N.Pahlawaththa and my other postgraduate colleagues G.Anderson, J.R.Camacho, J.de Souza, A.Medina, A.Miller, M.Villablanca, A.Wood and M.Zavahir for their helpful suggestions and friendship. Also, the encouragement and help given by my friend Dr.K.S.Chandrasekhar is greatly acknowledged.

Finally thanks are due to my family and friends for their support and understanding.

Publications Associated With This Thesis

The following publications are associated with research presented in this thesis.

Sankar,S., Arrillaga,J., Arnold,C.P and Watson,N.R.,"Inclusion of HVDC controller dynamics in transient convertor simulation", Transactions of IPENZ, Vol 16, 2/EMCh, Nov. 1989, pp 25-30.

Arrillaga,J., Sankar,S., Watson,N.R., and Arnold,C.P.,"Operational capability of generator-HVDC convertor units", presented at the 1991 IEEE PES Winter Meeting, New York.

Arrillaga,J., Sankar,S., Watson,N.R., and Arnold,C.P.,"A comparison of transient simulation algorithms", accepted for the 5th IEE International conf. on ac/dc systems, London, to be held in Sept. 1991.

The following paper has also been submitted for publication, but has yet to be officially accepted (as of 28 February, 1991).

Arrillaga,J., Sankar,S., Arnold,C.P. and Watson,N.R.,"Characteristics of unit connected generator-HVDC convertors operating at variable speeds", submitted for 1991 IEEE PES Summer Meeting.

Chapter 1

INTRODUCTION

1.1 Background

The modern HVdc technology which started with a simple 2-terminal dc link between Gotland and Mainland Sweden in 1954, has developed to a stage now where a 5-terminal dc system is a commercially viable possibility [IEEE 1990]. During this period, the dc power transfer capacity has increased from a mere 20 MW to 6000 MW. The reason for this rapid growth can be mainly attributed to the availability of cheaper high voltage, high power semi-conductor thyristors and the increasing confidence on the reliability of dc systems. In some of the projects, HVdc was the only option available to the system planners (e.g., Sakuma frequency convertor and New Zealand scheme). The present need of energy requires increase exploitation of renewable energy resources such as hydro-energy source located far away from load centres. At present, HVdc transmission is a recognised methodology for such applications.

In conventional HVdc design, the generators from isolated power plant are allocated to a common ac bus which feed all the convertors. Also the filters are connected at the convertor terminal. When the generated power is supplied exclusively to the HVdc transmission link, such as in an isolated power station, the unit connection of individual generators to HVdc convertors proposed as early as 1973 [Calverley] is an attractive alternative. The importance of HVdc system unit connection is realised to the extent that CIGRE has formed a separate working group to study various aspects of such systems [CIGRE 1988].

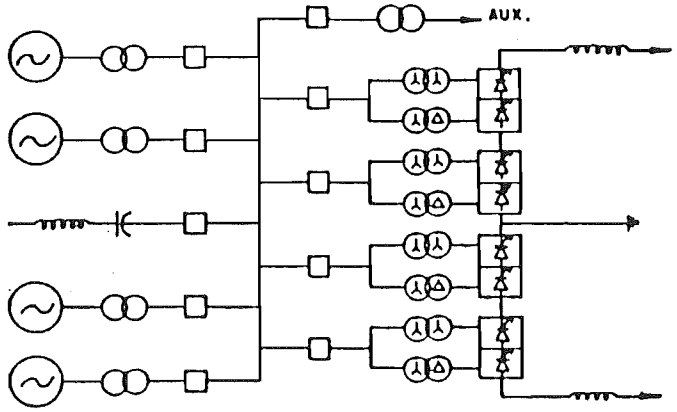

Figure 1.1: HVdc rectifier station- conventional arrangement

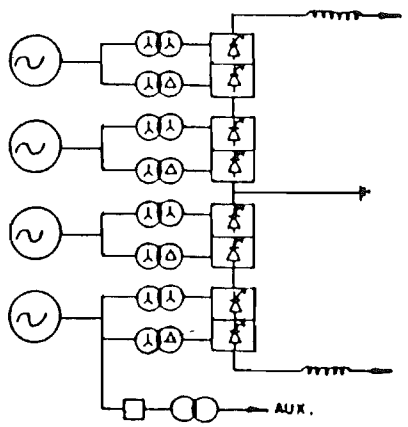

Figure 1.2: HVdc rectifier station- unit connected arrangement

1.2 The Unit Connected HVdc System

Figures 1.1 and 1.2 show the essential elements of a conventional scheme and unit connected scheme respectively. In the unit connected scheme, the generators are connected directly to the convertor transformers and the paralleling (or the series-parallel combination) of units is done at the dc side.

Advantages

The unit connected HVdc scheme has several advantages over the conventional scheme and they are summarized as follows:

- Each generator operates individually and so there is no synchronisation or stability problem among them.
- Elimination of ac harmonic filters result in the reduction of station cost and space and also eliminates the potential resonance and self-excitation problems.
- Only a single unit transformer is needed in place of generator and convertor transformers.
- Possible elimination of On-Load Tap-Changers on transformers.
- There is no need of an ac busbar system and also the layout eliminates one level of breakers.
- The unit connected HVdc station would possibly result in a compact and light design due to the absence of high-voltage ac switchyard and filters, separate convertor buildings and associated services and several ac collector lines between the power house and the switchyard.

The Manitoba HVdc Research Centre, Canada undertook a study [Ingram 1988] of the economic benefits of the unit connected concept, taking advantage of known costs from the Limestone generating station on the Nelson River. The conclusion of this study are that for a 1250 MW hydro plant with dimensions and ratings similar to Manitoba Hydro's Limestone station, a directly connected HVdc thyristor convertor would realise savings in the order of $M75 Cdn (in 1987 dollars) compared to a conventional design with separate convertor station.

Disadvantages

The unit connected schemes would have the following limitations:

- The generator must absorb the entire harmonics produced by the individual convertor units. Their major effect upon the generator is extra heating of the

rotor surface and the damper winding due to the induced harmonic currents in the rotor circuit.

- In the event that generators are operated at frequencies other than power frequency, a separate source of power for station auxiliaries must be arranged.
- A convertor unit outage would prevent the delivery of power from that unit generator and also would decrease the transmission voltage.

Applications

The potential application of unit-connected HVdc schemes are those cases where the whole output of the generating station can be transmitted via HVdc. Applications where this is possible could be:

- transfer of large power from very remote hydro generating stations to the load centres
- connection of large power stations into existing complex ac systems (such as Mine-Mouth application)
- interconnection of off-shore power station into existing ac networks
- variable frequency operation such as pump-storage schemes

Group Connection

A variation of unit connection has also been suggested in which instead of a single generator, two or more generators would be connected directly to the convertor transformer [Ingram 1988], as shown in Figure 1.3. The flexibility of operation and maintenance is enhanced in this configuration, but generator breakers become essential and though variable speed operation is still allowed, the group of synchronized generators would require some form of joint speed control. As far as the system studies are concerned, this type of connection is not different from the unit connection.

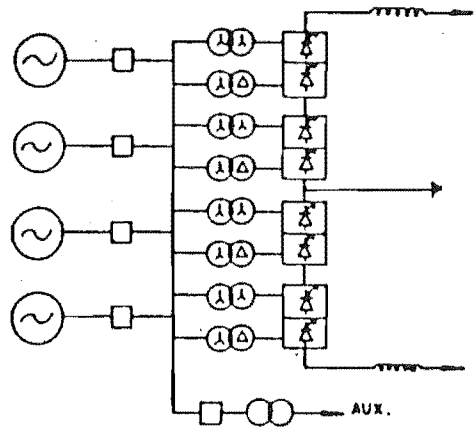

Figure 1.3: HVdc rectifier station- group connected arrangement

Diode-Rectifier Configuration

The HVdc convertor in the unit connected scheme can be either of thyristor or diode type. The use of diode-rectifier for HVdc applications has been proposed from time to time [EPRI 1983]. Since power reversal is not required of unit connected schemes (except in pump-storage), the diode-rectifier remains a major contender to the thyristor convertor due to cheaper cost and simplicity.

In the diode-rectifier scheme, the fast current control of rectifier would be taken over by the invertor, whose extinction angle has to be controlled by the slow acting transformer tap-changer [Bowles 1989]. DC and AC breakers have to be provided at the rectifier station for protection purposes. In order to prevent occurrence of commutation failures, the invertor must operate at higher firing angles than the conventional scheme. This results in higher costs for convertor valves, filtering and reactive power compensation equipment at the invertor station.

1.3 Modelling

In conventional HVdc schemes, the relatively low ac system impedance combined with the provision of filters achieves a practically sinusoidal voltage at the convertor terminals. Such voltage and the transformer leakage reactance can then be used as the commutating voltage and commutation reactance respectively. The generator's phase currents are also sinusoidal and hence the steady state operating

conditions can be derived using conventional single-frequency phasor theory.

At present, the operating characteristics of unit connection are also discussed with reference to the conventional steady state formulation [Krishnayya 1973, Hausler 1980, Campos Barros 1989].

However, in the absence of harmonic filters, the use of such formulation must be reconsidered. Each and every convertor commutation process represents a line-to-line short circuit across the generator terminal and hence the commutation reactance must include the generator sub-transient reactance as well as transformer leakage. The convertor terminal voltage is not sinusoidal and so the generator internal emf must be used as the commutating voltage.

Moreover, rotor saliency causes non-linear harmonic interaction between the generator and the convertor which affects the output voltage of the unit connection and this effect can not be analysed using single frequency steady state formulation.

Therefore the main objective of this work is to show the need for dynamic simulation in unit connection studies.

1.3.1 Dynamic Simulation

Dynamic simulation programs have already been used to establish the controllability of the unit connection during disturbances [Campos Barros 1977, Hungasutra 1989, Rangel 1989]. In this work, dynamic simulation is used to assess the applicability of the steady state formulation and derive the operating characteristics of the unit connected HVdc convertor.

Two basically different approaches are currently used in HVdc dynamic simulation, i.e the Electromagnetic Transient Program (EMTP) and the state variable technique. The EMTP type programs use constant step length, whereas the step length can be altered in state variable algorithms.

The equivalent circuit of a generator-HVdc convertor system contain time-varying parameters which require modification of the system impedance matrix from step to step in the dynamic simulation. Also the voltage crossings, firing instants and commutation intervals can not be predicted and hence the integration steps need to be adjusted accordingly. Such requirements and the relatively small number of components involved make the state variable algorithm ideally suited to the dynamic simulation of unit connected schemes.

A dynamic simulation program, TCS, developed at the University of Canterbury, NZ is used for this work. Transient Convertor Simulation (TCS) is a program specifically developed to analyse the dynamic behaviour HVdc systems and is formulated in terms of state space theory [Arrillaga 1983b].

The basic algorithm of TCS was established at the University of Manchester Institute of Science and Technology [Al-Khashali 1976, Campos Barros 1976]. Further work on TCS continued at the University of Canterbury by progressively improving the accuracy of the results by developing better models for the various power system components.

In ac/dc dynamic simulation programs, normally ac systems are represented as equivalents. The means of representing ac system as time varying equivalents was developed by Heffernan[1981] and Turner[1981]. Based on the recent advancements [Reeve 1988] on these models, further work on this topic is currently underway at the University of Canterbury, NZ.

Following HVdc disturbances, the convertor transformers may be subjected to overexcitation, dc magnetisation and in-rush effects, all of which must be accurately represented in dynamic simulation studies. Practical ways of modelling the magnetic history of the convertor transformer in TCS were developed by Joosten [1989].

The frequency response of power system components affects the transient response due to the multitude of frequencies present in transient waveforms. Given the size and complexity of a power system, it is not practical to model each of its components individually. Watson [1987] developed methods of obtaining a practical and computationally efficient equivalent circuit for TCS that accurately represents the frequency dependence of the actual system being represented.

During all these developments, TCS contained in-built basic controllers i.e., current and extinction angle controllers based on the direct digital control technique [Arrillaga 1970]. The representation of any other controllers other than basic controllers required expert understanding of the program in order to introduce appropriate modifications. Hence the starting point of this investigation was to implement a more realistic and flexible controller models in TCS which would make TCS more powerful in analysing ac/dc systems.

1.4 Thesis Outline

Chapter 2 describes the modelling of realistic and flexible HVdc controller models in TCS and also the importance of such models.

As in any other model simulations, in order to establish the confidence, the analytical tools must be validated. Chapter 3 discusses the process involved in comparing various simulation tools and the comparison between TCS and EMTDC for a sample dc system.

The TCS program is then used for unit connected HVdc system studies. Chapter 4 discusses the initialisation process and the derivation of steady state values involved with the dynamic simulation of generator-HVdc convertor units using TCS.

In chapter 5, the commutation process in unit connected HVdc systems is analysed and the inapplicability of conventional dc system equations for unit connections is demonstrated using TCS.

In order to evaluate the performance of a unit connected system compared to a conventional scheme, comparative operational capability charts must be developed. Chapter 6 analyses the operational capability of unit connected HVdc systems using TCS.

In the absence of local load, the unit connection concept could be extended to generate power at varying frequencies to suit the optimal operation of the turbines. Chapter 7 analyses the operating characteristics and harmonic problems of variable speed unit connected HVdc systems.

Finally, chapter 8 draws conclusions and offers suggestions for further research directions.

Chapter 2

INCORPORATION OF HVDC CONTROLLER DYNAMICS IN TCS

2.1 Introduction

The dynamic behaviour of ac/dc power systems is presently assessed in two separate ways.

The transient recovery of the convertors following ac or dc disturbances is normally tested in physical simulators. This is due to the ability of the simulators to represent the control systems realistically.

On the other hand, the assessment of voltage and power stability is carried out with the help of digital computer models using idealised controls and specified convertor recoveries.

However the accurate quantitative prediction of convertor and ac/dc system stability, requires a time domain simulation of the complete system with detailed representation of the power and control system components.

Such assessment cannot be realistically made by physical simulators due to their practical limitations [Mattensson 1986] in representing actual generators, transformers, frequency- dependent lines etc. The only feasible alternative is the digital solution.

It has already been shown that the Transient Convertor Simulation (TCS)

algorithm can include very accurate frequency-dependent ac system equivalents [Watson 1988] and time-varying machine dynamics [Heffernan 1981].

This chapter describes the incorporation of realistic and flexible HVDC controller models in TCS algorithm.

2.2 HVdc Controllers Hierarchy

HVdc controllers follow a strict hierarchical organisation and they are generally classified as follows:

- Thyristor and valve control

It is the lowest hierarchical level represented by thyristor and valve control units. The objective of a thyristor control unit is to convert a thyristor triggering signal from ground potential to a gate current pulse. In modern HVdc plants, the communication from ground to the thyristor level is realised using light and glass fibre light guides and the energy needed for firing the thyristor is normally obtained from the voltage across the thyristor. The valve control unit converts the control pulse for the valve from the convertor firing control system into light pulses for each individual thyristor.

- Convertor control

The next level in the hierarchy is the convertor control. When the convertors are connected in series, a separate convertor firing control system is needed for each convertor. Some protective actions are also implemented at the convertor level. Examples are the valve short-circuit protection, the commutation failure protection and convertor differential protection. Further, sequence control functions like blocking and deblocking of the convertor and equipment for measuring phase current and ac voltage are also found here.

- Pole control

The current control amplifier and the current order limiter with the voltage dependent current order limiter (VDCOL) are found in this level. A pole master control which makes use of the inter-station telecommunication system is also defined at this level. Many of the power modulation tasks like stabilization of connected ac networks by modulating the transmitted power from measured frequency deviation, are performed at the pole level.

- **Bipole and station control**

The complexity of the control equipment at the highest level is kept at a minimum whether this is the bipolar level or there is still a higher hierarchical level as for a transmission system, which includes two bipoles. A control desk with setting devices and reactive power control systems are normally found on the highest level.

The two lower levels of controls, valve and convertor controls and also the current controllers differ little from scheme to scheme and thus in earlier TCS studies, the logic of such modes was incorporated into the algorithm. Moreover, the representation of any other control modes required expert understanding of the program in order to introduce appropriate modifications.

A more flexible and realistic way of representing HVdc controllers including pole and station controls, has now been implemented whereby the control system is built-up in a modular form using a defined set of functions and inputs. However, the basic convertor control is built within the program.

2.3 Convertor Control

In the early dc schemes, convertor controllers used the individual phase control technique. With the experience gained from them, it was learnt that they are prone to harmonic instability due to non-characteristic harmonics generated by the convertor, especially when the ac system impedance is high [Ainsworth 1967]. Since then the equi-distant pulse control has been the norm for HVdc convertor control. Unlike the individual phase control, the equi-distant pulse control does not depend on the ac voltage waveform for firing angle calculation. The distance between the firings are equal under steady state and hence the non-characteristic harmonics are minimised.

The basic form of equi-distant pulse controller is based on the phase-locked oscillator principle proposed by Ainsworth [1968]. Since then various versions of the original phase-locked oscillator control system have subsequently appeared and they have been well documented in the literature also [Arrillaga 1983a]. The convertor controller model implemented in TCS is based on the phase locked oscillator principle. It is explained here with respect to a 6-pulse bridge convertor.

There are two possible ways in which the convertor controller can be specified

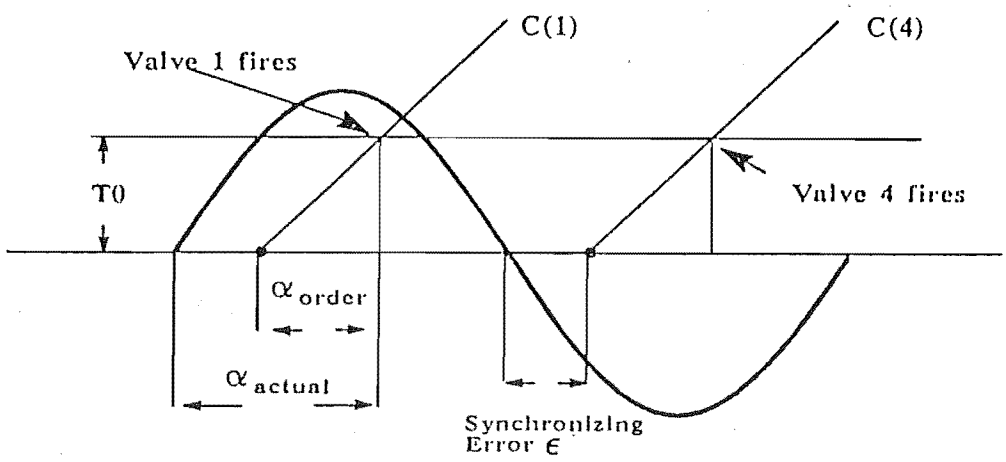

Figure 2.1: Phase locked oscillator reference

in the program: the input to the convertor controller can be either the firing angle order (α_{ord}) or the control voltage to the oscillator, in which case the firing angle is automatically adjusted.

The controller basically consists of a 6-pulse saw tooth oscillator, whose frequency is controllable. Under normal steady state operation, each pulse is displaced by 60 degrees in time. The output of the oscillator is compared with the firing angle order issued from the pole control and whenever an oscillator pulse exceeds α_{ord}, a firing pulse is issued. As an example, Figure 2.1 shows one phase of the commutating voltage at the convertor terminal (assuming a perfect filter) and also the first (C(1)) and fourth pulse (C(4)) from the oscillator. Whenever a firing pulse exceeds the level indicated by α_{ord}, whose value is converted to seconds (To) from degrees, that particular valve 'ON' pulse is applied.

If for some reason (which could occur during initialisation and disturbance), the oscillator frequency is out of phase with the power frequency, then the actual firing angle will be different from the firing angle order, as shown in Figure 2.1. Under such circumstances, the oscillator frequency needs to be varied so that it gets phase-locked with power frequency. This is accomplished through a negative feedback loop. If the duration between the zero crossing of the commutating voltage and the beginning of a corresponding oscillator pulse is ϵ (which could be called the synchronising error),

then the oscillator frequency is changed according to the following equation:

$$T_{60(osc)} = T_{60(ac)} - \frac{T_n \epsilon}{T_s} \tag{2.1}$$

where,

$T_{60(osc)}$	- 1/6 period of oscillator
$T_{60(ac)}$	- 1/6 period of ac system
T_n	- Nominal period of oscillator
	60 degrees for 6-pulse convertor
	30 degrees for 12-pulse convertor
ϵ	- synchronising error
T_s	- synchronising time constant

The ac system period is updated at every 60 degrees and so the synchronising error ϵ is redefined at every 60 degrees. The synchronising time constant allows the user to select the response of the phase-locked oscillator, i.e the speed of synchronisation. If the individual phase control is to be simulated, then T_s is selected to be a very small value.

The measured ac system periods are generally subject to jitter and sometimes even to multiple cross-over points. Hence if it is necessary in the program, it is possible to pass the ac system periods through a low-pass filter to calculate the correct values.

When a 12-pulse convertor configuration is modelled, a common firing controller is used for the two bridges, rather than two individual controllers. This is done automatically in the program by disabling the second firing controller. Instead of a six-pulse oscillator, a 12-pulse oscillator is used and correspondingly the oscillator frequency is updated at every 30 degrees.

2.4 Modular Approach to HVdc Controls

The controllers at higher levels vary from one application to another. Furthermore, during the planning phase it could be necessary to test a number of different control alternatives to solve a specific problem.

Table 2.1: Control system - TCS interface variables

Symbol	Variable
AV	AC bus voltage (instantaneous)
DV	DC bus voltage
DI	DC current
AO	Firing angle controller
VC	Control voltage of current controller's VCO
VA	Control voltage of ext. angle controller's VCO
EA	Lowest extinction angle
EH	Highest extinction angle
FA	Firing angle

The method used in TCS allows for control simulation by means of user-defined block diagrams. The concept of user-defined control simulation have previously been discussed with reference to transient stability programs [Williams 1986]. The user enters the control specification by means of elementary modules included in a data file. The connections between these modules are also defined in the same data file. There is no need to recompile the program whenever the controller configuration changes. A list of typical modules, compiled from existing HVdc controllers is summarised in Appendix A. These modules are accessed through input and output interface variables such as those listed in Table 2.1.

The basic elementary functions which form the control diagram are read from a data file created prior to the simulation runs. Control data file must be defined for each convertor, but since the control of rectifier and invertor are often achieved by the same functions, the same control data file can be repeated for different convertors.

The inputs and outputs of the controllers are defined as interface variables and they are listed in Table 2.1. A typical input to a control block could be bus voltage, dc current etc. The interface variables consist of a four character alpha-numeric name, in which the first two characters denote the electrical quantity and the last two characters denote the component number.

By way of example, consider the block diagram of Figure 2.2 (the symbols used in the diagram are from the list of interface variables in Table 2.1). A controller data file can then be prepared from the module library in the form shown in Table 2.2

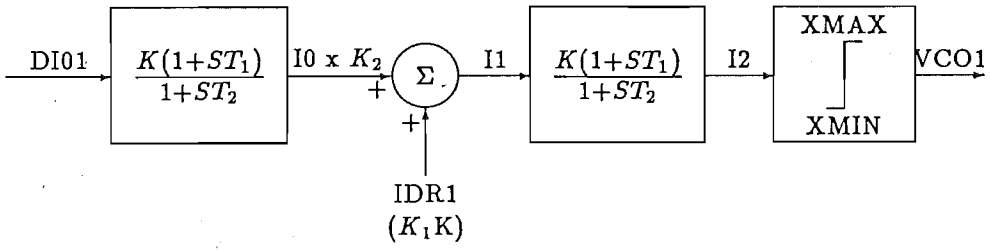

Figure 2.2: Example of controller corresponding with Table 2.2

Table 2.2: Sample control data file

FN	INP1	INP2	INP3	OUT	CON1	CON2	CON3
TRAP	DI01			IO	K	T_1	T_2
ADDI	IDR1	IO		I1	K_1	K_2	
TRAP	I1			I2	K	T_1	T_2
LIMC	I2			VC01	XMIN	YMIN	
INIT	I0				K		
INIT	IDR1				K		

for various modules used in the test controller, the modules used in the example being TRAP, ADDI, LIMC and INIT.

The Table 2.2 provides informations of inputs (INP), outputs (OUT) and Control Function Constants (CON).

The control system components listed in the data file are then stored in an array, so that they can be solved sequentially. The program has built-in capabilities to detect any data entry errors such as wrong bus type, invalid control function etc. during the input stage.

2.5 Combined Power and Control TCS Solution

The formulation of Transient Convertor Simulation (TCS) state-space equations is well documented [Arrillaga 1983b]. The skeleton of the state variable method is the simultaneous solution of a system of differential equations, which is achieved by means of an implicit integration routine.

State equations have the form:

$$\dot{X} = AX + BU + EZ \tag{2.2}$$

$$\dot{Y} = CX + DU \tag{2.3}$$

where,

U - input voltages and currents
X - state variables
Y - output voltages and currents
Z - dependent variables

The details of controller function type, inputs, outputs are stored in arrays. For the transfer functions, state-space equations (i.e differential equations) are written as in the basic TCS formulation and are solved one at a time in order down the arrays. The main steps involved in the computer solution of the modified TCS algorithm are shown in the flow diagram of Figure 2.3.

State-space equations are established for the network and initial values are derived for the state variables of the network and control systems from the initially assumed voltages and currents.

The set of differential equations 2.2 and 2.3 are then solved for one step using the Implicit Trapezoidal method [Arrillaga 1983b]. The control equations are incorporated within the iterative loop of the integration procedure and therefore additional time step delays are not introduced due to feedbacks.

Upon convergence at every time step, the results are stored in an output data file for further processing like plotting, FFT analysis etc.

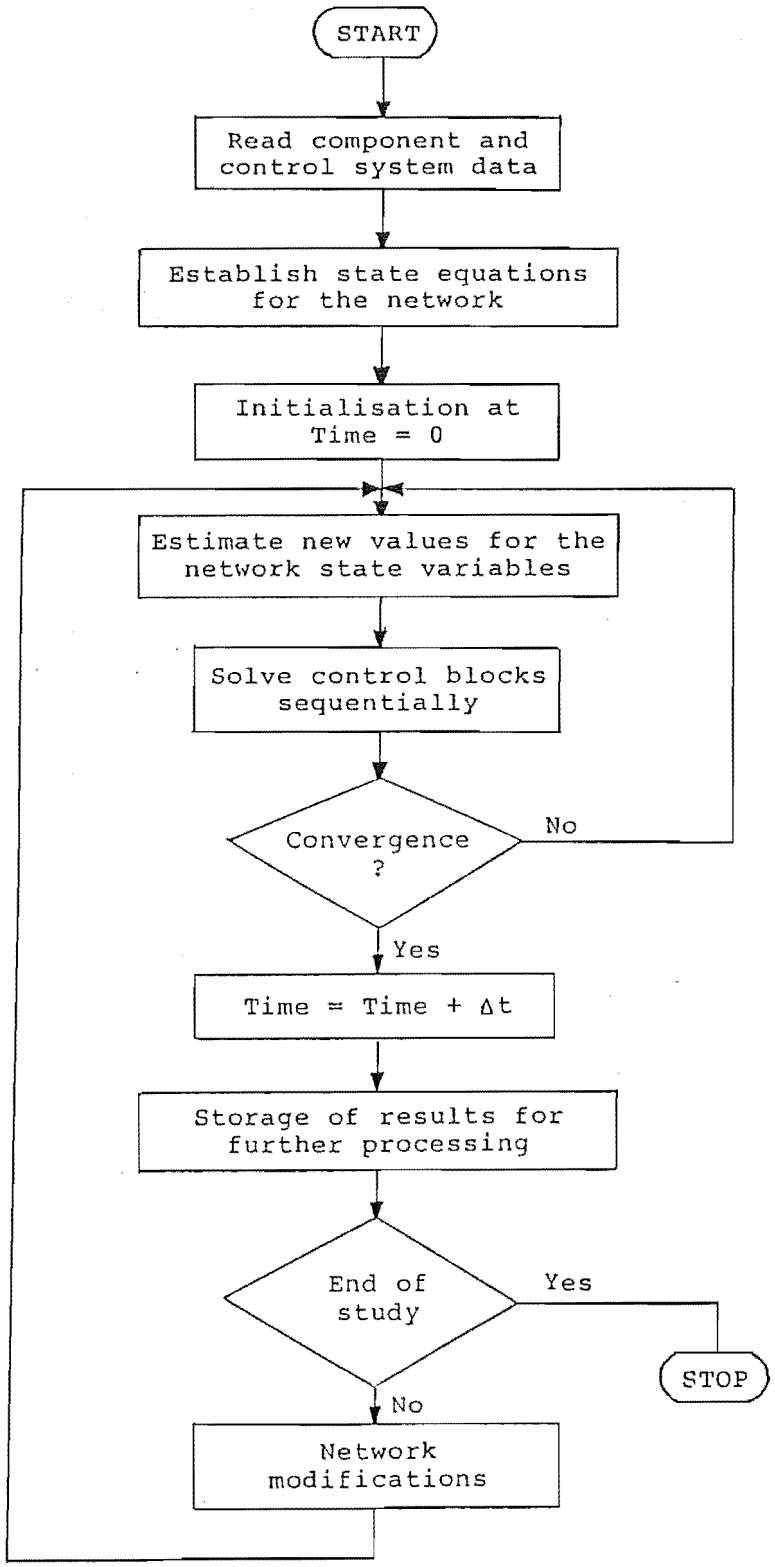

Figure 2.3: TCS flowchart

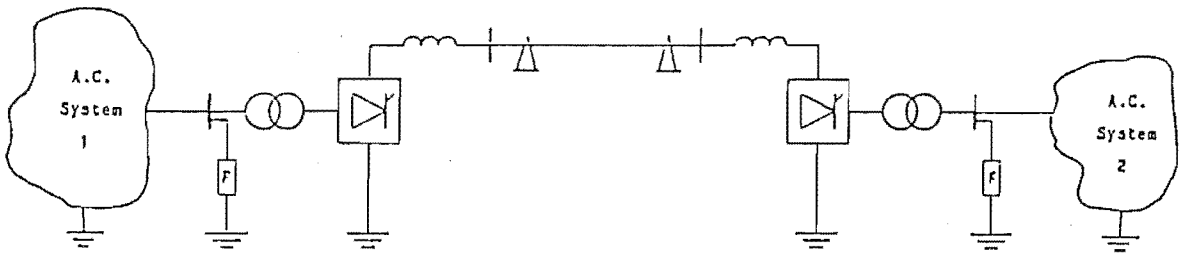

Figure 2.4: HVdc test system

The program has the ability to select automatically a suitable step length at the end of every time step. Also at each step of the integration process, the convertor bridges are tested for extinction, voltage crossover and conditions for firing. If indicated, changes in valve states are made and control system is activated to adjust the phase of firing. Moreover, when a valve switching takes place, the network equations and the convertor connection matrix are modified.

2.6 Illustrative Test Cases

In order to illustrate the need for representing the detailed control models, two test cases are considered here.

In the first test case, the performance of basic controller types are tested by considering 'instantaneous' and 'detailed' models.

In the second case, conventional transient stability results are compared with results obtained from detailed representation of the convertors and their controllers.

2.6.1 Test Case - 1

2.6.1.1 Test System

A monopolar equivalent of the New Zealand HVdc interconnection (Figure 2.4) is used as a test system. The two ac terminals contain 12-pulse related tuned filters, high pass filters and a frequency dependent equivalent circuit [Watson 1988] of the North and South Island systems respectively. Figures 2.5 and 2.6 show the basic current and extinction angle controllers.

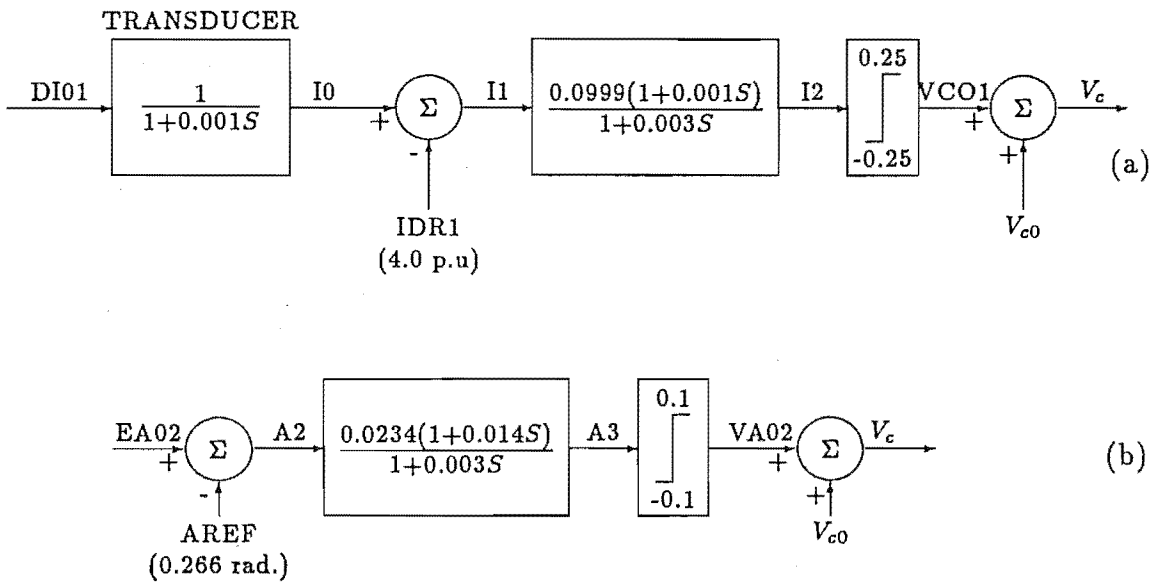

Figure 2.5: Controller dynamics-1: (a)Rectifier current controller (b)Invertor extinction angle controller

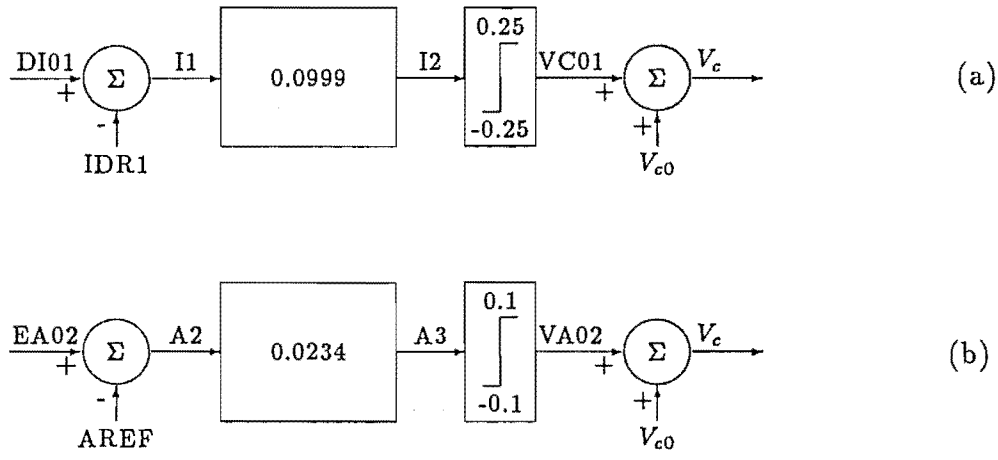

Figure 2.6: Controller dynamics-2: (a)Rectifier current controller (b)Invertor extinction angle controller

Referring to Figure 2.5(a), the dc current from convertor 1 (DI01) is the input to the current transducer, which is represented as a single-pole transfer function on the assumption that the DC-CT response is reasonably linear over the current range expected during disturbances. The transducer output I0 is compared with a current reference (IDR1), which is set using the function INIT. Their difference (I1) is the input to the controller dynamics function which, through a limiter, produces the control voltage (VC01) signal fed to the oscillator. A similar description applies to the extinction angle controller of Figure 2.6.

The HVdc system recovery from major disturbances is an essential criterion used in the selection of controller dynamics. Thus in order to test the performance of the basic controller types of Figures 2.5 and 2.6, a single phase to ground fault is applied at the invertor end of the test system.

2.6.1.2 Line to Ground Fault Recovery

The results of a solid line-to-line fault of two-cycles duration at the invertor end terminals are shown in Figure 2.7.

Figure 2.7 (a) displays the dc current during disturbance and after fault clearance by the circuit breaker; the continuous line indicates the modified TCS solution responses with detailed representation of the controller dynamics (controller-1) and the dotted line, the TCS solution with instantaneous controller (controller - 2). The voltage waveforms at the invertor end are shown in Figure 2.7 (b) for the case including the controller dynamics.

While in both 'ideal' (i.e. instantaneous) and 'real' (i.e. detailed) cases the link is seen to recover from the disturbance, the variation of dc current from fault occurrence to final recovery is very different in the two cases.

The dynamic behaviour of the convertor itself is better explained with reference to the valve conduction patterns, displayed for the 'ideal' and 'real' controllers in the bar-graph diagrams of Figures 2.8(a) and (b) respectively. These graphs show a number of consequential commutation failures following the application of the fault and a marginally faster recovery for the case with controller dynamics.

(a)

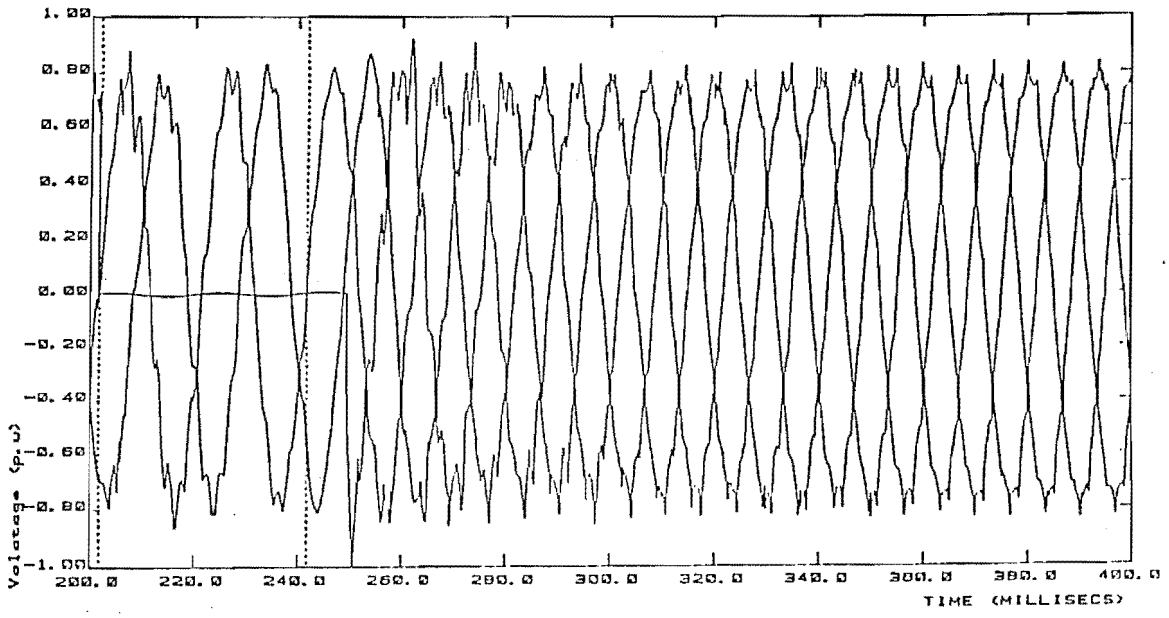

(b)

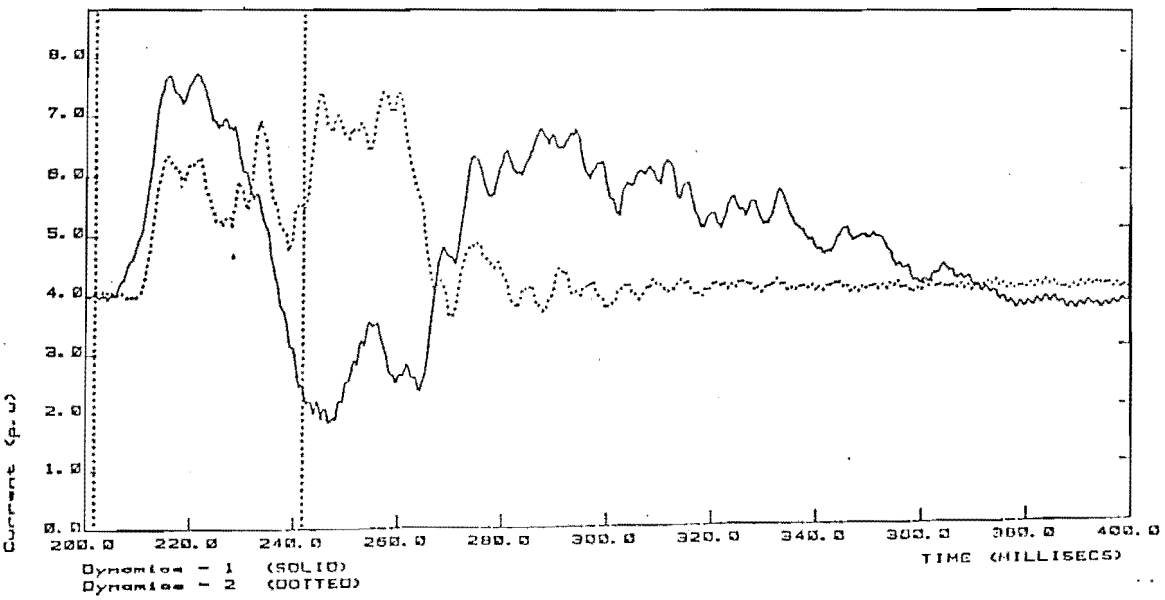

Figure 2.7: Invertor ac voltages and dc current waveforms for a single-phase to ground fault

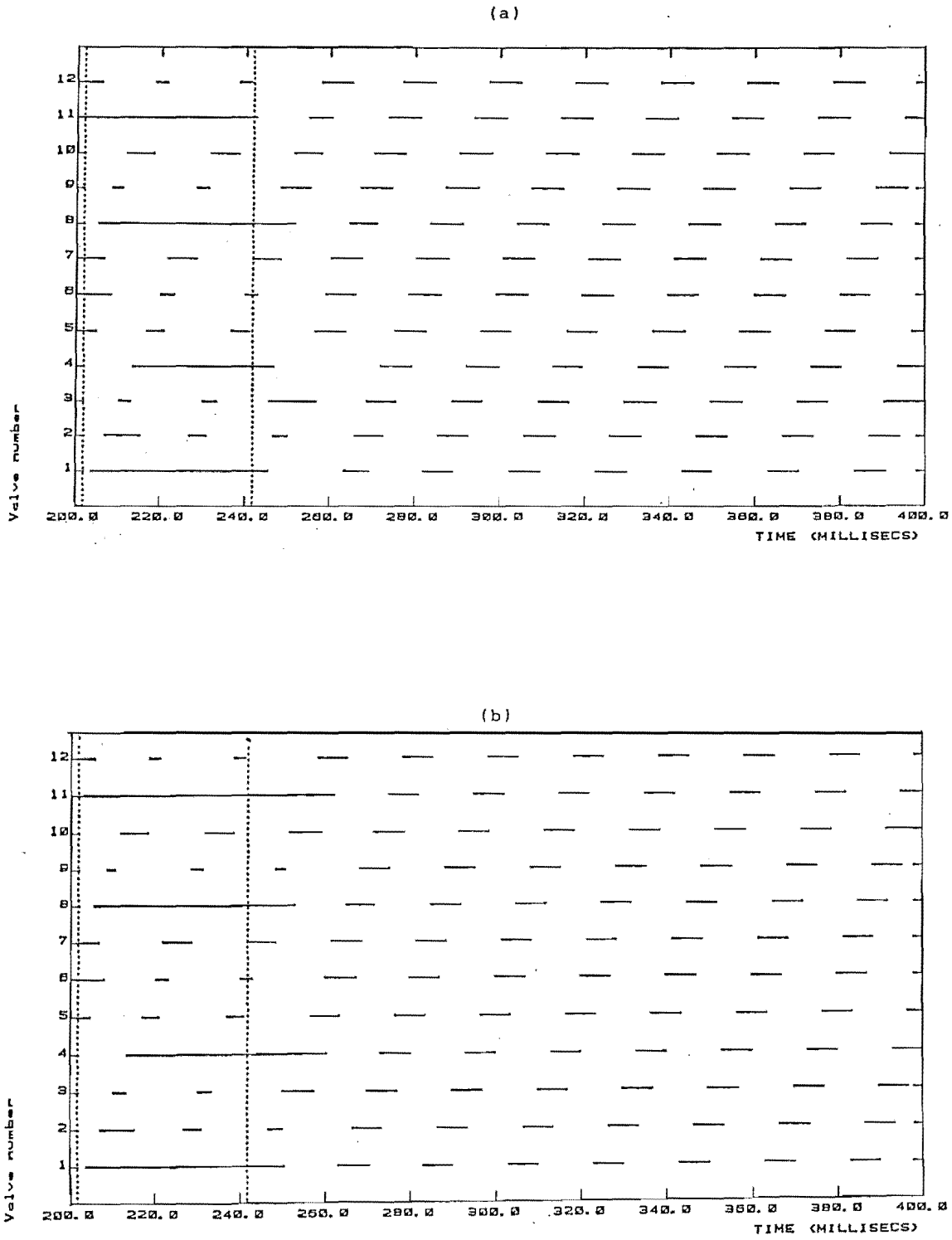

Figure 2.8: Invertor valve conduction patterns for a single-phase to ground fault. (a) Control dynamics-1 (b) Control dynamics-2

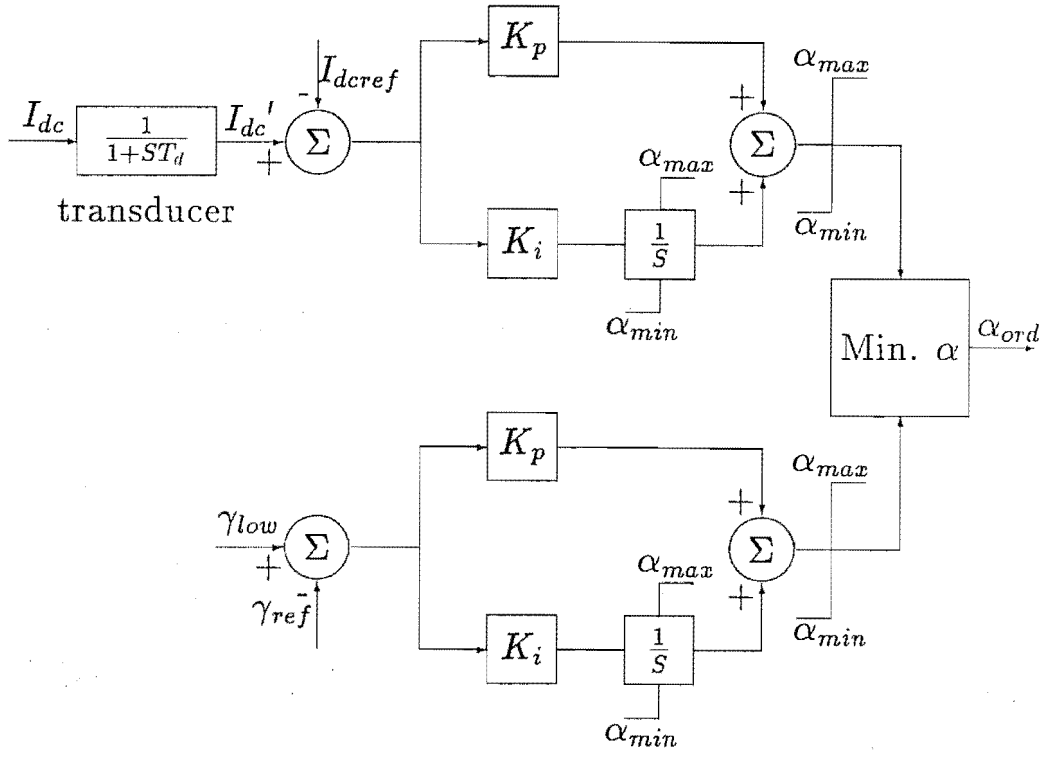

Figure 2.9: Controller blocks of Test case - 2

2.6.2 Test Case - 2

In present transient stability programs the HVdc convertors are modelled using Quasi-Steady-State (QSS) equations [Williams 1986] and the controller dynamics are represented with suitable transfer functions. In these programs, the implementation of firing angle control is instantaneous, whereas in practice firing signals occur at discrete intervals of about 1.5 or 3 mS depending on the pulse number. Moreover, transient stability programs can not realistically model the control system response following commutation failures.

An integrated approach was proposed [Heffernan 1980, Turner 1980] wherein the conventional single phase multi machine stability analysis is combined with a detailed 3-phase transient convertor simulation and detailed convertor controls.

In this example, with the help of TCS and the stability program, the effect of representing detailed control systems is illustrated.

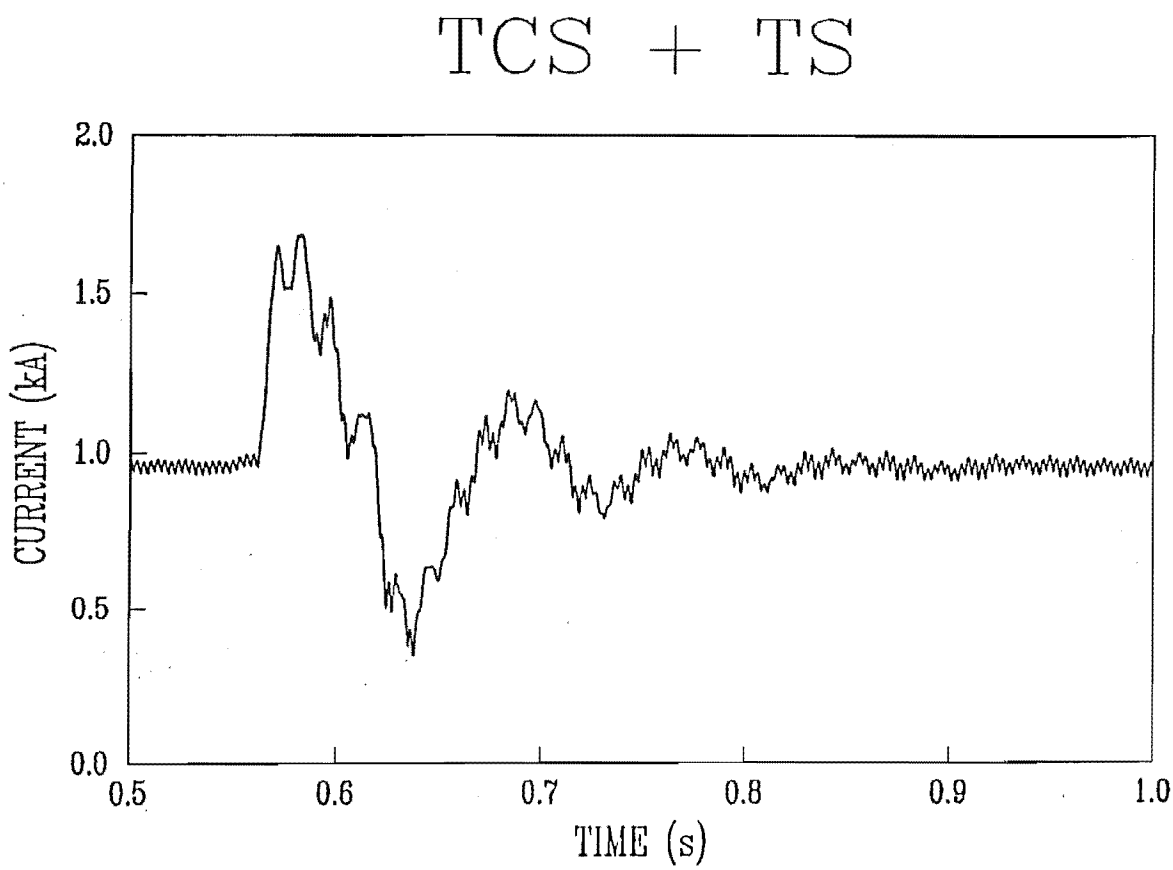

Figure 2.10: Rectifier dc current obtained from integrated TCS and stability program

2.6.2.1 Test System

The New Zealand ac/dc system is used as the test system. The ac system, represented in the transient stability program consists of 39 and 24 buses on the sending end and receiving end of the dc link respectively. Thevenin equivalents were derived using a Short Circuit program to represent the ac systems in TCS. Detailed current and extinction angle controllers, shown in Figure 2.9 are also modelled in TCS.

2.6.2.2 Fault Study

The results of a 3-phase fault of 2-cycles duration at the invertor end ac terminal are shown in Figures 2.10 to 2.12.

Figure 2.10 displays the dc current during the disturbance and fault recovery. The dc power transfer through the dc link is shown in Figure 2.11.

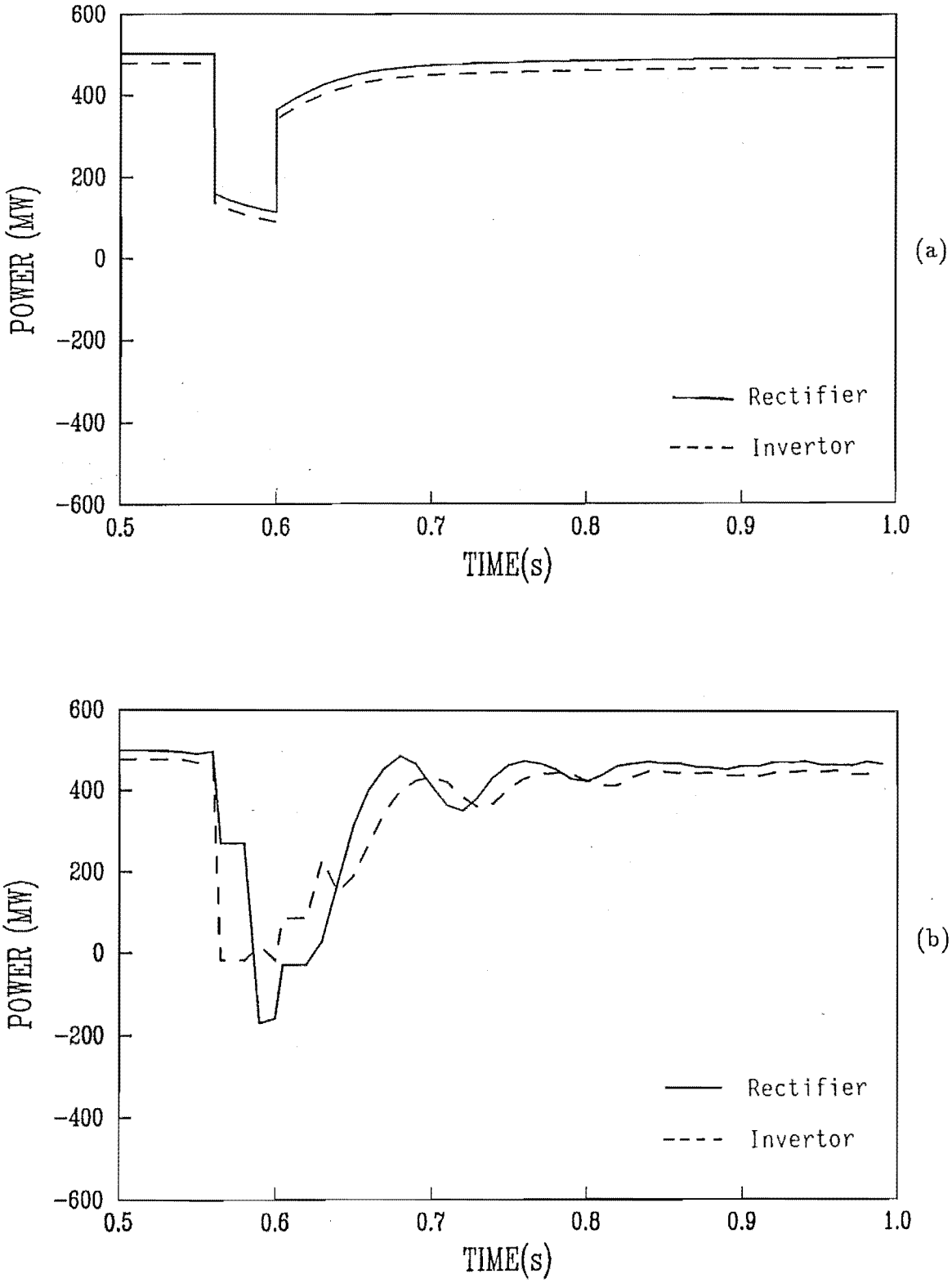

Figure 2.11: Rectifier and invertor powers from (a) stability program (b) integrated TCS and stability program

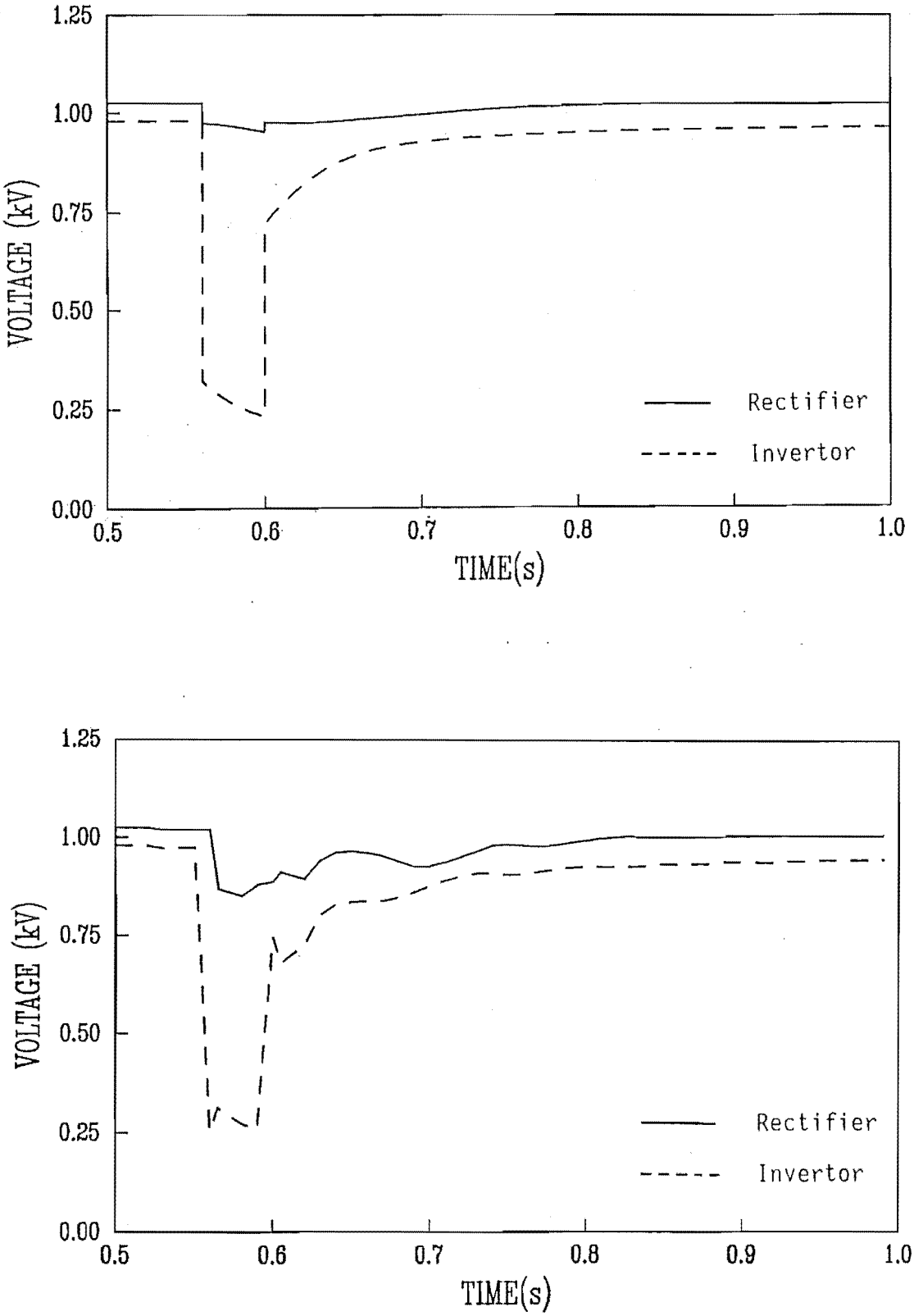

Figure 2.12: Rectifier and invertor terminal ac voltages from (a) stability program (b) integrated TCS and stability program

The response of the link obtained from the conventional transient stability program is shown in Figure 2.11(a) and the corresponding response obtained from the integrated TCS and stability program is displayed in Figure 2.11(b). The effect of detailed controller model during the disturbance and recovery period is clearly seen in Figures 2.11(a) and (b).

Figures 2.12(a) and (b) show the invertor terminal ac voltage obtained from the conventional and the integrated TCS-stability programs respectively.

2.6.3 General Discussion

The above test cases serve to illustrate the ability of the digital solution to model the effect of controller dynamics, which is shown to be of fundamental importance in the assessment of convertor recovery from disturbances.

The physical simulator is reputed to be an ideal tool for the setting of controller dynamics constants due to its ability to quickly perform repetitive studies.

The digital model, while slower in performing studies with different controller constants, is more flexible in altering the controller functions and can set up very accurately any specified point on wave of fault application, any level of transformer residual magnetisation, any pattern and duration of fault clearance etc. Moreover the digital solution can represent the ac system components as accurately as required (only limited by the availability of information). In particular, the ability to represent the convertor transformer magnetising history during the disturbance and the frequency-dependence of the ac system (even with detailed mutual effects) to any required degree of accuracy make the digital solution a viable alternative to the physical simulator.

The above remarks clearly show the difficulty involved in attempting 'quantitative' verifications of the computer results with reference to simulator studies. All that can be done is to check the 'qualitative' nature of the results with reference to typical patterns of fault recoveries expected; the results displayed in the last section are in line with such expected behaviour.

2.7 Conclusion

A detailed control system simulation has been added to the Transient Convertor Simulation (TCS) program currently used to predict the convertor recovery from disturbances. Apart from the extra modelling flexibility provided, representation of the control dynamics has been shown to influence dramatically the convertor performance following fault clearances.

The enhanced TCS program provides an important tool for the computer simulation of the operation of HVdc interconnections, particularly during ac and dc system disturbances. This program can be used to further develop control and protection schemes that will lead to improved overall system performance.

Chapter 3

A COMPARISON OF SIMULATION ALGORITHMS

3.1 Introduction

The incorporation of HVdc controller dynamics into TCS program was discussed in the previous chapter along with the need for such models. However, the simulation technique must be compared with another simulation tool for a wider acceptance.

Attempts to validate dynamic simulation algorithms for use in HVdc transmission are normally carried out by comparison to disturbances recorded from actual systems or physical simulators. This type of verification is by necessity of a qualitative nature.

A quantitative comparison is made in this chapter between the results predicted by two fundamentally different computer models, i.e. between algorithms derived from EMTP and state variable techniques (TCS program).

3.2 Criterion for Comparison

Three conditions must be met for a rigorous approach to the problem of verification of a computer algorithm, i.e.

1. Comparing the proposed algorithm with one or more fundamentally different models.

2. Setting up identical test system conditions in each model.

3. Presenting all the relevant information needed to detect any deviations and the instances of their occurrence.

With reference to HVdc transmission, the possibility of using real system information to assess the predictive ability of a computer simulation program, although often expected, is unrealistic owing to practical difficulties in meeting condition 2. Among the problems involved are the random 'points on wave' in which disturbances appear and disappear, the random states of magnetisation of convertor transformers upon fault clearances, the unavailability of realistic information of the actual system parameters prior to and throughout the disturbance etc. The use of a scaled-down physical simulator, still considered an acceptable alternative, is not entirely free from the problems listed above and its comparisons with computer models tend to emphasize the qualitative rather than quantitative behaviour [Cazzani 1988].

More often than not, 'good matches' are derived using the experimental information and adjusting by trial and error the computer model parameters [Mattensson 1986]. However such heuristic approaches give little confidence on the general applicability of the algorithm in question.

A more realistic comparison in terms of conditions 1 to 3 above is the use of two or more alternative and fundamentally different computer solutions. Two basically different approaches are currently used in HVdc transient simulation i.e the Electromagnetic Transient Program (EMTP) and the state variable technique. The EMTP method and a diakoptical solution have been combined into an efficient algorithm, the EMTDC, for the analysis of ac/dc power systems [Woodford 1983].

State variable solutions often reputed less efficient, are formulated in a more 'physical' form and use less approximations. They therefore provide suitable tools for a rigorous comparison. If the response of the two methods, i.e. EMTDC and TCS to various disturbances can be made to agree, it will be reasonable to accept the validity of both. If they do not agree, at least one of them will not meet the criterion and without additional information, it will be difficult to reach a positive conclusion as to the value of either.

3.3 Algorithmic Differences of TCS and EMTDC

TCS is a program specifically developed to analyse the dynamic behaviour of HVdc systems and is formulated in terms of state space theory [Arrillaga 1983b].

The EMTDC algorithm [Woodford 1983] is based on the Electromagnetic Transients Program, EMTP [Dommel 1969]. The trapezoidal rule is used for integrating the ordinary differential equations of lumped inductors and capacitors and converting them into a resistor in parallel with a current source, while lumped resistors are modelled simply as resistive branches. Hence a network of lumped R,L,C components is transformed into an equivalent circuit of resistive branches and current sources.

Using nodal analysis, a conductance matrix [G] is formed from the inverse resistance value of each branch in the circuit. A column matrix [I] is also formed, its elements consisting of the sum of the current sources at each node. The nodal voltages [V] are therefore,

$$[V] = [G]^{-1}[I] \tag{3.1}$$

Valve or ac system components switchings are implemented by changing the value of the appropriate resistors.

For greater efficiency, EMTDC uses the subsystem concept which groups the system into appropriate identifiable components such as generators, ac networks, convertors and dc lines, each of which is solved independently of the others at each time step. The subsystem solution requires the prediction of the incremental voltage waveform for the next step of the solution at the points of interface between subsystems. Thus to reduce error and avoid numerical instability, the use of subsystems requires the presence of sufficient capacitance and inductance to prevent large deviations of the voltages and currents from one step to the next.

The usage of subsystems result in greater reduction in computation time. Further efficiency is obtained by using a constant integration step throughout the solution.

The dc convertor along with a three phase transformer is modelled as a separate network, by taking advantage of the subsystem concept. It is also possible to model a convertor explicitly as a set of resistive branches (which represent valves),

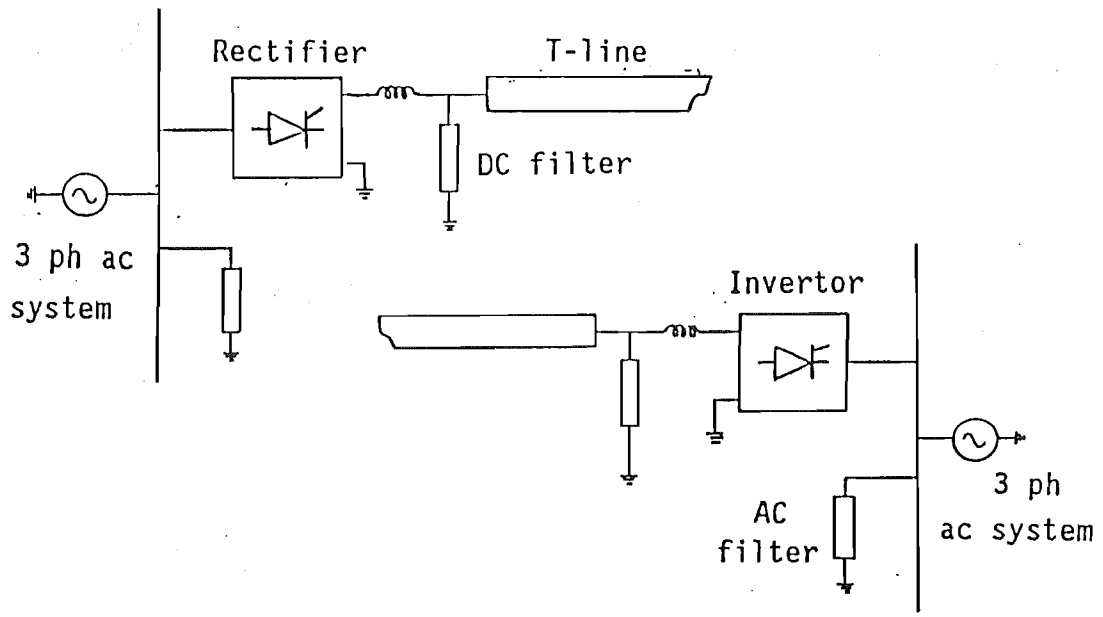

Figure 3.1: Test system for the comparison

in which case the dc system is solved as a unified solution.

3.4 Test System

The dynamic comparison will concentrate on the HVdc convertor, which constitutes the specific reason for the existence of the EMTDC and TCS programs.

A realistic comparison of the HVdc convertor behaviour provided by the two alternative algorithms can be achieved with reference to the simple test system illustrated in Figure 3.1. It consists of a monopolar dc link with a single bridge at each end provided with the basic control functions as illustrated in Figure 3.2.

The ac systems are modelled as modified Thevenin equivalents in parallel with the filters [Bowles 1970]. The dc line is represented by means of several pi-sections, dc filters and smoothing reactors. Details of the test system parameters are given in Appendix B.

In the TCS algorithm, the power system is built-up by appropriate connection of the network components and the control system is formed by cascading the individual controller functions available in the data file. Appendix C gives the TCS controller data file.

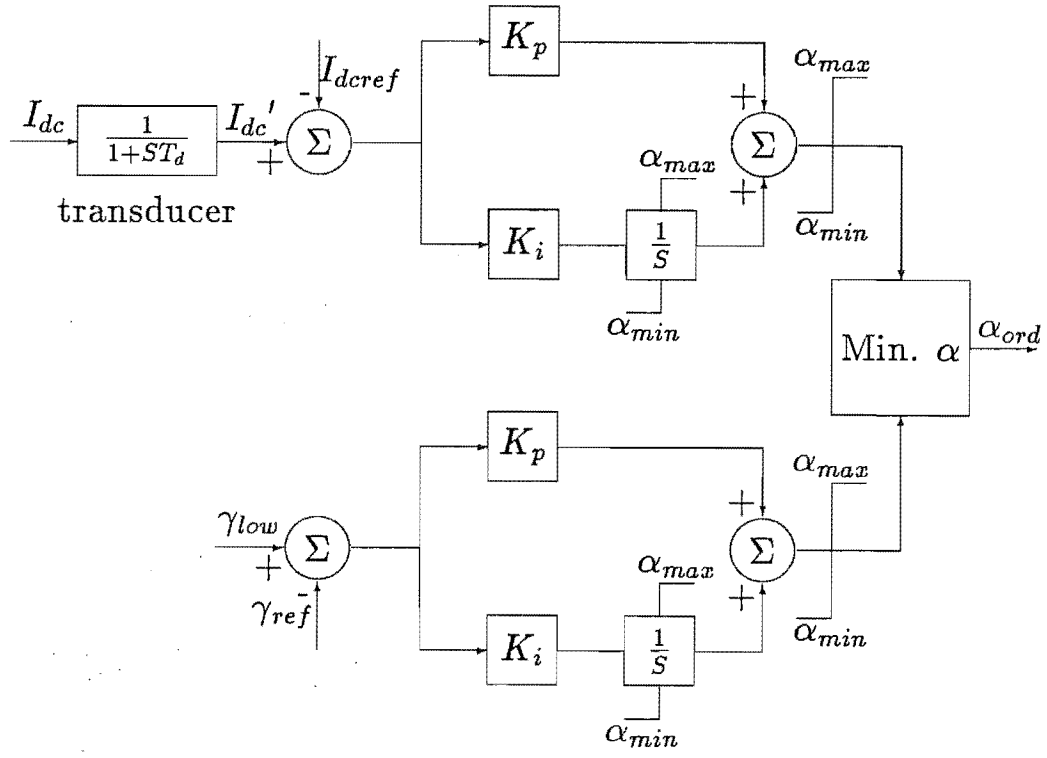

Figure 3.2: Test system controllers

In the EMTDC program, the power and control systems are formed using the data file and user defined subroutines. In the present test system, the electric network is conveniently divided into three subsystems comprising the sending and receiving end ac systems and the dc system [Manitoba 1988]. Also the convertors are modelled as separate subsystems.

3.5 Steady State Initialisation

Prior to the dynamic comparison, it is necessary to start up the system from a de-energised state and observe the operating conditions under steady state. For this purpose, both TCS and EMTDC were run for 0.5 seconds of simulation time to let the system settle down to the steady state. Both TCS and EMTDC have the facility to store the steady state results in a separate file for further studies and so a snapshot was taken at 0.5 seconds in both programs. The steady state run was first used to identify and correct various anomalies in data preparation (such as the per-unit systems) and information retrieval (such as the elimination of zero sequence

at the convertor voltages in the case of EMTDC).

It was observed then that the two programs settled down to the same operating point with the rectifier firing angle at 15 degrees and the extinction angle at 18 degrees. The reference dc current was 1.45 kA, with 0.1 pu current margin. The filter reactive powers were observed to be of the same magnitude in both programs and all the valve conducting states changes took place with less than one degree differences in the two programs.

3.6 Disturbance Simulation

Major disturbances in ac/dc power systems lead to multiple commutation failures at the invertors. Hence for a credible validation, the two transient algorithms should produce the same pattern of commutation failures. Such patterns together with full convertor recoveries are displayed in this section for typical severe ac system disturbances.

3.6.1 Symmetrical Fault

A three phase short-circuit of 2 cycles duration and causing a 40% voltage reduction in the three phases of receiving end system was used to determine the highest EMTDC integration step needed to reproduce the performance of the TCS algorithm. These were found to be 20 and 10μs for ac system and convertor models respectively.

Figures 3.3(a) and (c) show the dc current and three phase ac voltage waveforms derived with the TCS algorithm. Corresponding results simulated with the EMTDC program are illustrated in Figures 3.3(b) and (d).

For a rigorous approach to the question of algorithmic verification, it is important to present all the relevant information needed to detect any deviations between the results and the instances of their occurrence. This can be achieved without the need for large amounts of numerical information by comparing the valve conduction times. The bar diagrams of Figures 3.3(e) and (f) provide detailed information of the valve conduction times and with them a clear indication of commutation failure events.

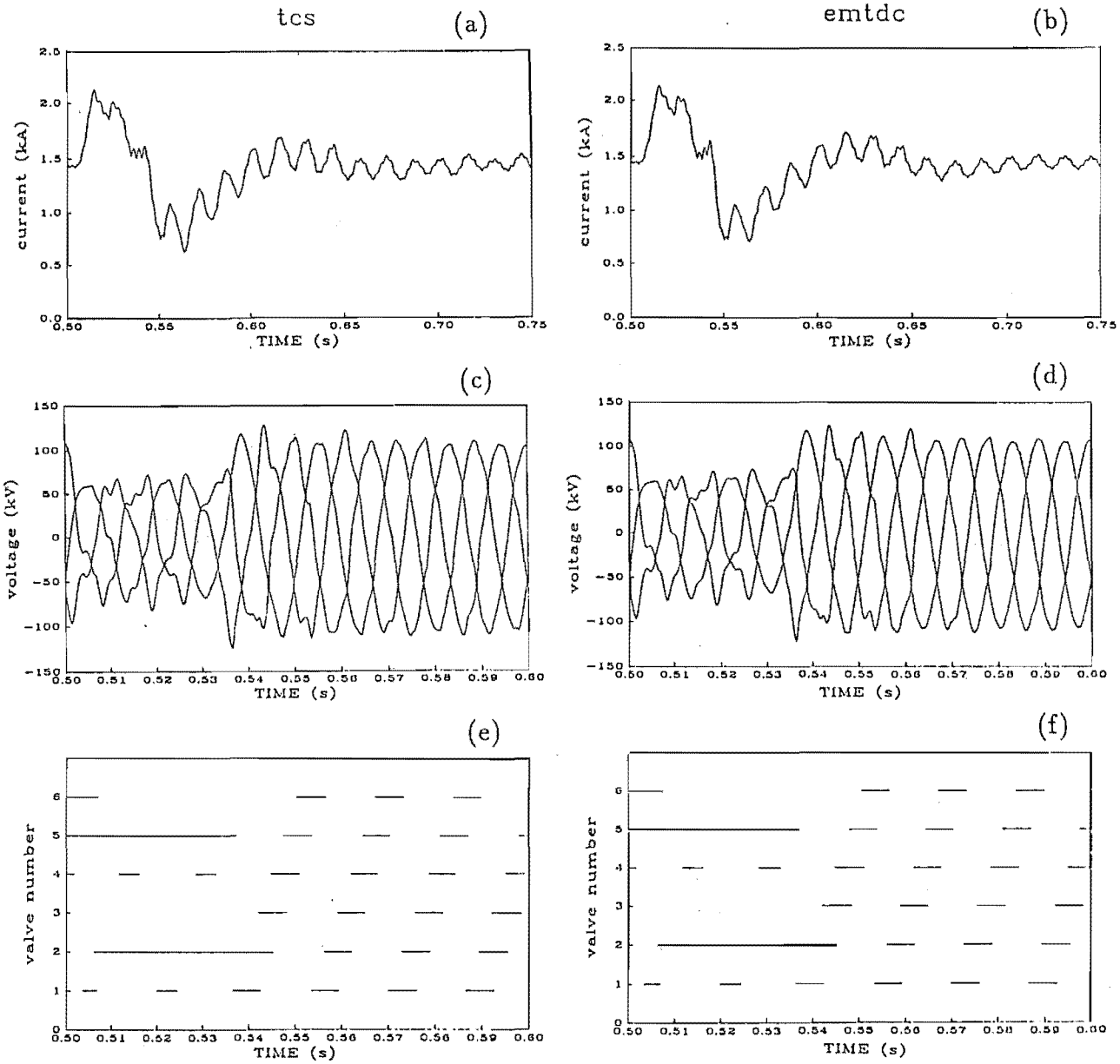

Figure 3.3: Three phase fault at the invertor end (a)(b) dc current, (c)(d) ac voltages, (e)(f) valves conduction

All the corresponding switching instants are within 0.5 degrees and the number of commutation failures predicted by both programs is eight. As a result, the convertor recovery following fault clearance is exactly the same in both cases. The severity of the disturbance simulated in this test case provides sufficient evidence of the validity of the two algorithms.

3.6.2 Asymmetrical Faults

Previous attempts to validate computer simulation versus field tests [Woodford 1985], while providing reasonable qualitative matches for balanced fault conditions, have shown unrealistic differences in cases of unbalanced disturbances.

The same integration step that achieved perfect matching for the symmetrical fault were used to assess the convertor response to a line-to-ground (L-G) fault, causing a complete loss of voltage in one phase of the receiving end ac system voltage.

While the overall recovery time and the number of commutation failures are the same for the specified disturbance, small differences are now observed in the valve conducting patterns. For instance, with reference to Figures 3.4(a) and (b), valve 5 attempts to conduct at about 0.515 seconds in the EMTDC simulation, whereas it does not conduct at all in the TCS simulation. Thus some small deviations are observed in the dc current and ac voltage waveforms illustrated in Figures 3.4(c),(d) and 3.4(e),(f) respectively.

A further test case was carried out consisting of a 2 cycle line-to-line (L-L) fault causing a 70% voltage reduction in two phases of the receiving end system. The results, shown in Figure 3.5, again indicate similar fault recoveries for the two algorithms. However, the valve conducting patterns of Figure 3.5(e), (f), although showing the same number of commutation failures, illustrate some differences between TCS and EMTDC; for instance, valve 4 has two brief conduction periods in EMTDC which are totally absent in the TCS simulation.

The above differences in valves conducting patterns in the asymmetrical cases are not due to the differences in the controller outputs, which have been checked to be the same at those particular instants and therefore, they must be due to differences in the software implementation.

An important algorithmic difference between TCS and EMTDC is the use of the subsystem concept by the latter. In EMTDC, the commutating voltages at

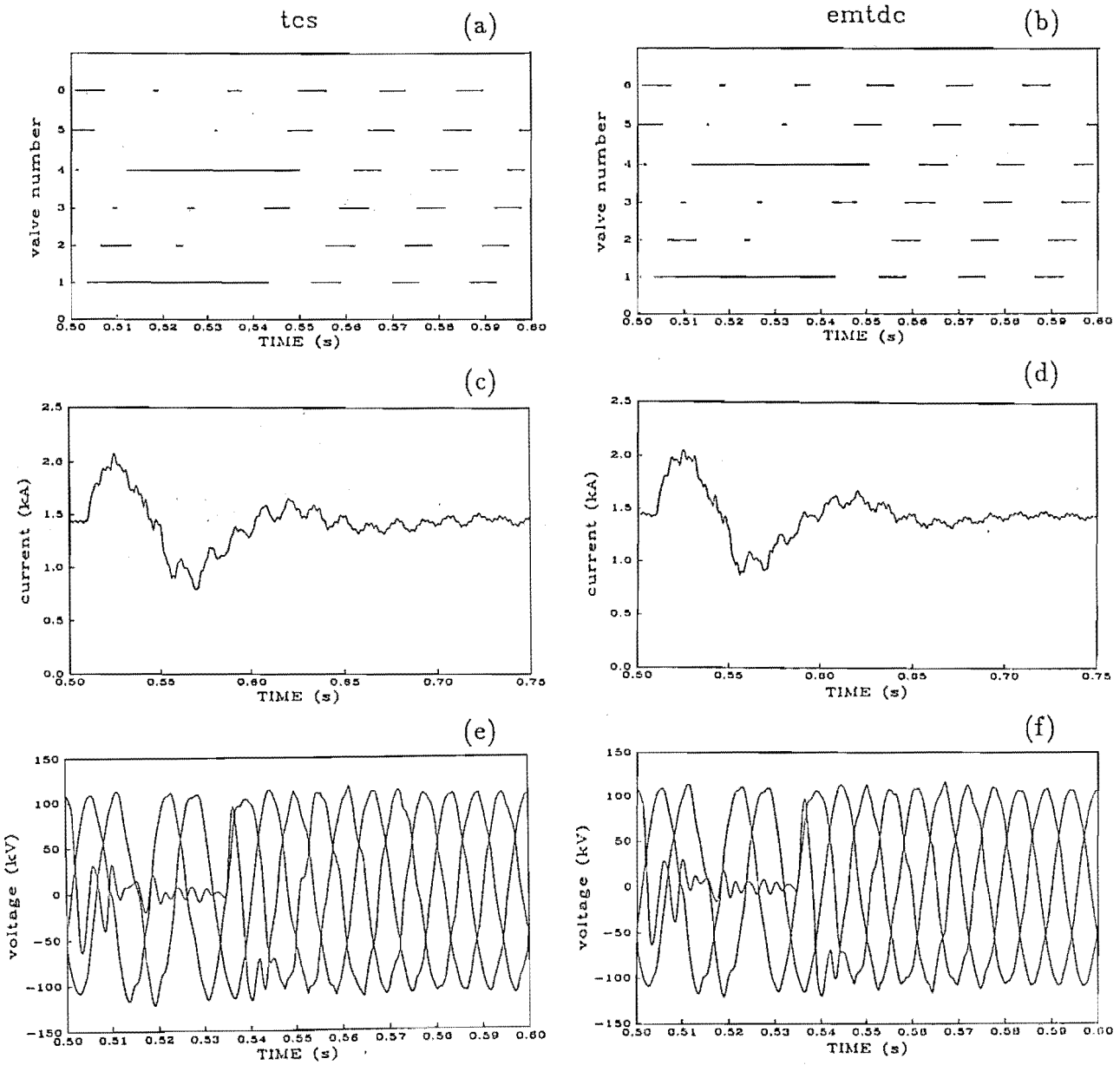

Figure 3.4: Line-to-Ground fault at the invertor end (a)(b) valves conduction, (c)(d) dc current, (e)(f) ac voltages

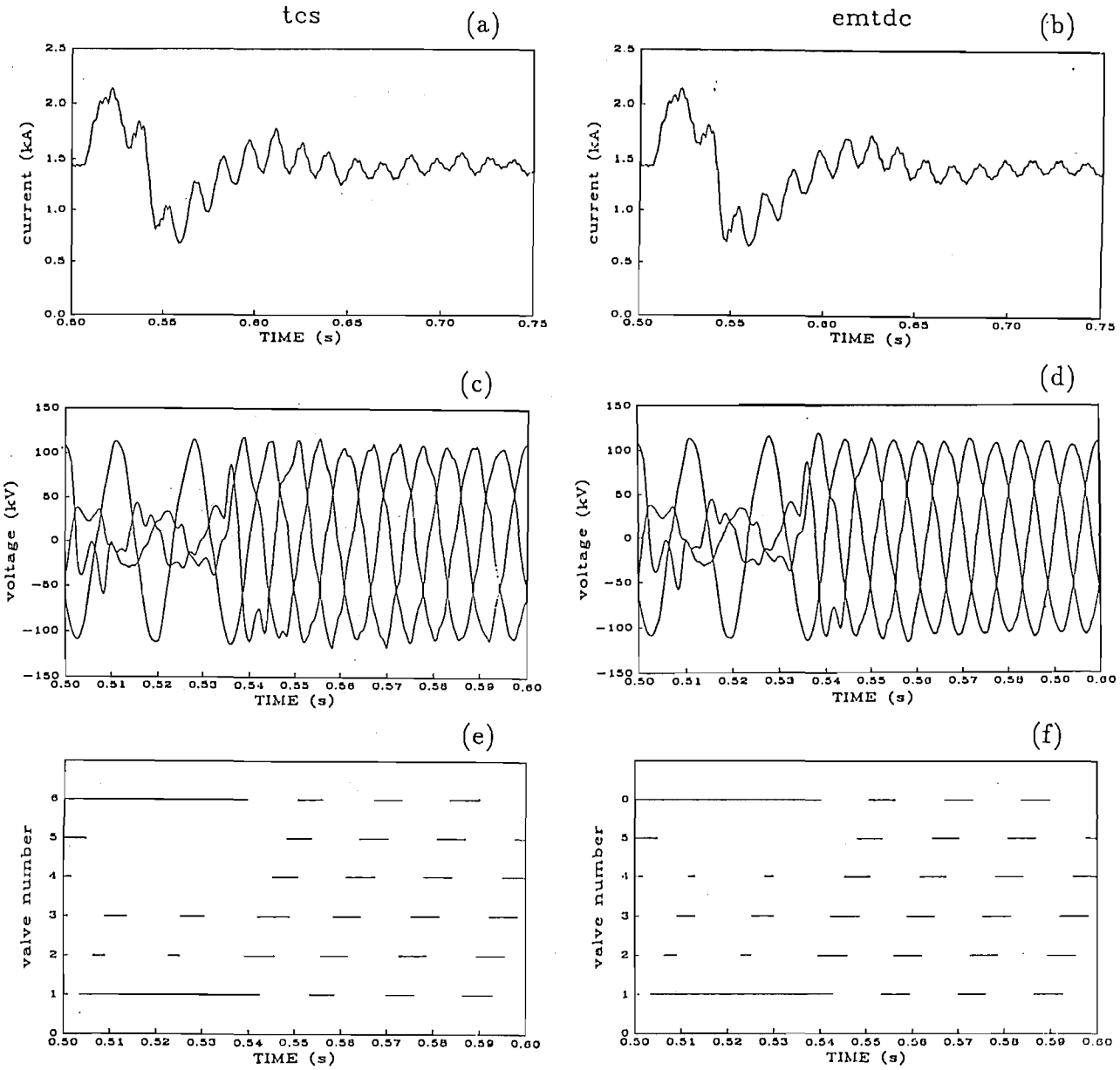

Figure 3.5: Line-Line fault at the invertor end (a)(b) dc current, (c)(d) ac voltages, (e)(f) valves conduction

the t^{th} interval are derived from those calculated in the previous interval $(t - \Delta t)$ by an approximate phase advance prediction [Manitoba 1988]. This is achieved by the following equation (for phase-A voltage) :

$$V_t = (1 - \omega^2 \Delta t^2) V_{a(t-\Delta t)} + \frac{\omega \Delta t}{\sqrt{3}} \{V_{c(t-\Delta t)} - V_{b(t-\Delta t)}\} \tag{3.2}$$

However, this equation is based on the assumption that the voltages are perfectly balanced and therefore their use is only accurate under balanced steady-state or symmetrical faults conditions. Thus neglecting the considerable negative sequence voltage content during L-G and L-L fault simulations can cause some error in the derivation of the commutating voltages (which alters the valve commutation intervals) and voltage crossings (which alters the valve extinction angles). This may account for the small differences in the valve conduction patterns between the EMTDC and TCS results observed during the asymmetric disturbances.

In order to test the effect of the phase advance prediction, the L-L fault was repeated without using the subsystem concept, that is with the whole system analysed simultaneously. A comparison of bar diagrams while the fault (and therefore the asymmetry) is ON is illustrated in Figure 3.6. Clearly the EMTDC response without system subdivision (Figure 3.6(a)) is much closer to that of TCS (Figure 3.6(b)) than the standard EMTDC using the subsystem concept (Figure 3.6(c)).

3.7 Algorithmic Efficiencies

The comparison of algorithmic efficiency is not straightforward, as it depends on subjective judgements regarding what constitutes an equivalent dynamic performance.

As expected, the use of the standard EMTDC algorithm, with the recommended integration steps, provides a very efficient solution. If the results plotted in Figure 3.5 are considered sufficiently close, the EMTDC program is about four times faster than TCS.

However if a closer agreement is required, such as that provided by the unified solution (displayed in Figure 3.6(a) and (b)) with a step length of 10μS, the situation changes quite dramatically. For the test system with a L-L fault and a 250 mS simulation run, the total computing times on a VAX-3500 computer were as

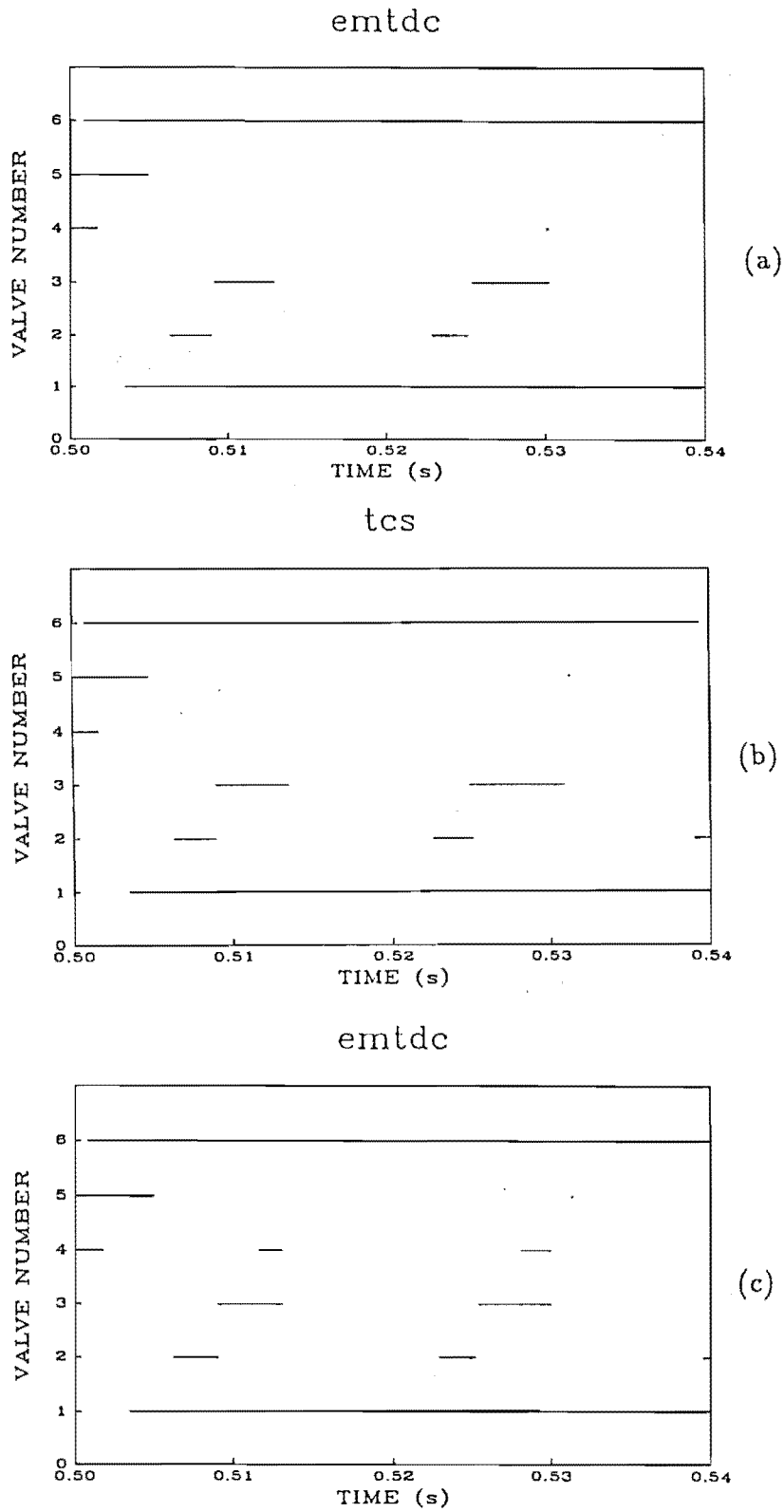

Figure 3.6: Comparison of valve conduction pattern (L-L fault) (a) EMTDC without system subdivision, (b) TCS, (c) EMTDC with system subdivision

follows:

TCS - 42 minutes

EMTDC - 41 minutes

3.8 Conclusion

By setting up an identical test system, it has been shown that the two main algorithms currently used for the simulation of ac/dc disturbances, namely TCS and EMTDC, can be made to agree in their prediction of the dynamic responses.

The TCS algorithm, though reputed to be less efficient, uses fewer approximations and provides automatic selection of optimal integration steps. As a result the TCS responses are very consistent.

With careful selection of the integration step, the EMTDC program can produce practically the same responses as the state variable technique for reasonably symmetrical conditions. However, some deterioration occurs with highly asymmetrical disturbances. This has been traced to the phase advance prediction, required by the subsystem concept, thus the EMTDC algorithm provides a very efficient solution at the expense of some accuracy.

The comparison has not included ac system components such as generators and SVC, but has concentrated on the modelling of the convertor algorithms. It can be concluded that both the EMTDC and TCS algorithms can be used with confidence to simulate the transient response of ac/dc convertors.

The results of this preliminary investigation indicate that the best features of EMTDC and TCS can be combined into a new algorithm called EMTCS and it is currently underway at the University of Canterbury.

Chapter 4

DYNAMIC SIMULATION OF GENERATOR-HVDC CONVERTOR UNITS

4.1 Introduction

Dynamic simulation of generator and HVdc convertors using TCS algorithms have previously been used to establish the controllability of generator-HVdc convertor units during disturbances [Campos Barros 1976] and in thyristor bridge excitation system studies [Heffernan 1980]. In this work, TCS is used to assess the applicability of conventional steady state formulation and derive the operating characteristics of unit connections.

Iterative analysis in harmonic space [Eggleston 1985] and EMTDC program [Naidu 1989] have also been used to study the generator-convertor units. These studies were restricted to harmonic analysis.

The synchronous machine model in TCS is represented in phase quantities, in order to handle assymetries, non-linearities and distortion effects by direct parameter modification or indirectly. A d-q axis representation is used for the rotor circuit, which uses the main field winding in the d-axis with two damper windings . The machine is treated as a motor when writing down its electrical axes equations; the terminal voltage can be expressed in matrix form as [Campos Barros 1976],

$$\begin{aligned} V_g &= p(L_g I_g) + R_g I_g \\ &= L_g \frac{d}{dt} I_g + \omega \frac{d}{d\theta} L_g I_g + R_g I_g \end{aligned} \tag{4.1}$$

where,

$\omega = \frac{d\theta}{dt}$ is the angular velocity.

$$L_g = \begin{bmatrix} L_{ss} & L_{sr} \\ L_{rs} & L_{rr} \end{bmatrix}$$

the subscripts s and r are stator and rotor respectively. Since most manufacturer data is in the two axes d-q-0 form, this must be transformed to yield the direct phase quantities (a,b,c).

Appendix D gives the transformation of manufacturer's data into the phase quantities.

In this chapter, the per-unit system used to simulate the unit connections and the validation of the generator model are given. Also the initialisation process involved in TCS to study the unit connections and the calculation of steady state quantities from the waveforms are explained.

4.2 Per-Unit System

In steady state analysis such as load flow, the convention is to choose rated current and voltage (fundamental frequency rms values) as base values. Ac/dc convertors are treated as voltage and frequency transformers and the base values of the dc side variables are defined according to their relation with the ac side variables [Arrillaga 1983b].

In a transient program like TCS, the valves are treated as switches and hence the instantaneous ac line voltage and current will be the same on both sides of the switch, i.e. on the ac and dc sides. For this reason, the base values of the dc side must be chosen as the base values of the ac side and so it is preferable to take instantaneous rather than rms base values.

In order to keep the figures for the per unit values of transformers and generators within the usual bounds, the base values are chosen such that the base

impedance is kept equal to the three-phase value. A system that would satisfy this requirement is as follows:

Base current : peak phase current of the star equivalent
Base current : peak phase voltage of the star equivalent
Base power : peak phase power of the star equivalent

In terms of usual three phase values it gives:

$$I_{base} = \sqrt{2} I_{line,rms} \tag{4.2}$$

$$V_{base} = \sqrt{2} V_{phase,rms} = \frac{\sqrt{2} V_{line,rms}}{\sqrt{3}} \tag{4.3}$$

$$Basepower = \frac{2}{3} \ (Three\ phase\ base\ power) \tag{4.4}$$

4.3 Validation of Generator Model

Even though the generator model in TCS is an established one and has been used for other studies [Campos Barros 1976 and Heffernan 1980], validation tests are still required to make sure that the program represents the required synchronous machine parameters. Computer simulated open-circuit and short-circuit tests are used for this purpose.

Simultaneously short-circuiting the three phases of a synchronous machine when running unloaded is an accepted method of determining the principal transient reactances.

For an unloaded machine, neglecting resistance, the short circuit stator current of any phase is given by [Concordia 1951],

$$i = \frac{e}{X''_d} cos(t + \theta_o) - (\frac{1}{X''_d} + \frac{1}{X''_q}) \frac{e}{2} \theta_o - (\frac{1}{X''_d} - \frac{1}{X''_q}) \frac{e}{2} cos(2t + \theta_o) \tag{4.5}$$

where θ_o is the switching angle. The above equation shows that the initial current is composed of a fundamental component depending only on X''_d, a dc component depending on X''_q and X''_d and a small double frequency component depending on the difference between X''_d and X''_q, i.e. the sub-transient saliency.

Figure 4.1 shows oscillogram of the open-circuit voltage and short-circuit stator currents of the salient machine given in Appendix E. The peak-to-peak open circuit voltage is, e= 1.5472 pu and the initial short circuit stator current is, i= 7.677 pu. So,

$$X_d'' = \frac{e}{i} = 0.2015 \tag{4.6}$$

The direct axis sub-transient reactance for the machine as given in Appendix E is 0.2 pu.

Figure 4.2 shows oscillogram of the open circuit and short circuit stator currents of the non-salient machine given in Appendix E. From the initial short circuit current and open circuit voltage , X_d'' is calculated to be 0.149 pu and the value given in Appendix E is 0.145 pu. It can be seen from the oscillogram shown in Figure 4.2 that the short circuit current does not have any double frequency component.

The close agreement of the calculated subtransient reactances together with the general pattern of the subtransient and transient periods indicate the correctness of the programmed data.

4.4 Initialisation of Unit Connection Simulation

The susceptibility of simulations involving detailed synchronous machine models to inaccurate initial conditions was shown by Campos Barros [1976] and Heffernan [1980] to be a major problem in their work, which involved generator-rectifier systems. When the dynamic simulation is started with idealised steady state conditions derived from fundamental frequency power flow, the initial estimate of state variables introduce transients in machine currents. These transients decay very slowly with the machine time constants. This difficulty is solved without extra-long adjustment runs by increasing the resistances of the rotor circuits and thereby artificially reducing the machine time constants. The inflated resistances are reduced to the original value after a few cycles and the desired operating point is reached. Figure 4.3 shows the dc current and machine rotor currents during the initialisation period.

During the initialisation, it is very important to specify accurate values for convertor transformer magnetisation currents. If inaccurate initial magnetisation

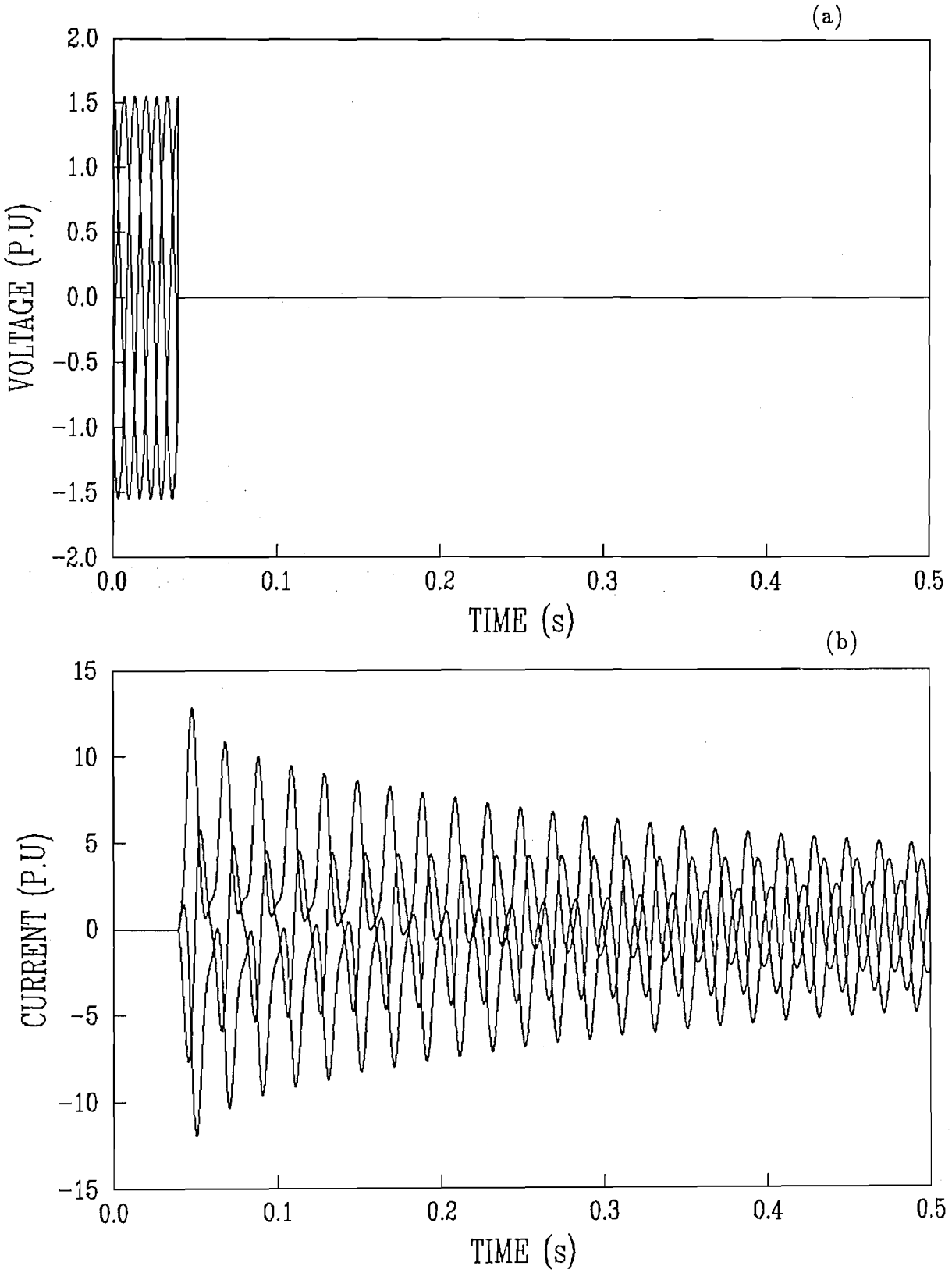

Figure 4.1: Short circuit test waveforms of the salient machine (a) terminal voltages (b) stator currents

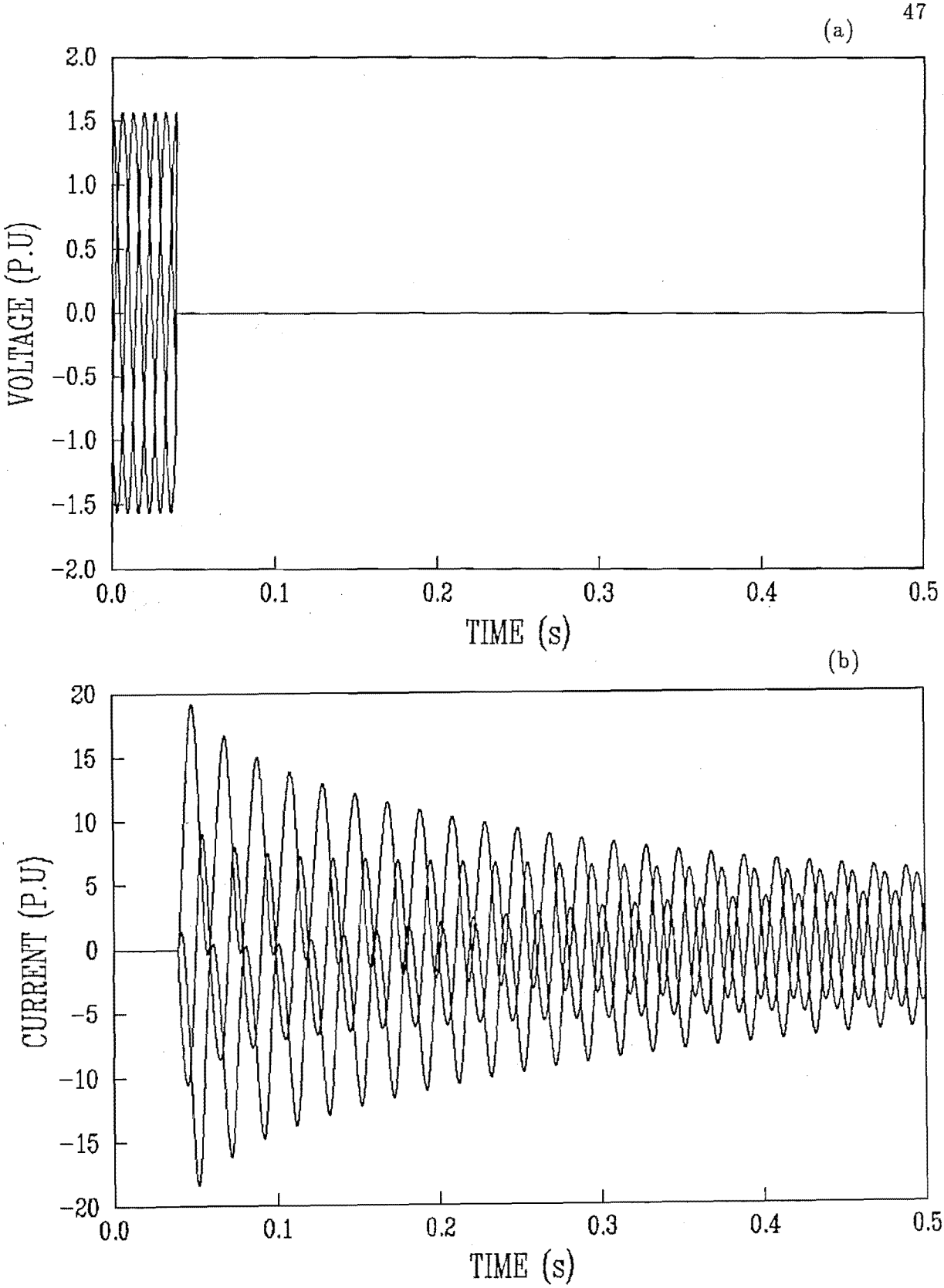

Figure 4.2: Short circuit test waveforms of the non-salient machine (a) terminal voltages (b) stator currents

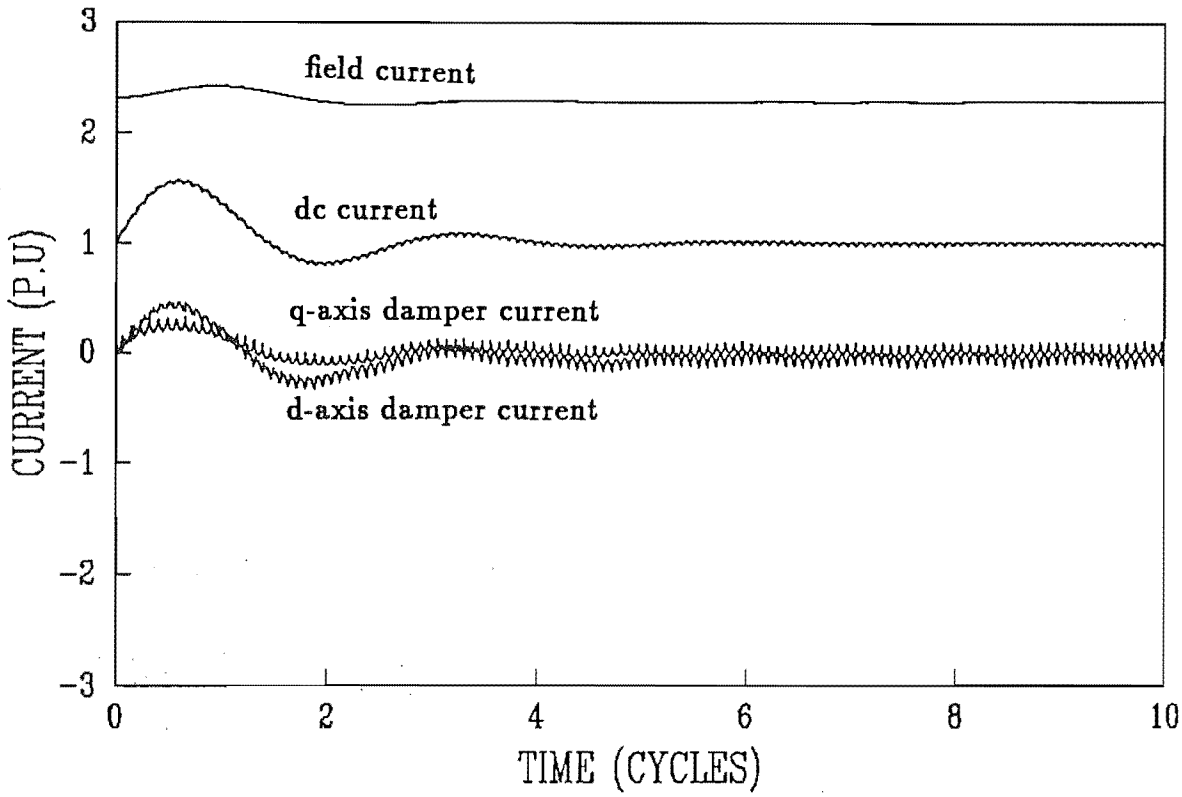

Figure 4.3: Generator rotor currents and dc current derived from dynamic simulation

currents are specified, then a dc offset is introduced in the magnetising current whose value depends on the error. The rate of decay of this magnetising current offset is dependent on the transformer resistance involved. Since this is usually low for power transformers, the time taken for the offset to disappear is considerably high and this problem has been reported by Heffernan also. The effect of this magnetisation offset is to create a dc component in the stator currents. In this work, the correct values of magnetisation current for a particular loading condition are obtained by doing a preliminary run (e.g. for 0.5 degrees).

Figures 4.4 and 4.5 show the generator terminal voltage (only two phases of the voltage waveform are shown for clarity) and stator currents derived from TCS.

Since there are no harmonic filters at the generator terminal, it would be difficult to know the excitation required for a particular dc voltage and dc current. One way to get around this problem is to model the excitation control with dc voltage as the controlled quantity instead of machine terminal voltage.

Dynamic simulation is extremely demanding computationally, as the program must run for many cycles to remove the transient components from the wave-

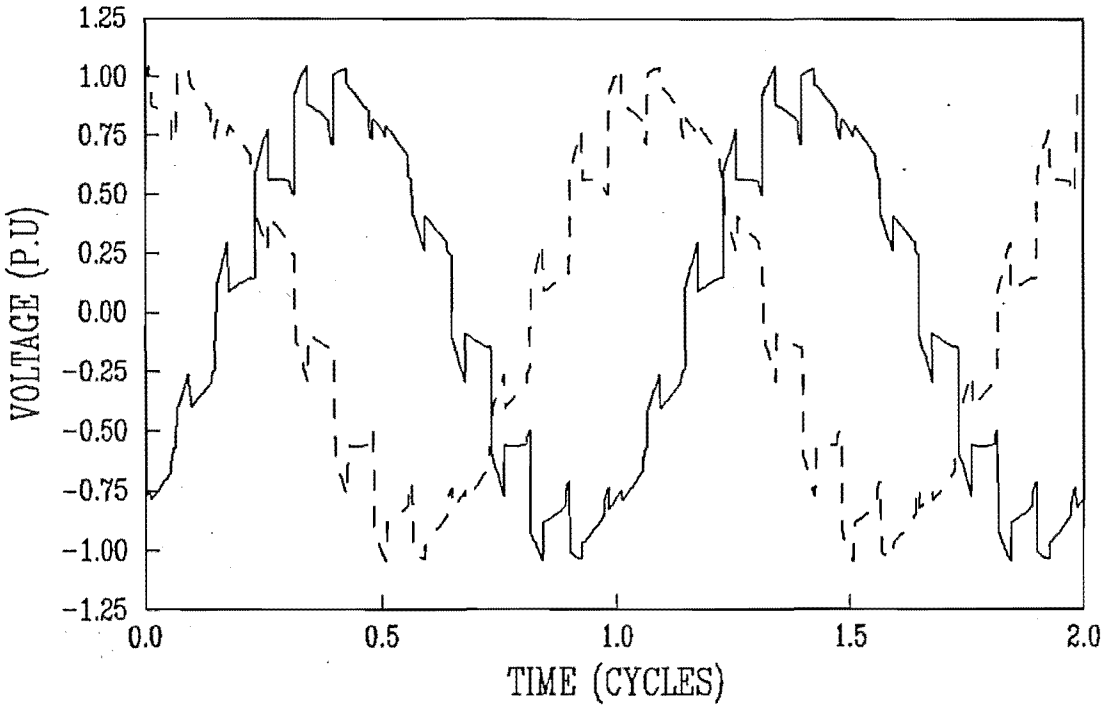

Figure 4.4: Generator terminal voltages (two phases) derived from dynamic simulation

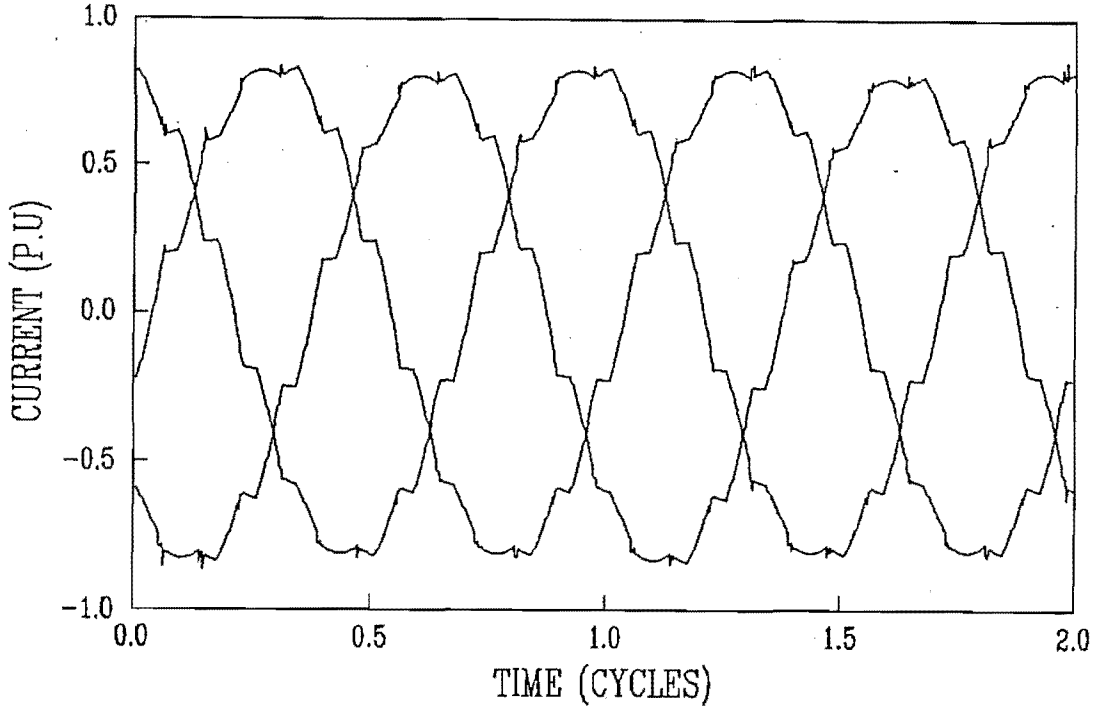

Figure 4.5: Generator phase currents derived from dynamic simulation

forms. The initialisation process can be speeded up by a preliminary study using the simplified steady state formulation described in section 5.6.

An approximate value of field current can be calculated using the steady state simulation. The field current gets adjusted to the exact value by the excitation control modelled in TCS, to obtain the specified operating point.

4.5 Notch Removal for Firing Angle Measurement

In the absence of harmonic filters, the terminal voltage waveform would be severely distorted and such a waveform is shown in Figure 4.4. A look at the waveform clearly shows that the use of generator terminal voltage as the reference waveform for the firing controller will introduce considerable discontinuities in the voltage crossings caused by the commutation notches. On the other hand, the internal emf is inaccessible for monitoring purposes. One possible solution is the provision of control filters to obtain the fundamental voltages; however the phase of such a filtered signal will alter with the firing angle and the loading conditions.

A better alternative is to 'ignore' the commutation notches, that is to use a sine wave derived 'on-line' from the actual waveform by filling-in the gaps during the commutation regions. This is not equivalent to 'filtering' and the fundamental frequency wave will therefore not be phase-shifted.

4.6 Calculation of Steady State Quantities

In this work, the dynamic simulation program is used to derive the steady state characteristics of unit connections. The steady state quantities like dc voltage, dc current, terminal voltage and machine currents are calculated from the TCS waveforms using the FFT. To reduce sampling errors at points of discontinuity, a high number of samples (1024 samples per cycle) is used.

In order to determine whether a particular run has reached steady state or not, FFT analysis is carried out at intervals of 5 cycles. The absence of any significant

Table 4.1: Variation of dc component in the stator current

Time (cycle number)	R - phase (%)	Y - phase (%)	B - phase (%)
40	-1.597	1.558	0.038
41	-2.616	2.070	0.553
44	-2.227	2.083	0.190
45	-2.291	2.056	0.236

difference in the fundamental quantities between two consecutive FFT sets of results indicates steady state. In this work, 0.005 pu has been used as the steady state criterion.

The computation time for a back-to-back system comprising generator, 12-pulse rectifier & invertor and primary controls is about 7 minutes per cycle on a VAX 3500, with a time step of 1 degree. Normally, 20 to 25 cycles would be required to reach a steady state with reasonable initial values.

In spite of adopting the techniques described in section 4.4 for initialising generator-HVdc convertor units, the FFT analysis detects the presence of small amounts of dc components in the stator currents. The magnitude of this dc component from a sample run is indicated in Table 4.1.

It can be seen from the Table 4.1 that the dc component magnitude does not follow any defined pattern and varies from one phase to another. From the numerous runs carried out during this work, the maximum value of the dc component was found to be less than 3%.

When the convergence tolerance for the state variables is changed from 10^{-5} to 10^{-10} and the step length reduced from 1 degree to 0.2 degree, the dc off-set levels decrease by almost 50%. But still they were in the order of 1.5 to 1.8%. With this reduced step length and improved convergence tolerance for the state variables, the computational time was extremely high (30 minutes of cpu time per cycle).

The effect of this dc component is to create a small component of power frequency rotor current and a power frequency component on dc current.

4.7 Conclusion

Various runs using generator-convertor units have showed the validity of generator model and per-unit systems adopted in TCS. Proper initialisation techniques and identification of steady state for unit connected systems have been established for further studies. An alternative to the control system filter has been proposed for firing angle reference. Further work is still required to eliminate the dc component completely from the machine stator currents.

Chapter 5

ANALYSIS OF THE COMMUTATION PROCESS IN A GENERATOR-HVDC CONVERTOR UNIT

5.1 Introduction

The mechanism of commutation in a static convertor connected to an ac system is a well-known process, in which the commutation is considered as a short-circuting process between the phases connected to incoming and outgoing valves. The difference in the open-circuit voltages of the two phases is treated as the effective voltage for commutation and during commutation, this effective voltage produces a circulating current flowing through the valves from the incoming valve to outgoing valve. Under normal condition, the commutation process is completed when the magnitude of the circulating current reaches the total current value, i.e. when the current in the outgoing valve reaches zero.

During commutation, circulating currents are reflected in the convertor transformer primary circuit and in the ac system. Thus any impedances associated with the paths of the circulating currents affect the build-up of circulating currents and hence influence the commutation process. The combined effect of such impedances causes an equivalent commutation impedance which includes one com-

ponent due to the convertor transformer and another due to the ac system.

The influence of convertor transformer impedance on the commutation process was thoroughly investigated by Chen [1962]. He showed that the winding resistances, stray and distributed capacitances and the mutual inductance effects have little effect on the commutation process. The reactance that influences the commutation process is independent of dc current and the dc ripple level and this reactance is equal to the transformer leakage reactance.

With perfect filtering or with a combination of filters and transformer phase-shift, the voltage on the ac side of the convertor transformers may be assumed to be sinusoidal and hence the system reactance has no influence on the commutation process. In the absence of filters, pure sinusoidal voltages only exist behind the system source reactance and in such case, the commutation reactance is the sum of transformer reactance and the system reactance.

In the case of a unit connected HVdc system, the generator, unit transformers and HVdc convertors are connected as a unit isolated from the rest of the system. This arrangement is different from the conventional arrangement due to the absence of harmonic filters and its isolation from the rest of the system. Hence the commutation process would be influenced not just by the convertor transformers alone.

The farthest component from the convertor is the turbine, which is a mechanical element. The typical response of a turbine governor is of the order of a second and compared to the convertor commutation period, the turbine governor will have no effect on the commutation process.

The other components in the system are the two electromagnetic elements: generator and transformer. The influence of transformer on the commutation process is same as in the conventional arrangement. The effect of the generator on the commutation process is analysed in this chapter. Earlier studies on Generator-HVdc convertors have been restricted to the harmonic analysis [El-Serafi 1980, Eggleston 1988].

5.2 Factors Affecting the Commutation Process

In a generator-HVdc convertor unit, in the absence of ac harmonic filters, each and every commutation represents a line-to-line short circuit across the generator terminal. As a result, the machine is driven into sub-transient state every 60 degrees in a 6-pulse convertor system and every 30 degrees in a 12-pulse convertor system. So, the reactance that effects the commutation process is the sub-transient reactance and the commutating voltage seen by the convertor would be the machine internal emf behind the sub-transient reactance.

There are two different effects on these parameters. Firstly, during the commutation period, which would be close to 30 degrees in a 12-pulse convertor system, the machine reactance would vary towards the direction of transient value. For a typical machine (given in Appendix E), the variation in the reactance value for a commutation period of 30 degrees is calculated to be only 3.8%.

Secondly, due to the unsymmetrical nature of the rotor, the machine reactance varies around the rotor surface. This reactance value depends on the rotor position and has minimum and maximum values of direct and quadrature axis sub-transient reactances respectively.

Apart from the above two effects, the frequency conversion nature of the synchronous machine introduces another dimension of complexity to the commutation process. In a perfectly non-salient machine, when a harmonic current of order h enters the stator, a flux of harmonic order (h-1) is set up in the rotor, which in turn induces a stator voltage of the original harmonic order h of the same sequence. On the other hand, in the case of a salient machine, when a positive sequence current of harmonic order h enters the stator, it sets up two counter rotating fields of (h-1), inducing a positive sequence component of order h and a negative sequence voltage of order (h-2). Similarly, a negative sequence current of order h produces a negative sequence voltage component of order h and a positive sequence voltage component of order (h+2). Thus in the presence of stator harmonic currents and also rotor saliency, the internal generator emf will contain frequencies other than the fundamental and thus the commutating voltage will not be sinusoidal.

5.3 Modelling of the Commutation Process

In conventional schemes involving power generating plants and HVdc conversion , the relatively low ac system impedance combined with the provision of filters achieves a practically sinusoidal voltage at the convertor terminals. Such voltage and the transformer leakage can then be used as the commutating voltage and commutation reactance respectively.

The generator's phase currents are also sinusoidal and therefore the steady state operating conditions can be derived using conventional single-frequency phasor theory. Under these conditions, the excitation field of the generators produces an internal emf behind synchronous reactance. The equations which describe the commutation are [Arrillaga 1983a]:

$$u = cos^{-1}(cos\alpha - \frac{\sqrt{2}X_c I_{dc}}{E_c}) - \alpha \tag{5.1}$$

$$V_{dc} = \frac{3\sqrt{2}}{\pi} E_c cos\alpha - \frac{3}{\pi} X_c I_{dc} \tag{5.2}$$

$$cos\phi = \frac{1}{2}(cos\alpha + cos(\alpha + u)) \tag{5.3}$$

At present, similar equations are used to represent the commutation process for unit connections also [Hausler 1980, Campos Barros 1989]. The commutation reactance is taken as a linear combination of generator sub-transient reactance X'' and transformer reactance X_t that depend on the chosen pulse number.

For a six-pulse configuration, the commutation reactance X_c of a unit connected bridge convertor is taken as,

$$X_c = X'' + X_t \tag{5.4}$$

For a 12-pulse configuration and using as the power base the nominal rating of one convertor transformer, the commutation reactance in per-unit is:

$$X_c = \frac{X''}{2} + X_t \tag{5.5}$$

If the generator rotor is non-salient, the machine sub-transient reactance is:

$$X'' = X''_d$$

where X''_d is direct-axis sub-transient reactance.

For a salient machine, the value of X'' is normally taken as the average of X''_d and X''_q [Eggleston 1985], i.e.,

$$X'' = \frac{1}{2}(X''_d + X''_q)$$

When the dc power and dc voltage are specified, the nominal valve side commutating voltage (E_c) is calculated from equation 5.2. Once the commutating voltage is calculated for the nominal case, the dc voltage for other operating points (e.g. for different dc currents and firing angles) is found by keeping the same commutating voltage. This voltage is adjusted only when the generator is operated at a frequency other than the nominal frequency and for a different transformer ratio.

The problem with the above formulation is the variant nature of generator emf behind the sub-transient reactance and the effect of saliency as explained in section 5.2.

Alternatively, unit connected system studies can be studied using the following models:

1. Simplified model using voltage behind reactance

2. Detailed dynamic simulation of generator-HVdc convertor units

3. Finite Element technique

A simplified single phase model which takes into account the variation of commutation voltage and reactance has been developed to study unit connected systems and this is explained in section 5.6.

A more realistic tool for the unit connection is dynamic simulation and will be used here to show the inapplicability of conventional quasi-steady state equations and the limitations of the simplified model.

Finally, Finite Element techniques have been successfully applied in the field of electromagnetics and are at present used to design electrical machines. It is understood that GEC, United Kingdom has developed a program to study generator-HVdc convertor units using Finite Element technique which involves the detailed simulation of dc convertors also [Preston 1990].

5.4 Limitation of Commutation Reactance

As seen from equation 5.1, the commutation period is a function of commutation reactance and firing angle, for the same commutating voltage and dc current. If the reactances are too high, the commutation lasts longer than the interval between firings. Hence a new commutation is started in the valve firing sequence before the previous one has been completed. In the case of a six-pulse convertor, if the commutation angle is greater than 60 degrees, it causes a pole-to-pole dc short circuit. For a 12-pulse convertor, a commutation angle larger than 30 degrees causes the two bridges to have regions of simultaneous commutation on the same phases and this will increase the commutation reactance in proportion to the duration of the simultaneous overlapping region. The resulting commutation reactance for commutation angles greater than 30 degrees becomes [Hausler 1980],

$$X_c = \{(u-30)X_{c1} + (60-u)X_{c2}\}/30 \tag{5.6}$$

where ,

$$X_{c1} = \frac{X''}{2} + X_t$$
$$X_{c2} = X'' + X_t$$

In the conventional scheme, the effective commutating reactance is the convertor transformer leakage reactance and so the commutation angle is always well below these limits during normal operation. As explained in section 5.3, the commutation reactance of the unit connected systems includes the generator sub-transient reactance also and so it will be much higher than the conventional scheme. One way of reducing the commutation reactance is to keep the transformer leakage reactance comparatively low. The commutation angle can also be reduced by operating the convertor at a slightly higher firing angle, but this increases the harmonic levels.

Another way of reducing commutation reactance is to design generators with low X''_d. Reduction in X''_d would tend to lead to designs with a reduced stator electric loading and a slightly oversized machine to get sub-transient reactances down to 0.1 to 0.15 p.u level. The lower reactances will lead to higher fault currents and torques but these conditions will only occur for faults on the ac system between the machine and the convertor.

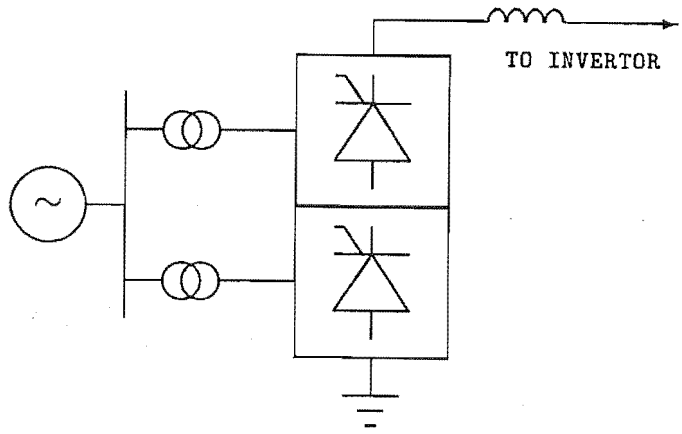

Figure 5.1: Twelve pulse unit connected generator-HVdc convertor

5.5 Inapplicability of Conventional Formulation

In order to show the inapplicability of using conventional quasi-steady state equations for unit connected dc systems and in particular the use of specified commutating voltage, a test system consisting of typical components has been considered for the dynamic simulations. The standard HVdc convertor consists of 12-pulse units and the corresponding unit connected configuration shown in Figure 5.1 is used as the test system. The dc side of the convertor is connected to an invertor through a smoothing reactor and line impedance.

The potential applications of unit connection include both salient pole generators and as well as turbo-generators, and hence both type of machines are considered here to illustrate the inapplicability of conventional approach. The dc system data and machine parameters are given in Appendix E.

The objective of this study is to calculate the dc voltage and commutation angle of the unit connected system under steady state for various dc currents and firing angles by keeping the same generator field excitation. In order to achieve this, the rectifier was modelled with constant firing angle control and the invertor with constant current control. Various operating points were obtained by changing firing angle and current settings.

The dynamic simulation program TCS was run for a particular operating condition, i.e., for a specified dc current and firing angle. Once the simulation reached

the steady state, the dc voltage was calculated by averaging the dc voltage waveform over one cycle. The commutation angle is readily available from the valve switching times. From the values of V_{dc}, I_{dc}, α and u and using the equations 5.1 and 5.2, the commutating voltage and reactance are given by,

$$E_c = \frac{V_{dc}}{2} \frac{1}{\frac{3\sqrt{2}}{\pi}(cos\alpha - \frac{1}{2}(cos\alpha - cos(\alpha + u)))} \tag{5.7}$$

$$X_c = \frac{(cos\alpha - cos(\alpha + u))E_c}{\sqrt{2}I_{dc}} \tag{5.8}$$

The commutation reactance X_c includes both machine and transformer reactances.

5.5.1 Unit Connection with Rotor Symmetry

To illustrate the limitations of the steady state formulation and in particular the use of a specified commutating voltage, a range of operating points were analysed using TCS, for constant excitation. From the results, the commutating voltage E_c and the reactance X_c were calculated using equations 5.7 and 5.8. The results listed in Tables 5.1 and 5.2 for varying dc current and firing angle respectively show considerable variation in the commutation parameters. The commutation reactances shown in the tables are the machine contribution to the total commutation reactance.

For operating conditions close to the nominal, the values of E_c and X_c are accurate. This can be explained with reference to the current waveform shown in Figure 5.2, which consists mainly of commutation (or short circuit) regions and are thus accurately represented by conventional sub-transient theory. However, as the dc current reduces, the commutation intervals also diminish while the dc regions increase. Moreover, the error introduced by neglecting the dc current ripple increases at lower current levels because the ripple is mainly voltage dependant.

In a HVdc convertor system, during the non-commutation period, the terminal voltage would follow the commutating voltage and if the commutation voltage is E_c (ph-ph rms), then the peak value of convertor terminal voltage is $\frac{E_c\sqrt{2}}{\sqrt{3}}$. From Table 5.1, the commutating voltage is 1.325 pu and so the peak voltage should be 1.082 pu, which can be seen in Figure 5.3.

Table 5.1: Variation of commutation parameters of the non-salient rotor generator with dc current (α=0)

I_{dc} (p.u)	u (deg)	E_c (p.u)	X_c(p.u)
1.0	25.52	1.325	0.146
0.8	21.98	1.414	0.144
0.7	19.53	1.502	0.135
0.6	16.99	1.532	0.112
0.5	15.14	1.596	0.114
0.2	9.4	1.683	0.115

Table 5.2: Variation of commutation parameters for the non-salient rotor generator with firing angle (I_{dc}=1.0 pu)

$\alpha(deg)$	u (deg)	E_c (p.u)	X_c (p.u)
0	25.52	1.325	0.146
5	21.56	1.283	0.148
10	17.91	1.277	0.145
45	9.39	1.042	0.147

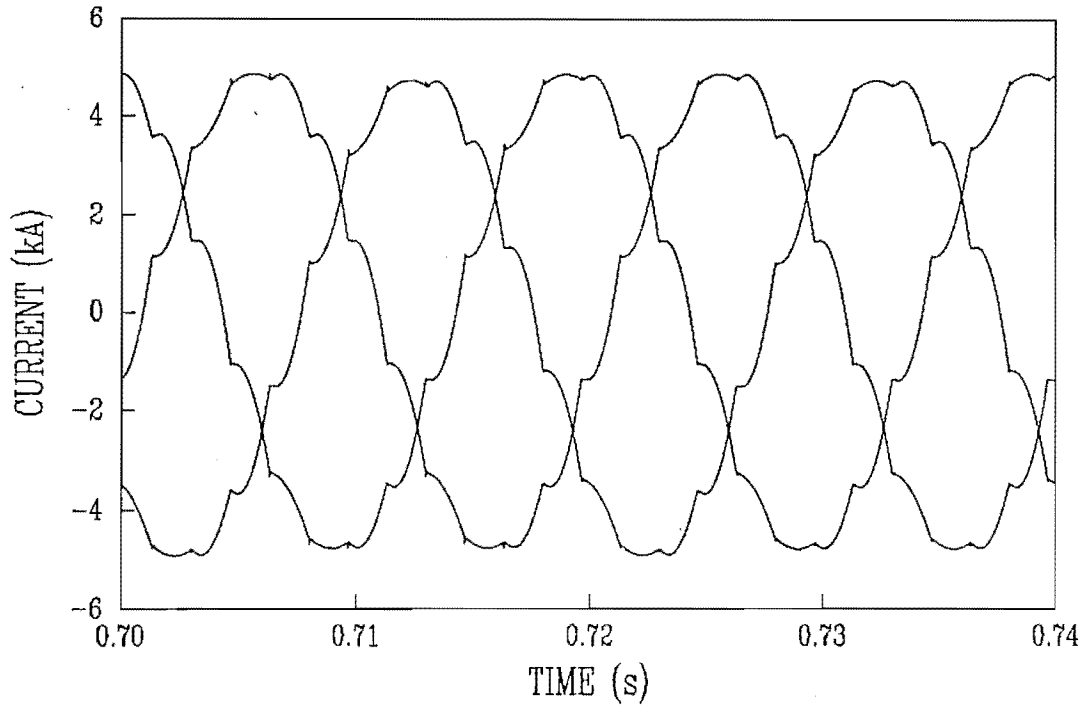

Figure 5.2: Generator currents derived from TCS for α=0 and I_{dc}=1.0 pu

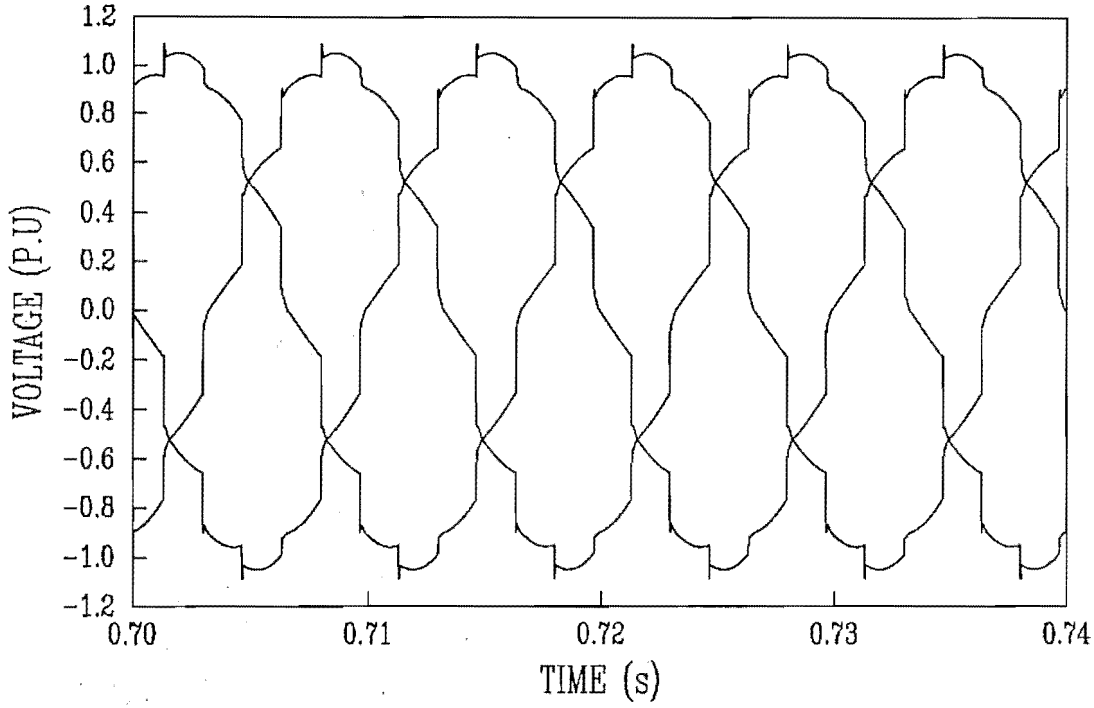

Figure 5.3: Generator terminal voltages derived from TCS for α=0 and I_{dc}=1.0 pu

5.5.2 Unit Connection with Rotor Saliency

In this type of machine, the rotor saliency causes the subtransient reactances to vary depending on the rotor position. For a unit connected salient generator-HVdc convertor, the rotor position and therefore the commutation reactance varies with the convertor firing angle. In order to demonstrate the rotor saliency effect and also the inapplicability of conventional steady state formulation, a range of dynamic simulation cases were run for varying levels of I_{dc} and α. The overlap angle (u) and the averaged dc voltage (V_{dc}) derived from the dynamic simulation were used in equations 5.7 and 5.8 to calculate the commutation voltage and reactance.

As in the case of a non-salient rotor, the steady state results are subject to increasing error as the dc current reduces. The saliency effect is clearly demonstrated in Table 5.3 for a constant (nominal) current and variable α. Table 5.3 shows the commutating voltage and the machine sub-transient reactance derived from the calculated commutation reactance. The machine contribution to the commutation reactance starts at 0.204 p.u for α=0, increases to a peak of 0.32 at α=65 degrees and then decreases to 0.25 when α=80 degrees. All these values are between the

Table 5.3: Variation of commutation parameters for the salient-rotor generator with firing angle (I_{dc}=1.0 pu)

$\alpha(deg)$	E_c (p.u)	X_c (p.u)
0	1.277	0.204
5	1.266	0.237
10	1.238	0.235
20	1.250	0.253
30	1.212	0.270
45	1.195	0.293
50	1.201	0.307
65	1.180	0.321
80	0.885	0.253

$X''_d(0.2)$ and $X''_q(0.367)$ machine sub-transient reactances. As the correspondence between convertor firing and machine rotor angle can not be pre-determined, the steady state formulation is impractical.

Moreover the commutating voltage of the unit connection (i.e. the machine internal emf) will contain unspecifiable levels of harmonic distortion, due to the frequency conversion process as explained in section 5.2. Consequently the conventional formulation of the commutation process and its incorporation with steady state equations is inapplicable to the unit connection.

5.6 Simplified Machine - HVdc Convertor Simulation

The generator-HVdc convertor units can be simulated in a simplified manner using approximate single phase, single frequency equations. In this method, the conventional dc system equations are combined with the well-known synchronous machine equations to form a set of non-linear equations. This set of non-linear equations is solved iteratively to get the operating point. With reference to the unit connection scheme depicted in Figure 5.1 and assuming a smooth dc current, the phasor diagram

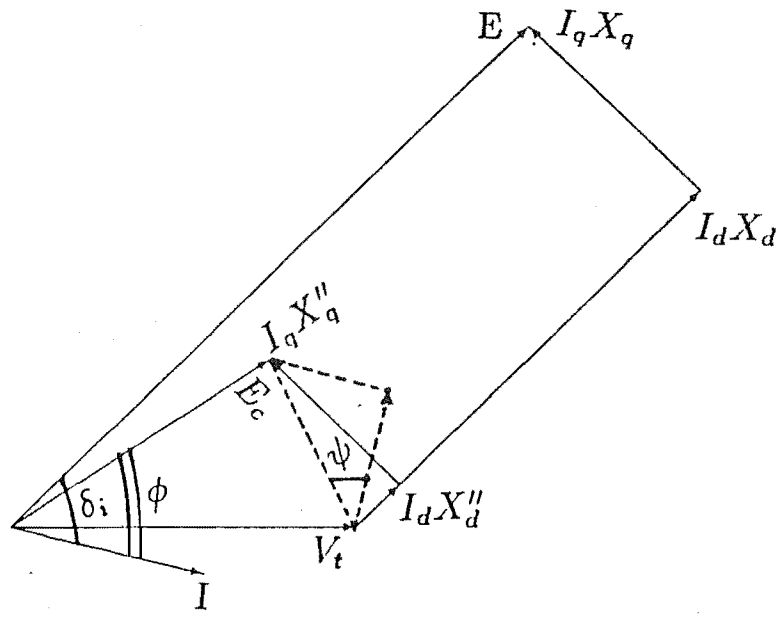

Figure 5.4: Phasor diagram of a salient pole machine

of Figure 5.4 interrelates the machine fundamental quantities.

It has been explained in the last section that a major difficulty in using the conventional dc system equations for unit connection is the varying nature of the machine contribution to the commutation reactance and whose value depends on the rotor position. In this model, the machine contribution of the commutation reactance is considered to be of two equivalent components X_i and X_r that produce voltages which are in-phase and quadrature to the ac current respectively. With respect to the phasor diagram shown in Figure 5.4, the following equations can be written:

$$\psi = tan^{-1}\frac{I_qX''_q}{I_dX''_d} - tan^{-1}\frac{I_q}{I_d} \tag{5.9}$$

Let,

$$\Delta V = (I_d^2X_d''^2 + I_q^2X_q''^2)^{\frac{1}{2}} \tag{5.10}$$

$$X_r = \frac{\Delta V sin\psi}{|I|} \tag{5.11}$$

$$X_i = \frac{\Delta V cos\psi}{|I|} \tag{5.12}$$

In the case of a perfectly non-salient machine,

$$X_r{=}0 \text{ and } X_i{=}X''_d$$

For a given unit connected system, if the nominal dc power, dc current and firing angle are specified, the following steps can be carried out until convergence to calculate the other quantities like commutation overlap angle, power factor, terminal voltage and field excitation requirement:

step-1 : Assume δ_i

step-2 : $|I| = \frac{\sqrt{6}}{\pi} I_{dc}$

$I_d = |I| \, sin\delta_i$

$I_q = |I| \, cos\delta_i$

step-3 : $\Delta V = (I_d^2 X_d''^2 + I_q^2 X_q''^2)^{\frac{1}{2}}$

$X_i = \frac{\Delta V cos\psi}{|I|}$

$X_r = \frac{\Delta V sin\psi}{|I|}$

step-4 : $E_c = \frac{V_{dc} + (\frac{3}{\pi} I_{dc}(X_i + X_t))}{\frac{3\sqrt{2}}{\pi} cos\alpha}$

$u = cos^{-1}(cos\alpha - \frac{\sqrt{2}(X_i + X_t)}{E_c} I_{dc}) - \alpha$

$cos\phi = \frac{1}{2}(cos\alpha + cos(\alpha + u))$

step-5 : update δ_i using

$\hat{E} = \hat{E}_c + j\hat{I}_d(X_d - X_d'') + j\hat{I}_q(X_q - X_q'')$

step-6 : Proceed to step-2 until convergence

If another operating point is to be determined for the same excitation, a similar procedure can be adopted by specifying any two of the following quantities: dc power, dc voltage, dc current and firing angle. The dc equations used in the above analysis are valid only when the commutation angle is less than 30 degrees.

When variable speed operation is considered, the internal emf has to be adjusted according to the following:

$$\frac{E}{E_n} = \frac{f}{f_n} K_f \tag{5.13}$$

where E_n is the emf corresponds to the nominal frequency, f_n is the nominal frequency

Table 5.4: Commutation angle in degrees from TCS and simplified models for non-salient machine

I_{dc} (p.u)	TCS	simplified model
1.0	25.52	25.35
0.8	21.98	21.20
0.7	19.53	19.33
0.6	16.99	17.51
0.5	15.14	15.70
0.2	9.40	9.57

and K_f is the factor due to induction. Typical values of K_f are 1.0 at 50.0 Hz and 1.1 at 34.0 Hz.

5.7 Comparison of Results

The simplified Generator-HVdc convertor simulation described in the previous section is based on the single-phase, single-frequency formulation. Also it does not represent the saliency adequately. In order to assess the validity of the simplified analysis, a comparison has been made with TCS results. For the same test system described in section 5.5, the commutation angle was calculated for various operating points using both TCS and the simplified simulation.

Table 5.4 shows the commutation angle calculated using both methods for the non-salient machine by keeping the same field excitation and firing angle. Table 5.5 shows the commutation angle for the same system at different firing angles. These tables show a difference of 3.5% for the commutation angles obtained from the simplified simulation as compared with the TCS results.

Table 5.6 shows the commutation angle calculated for the system using salient machine from TCS and the simplified simulation. It is seen that the commutation angles calculated from the simplified simulation for the salient case have a

Table 5.5: Commutation angle in degrees from TCS and simplified models for non-salient machine

$\alpha(deg)$	TCS	simplified model
0	25.52	25.35
5	21.56	20.96
10	17.91	17.66
45	9.39	9.43

Table 5.6: Commutation angle in degrees from TCS and simplified models for salient machine

$\alpha(deg)$	TCS	simplified model
5	26.10	28.34
10	22.60	24.60
20	17.70	19.20
30	15.15	15.73
45	12.70	12.66
50	12.33	11.99

maximum difference of 8.8% as compared with TCS. This is due to the fact that the simplified model does not represent the frequency conversion.

Moreover, the simplified analysis is based on the assumption that the dc current is perfectly smooth. Figure 5.5 shows the dc current obtained from TCS with the smoothing reactances of 0.4 H each at rectifier and invertor ends. Neglecting the dc ripple in the dc system formulation introduces additional error in the simplified analysis.

5.8 Conclusion

The limitations of the formulation based on the concepts of commutating voltage and commutating reactance when applied to unit connected generators-HVdc convertors have been demonstrated.

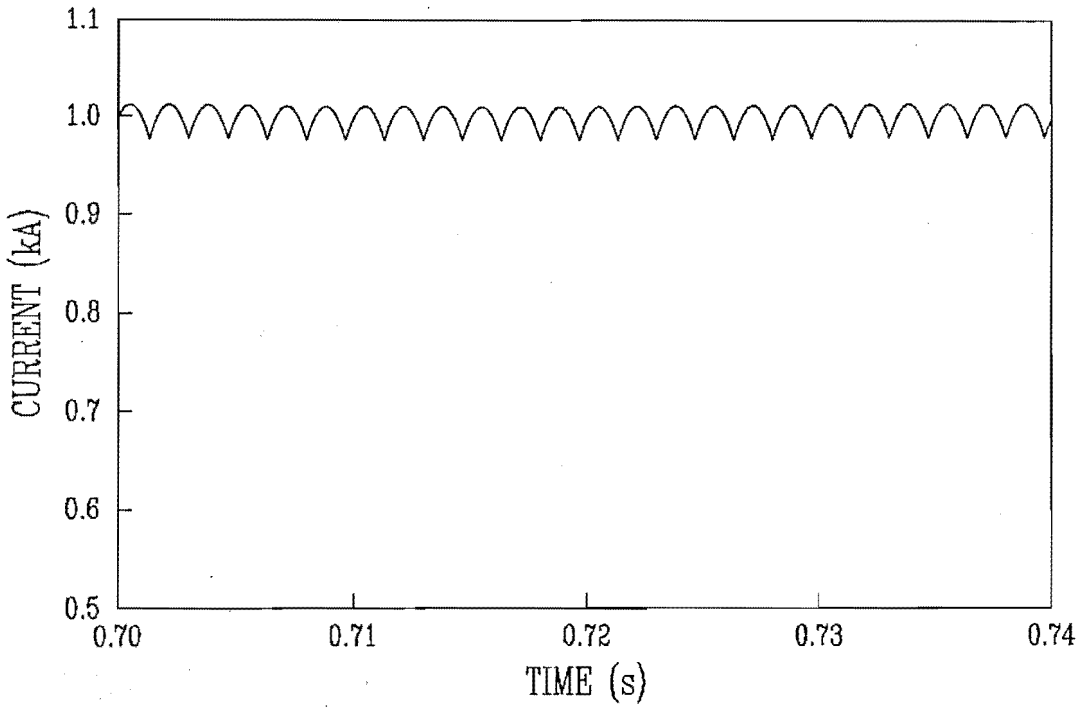

Figure 5.5: A typical dc current waveform derived from TCS

A simplified machine-HVdc convertor simulation is presented. Although this analysis is useful to initialise the time domain simulation, they have been shown to be inadequate by themselves in providing accurate information, particularly in the presence of generator rotor saliency.

Only dynamic simulation can provide the dc voltage/current regulation characteristic of the unit connection.

Chapter 6

OPERATIONAL CAPABILITY OF UNIT CONNECTIONS

6.1 Introduction

Existing information on the subject of unit connected generator-HVdc convertors emphasizes the reduced number and cost of components involved as compared with conventional configurations [Calverley 1973, Krishnayya 1987, Kanngiesser 1983]. Thus the main arguments currently used in favour of the unit connection are the absence of harmonic filters, generator transformer and convertor transformer tap changers. Other important properties making the unit connection a cost effective solution are its flexibility in the selection of generator frequency [Naidu 1989], the simplicity of generator controls and even the possibility of using diode instead of thyristor controlled rectification [Bowles 1989].

A critical factor so far ignored in the comparison between conventional and unit connected schemes is the maximum operational capability of the system rather than the rating capability of the individual plant components. Normally, dc systems are designed to permit certain continuous and temporary overloads. As an example, the New Zealand hybrid dc link is designed to operate with 25% continuous overload [Gleadow 1989]. The temporary over loading capability is necessary for transient stability purposes. When comparing the unit connection with the conventional scheme, this additional capability must be taken into consideration, or in other words the maximum capability of unit connection must be known.

Capability charts represent a method of graphically displaying power system performance. Normally, the capability charts are drawn on the complex power plane and define the real and reactive power that may be supplied from a busbar during steady state operation [Walker 1953]. The power available is depicted by a region on the plane, the boundaries of the region represent the critical operating limits of the system. In recent times, algorithms have been developed to draw capability charts to include HVdc convertors and dc links also [de Silva 1987].

For operational purposes the unit connected group can be considered as an HVdc generator that provides P_{dc} and V_{dc} at the convertor output. Hence, in this work the operational capability of unit connections are demonstrated with the help of V_{dc}-I_{dc}-P_{dc} characteristics rather than the conventional P-Q charts.

As demonstrated in the previous chapter, the unit connected HVdc schemes can not be analysed using single frequency steady state formulation. The dynamic simulation algorithms have already been used to establish the controllability of the unit connection during disturbances [Campos Barros 1977]. The same algorithms are used here to develop realistic capability charts.

Harmonic current and voltage ratings spectra for the region of operational capability of the unit connection are also derived in this chapter.

6.2 Control Philosophy and Test System

One of the major advantages of dc transmission is its controllability. In the conventional schemes, the active power (or current) is controlled by the rectifier and the ac terminal voltage at the sending end is kept to the nominal value by the generator excitation control. The invertor usually determines the direct voltage in such a way that the maximum permissible value is kept constant at the rectifier dc terminals independent of the load. The tap changers on the convertor transformers are adjusted to keep the firing angle, α , within a band in order to provide a sufficient control margin. Under such circumstances, the dc system capability is matched with ac system requirements during the steady state.

In the case of unit connection, the terminal ac voltage magnitude becomes

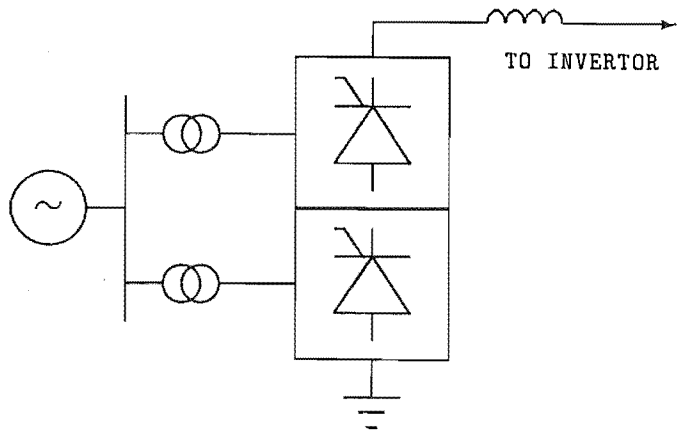

Figure 6.1: Twelve pulse unit connected generator-HVdc convertor

irrelevant due to the absence of local loads and also the fact that the dc voltage is influenced by the voltage behind the sub-transient reactance rather than the terminal voltage. So the conventional AVR action that maintains the terminal voltage constant becomes irrelevant. Instead, the generator excitation control could be used to take over the function of on-load tap changers to keep the firing angle, α , within the predetermined range [Kanngiesser 1989]. This control philosophy has been taken into consideration in deriving the operational capability of the unit connection.

The circuit of Figure 6.1 is used as a basis for the development of capability charts. That is a 12-pulse standard HVdc convertor group connected directly to the terminals of a single generator. The parameters used for the simulation can be found in Appendix E.

The critical operating factor of a unit connected generator-HVdc convertor unit will be to maintain the specified dc power (or current) under control at minimum delay angle to try and reduce generator losses in the rotor (by using minimum excitation) and the stator (by reducing the harmonic current). Hence the model assumes that the immediate control action following small changes or large disturbances will be taken care of by the convertor controller, whereas in the steady state the AVR will attempt to reduce the control angle to the minimum setting. The overall control of a unit connected scheme will thus be faster and continuous as compared with tap-changer control action and consequently the overall energy loss should reduce. The reduction of generator losses is more critical in the case of the unit connection as the generator rating must take into account the convertor harmonics.

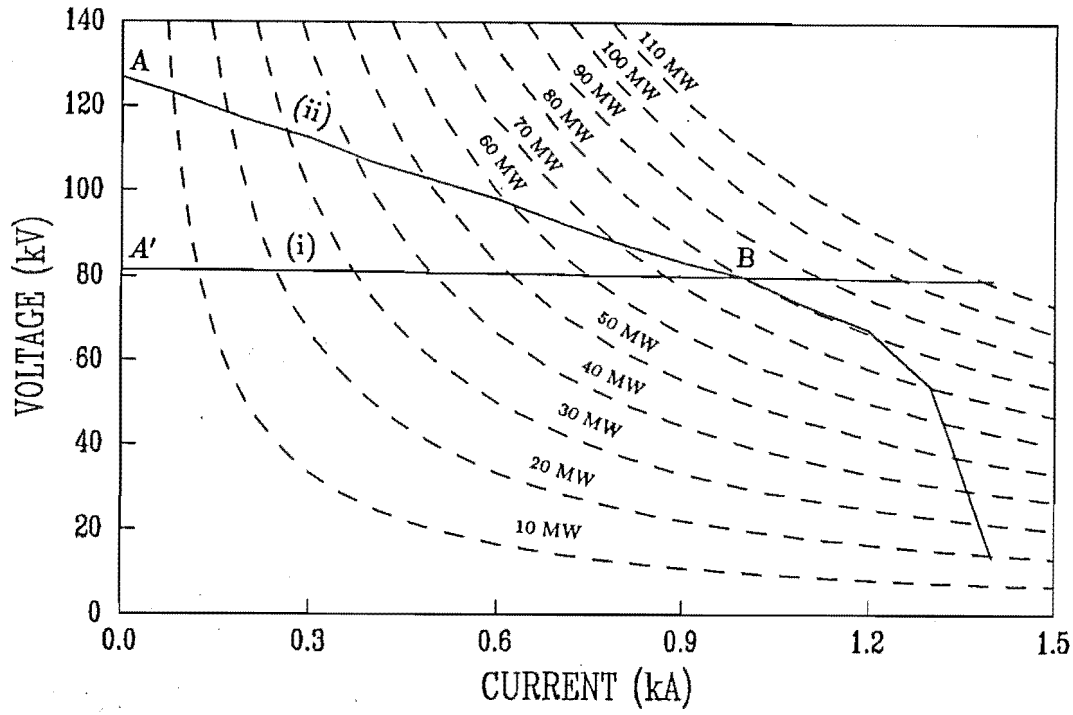

Figure 6.2: Operational capability charts with α_{min} (i) Conventional (ii) Unit connection

6.3 Capability Charts

In many cases the unit connection application will relate to hydroelectric schemes and hence a salient pole generator is considered here to derive the capability charts. Also to try and keep the commutation reactance within reasonable limits, the transformer leakage reactance has been reduced to a low but realizable 5% level.

The absence of simple equations capable of establishing general relationships in terms of commutating voltage and commutation reactance makes it impossible to provide charts of general applicability. Each individual scheme needs to be modelled to derive operating capability charts.

The average dc voltages for each value of α and I_{dc} are derived from the TCS results as described in Chapter 4. Figure 6.2 displays the voltage regulation characteristic for the unit connected test system. The convertor open circuit voltage is fixed by the maximum level of excitation (point A).

In order to compare the operating capability of the unit connection with that of a conventional scheme, it is necessary to start by assuming that both have been designed to provide a nominal operating point (say point B in Figure 6.2) that

Table 6.1: Relationship between dc current setting and power levels

D.C. Current (p.u)	Unit connection (MW)	Conventional (MW)
0.8	70.46	64.45
0.9	75.36	72.29
1.0	80.00	80.00
1.1	80.65	87.96
1.2	81.15	95.76
1.3	70.25	103.51
1.4	18.96	111.22

provides a specified power of 80 MW with a current of 1 kA. To obtain this operating point with a conventional scheme and a commutation reactance equal to the transformer leakage, the regulation characteristic is a straight line (i). Thus the no-load voltage required (point A') is substantially reduced with respect to the corresponding level of the unit connection.

In Figure 6.2 the unit connection characteristic (graph (ii)) has been obtained with minimum delay angle (i.e α_{min}) and therefore indicates the capability boundary. The Figure 6.2 also shows constant power characteristics (in dotted lines).

The power setting curve which is tangent to the capability chart that determines the maximum operating power possible. For the unit connection of the test system, the limit is 80 MW. In contrast, the conventional configuration permits considerably higher power settings, subject to increasing current overloading margins.

A few discrete points derived from the graph are compared in Table 6.1, which show that there is a dramatic loss of temporary overload capability in the case of the unit connected scheme. The main reason for the power collapse at higher ratings is the large nominal commutation overlap (close to 30 degrees) which even for a small increment in current causes simultaneous commutations on both bridges.

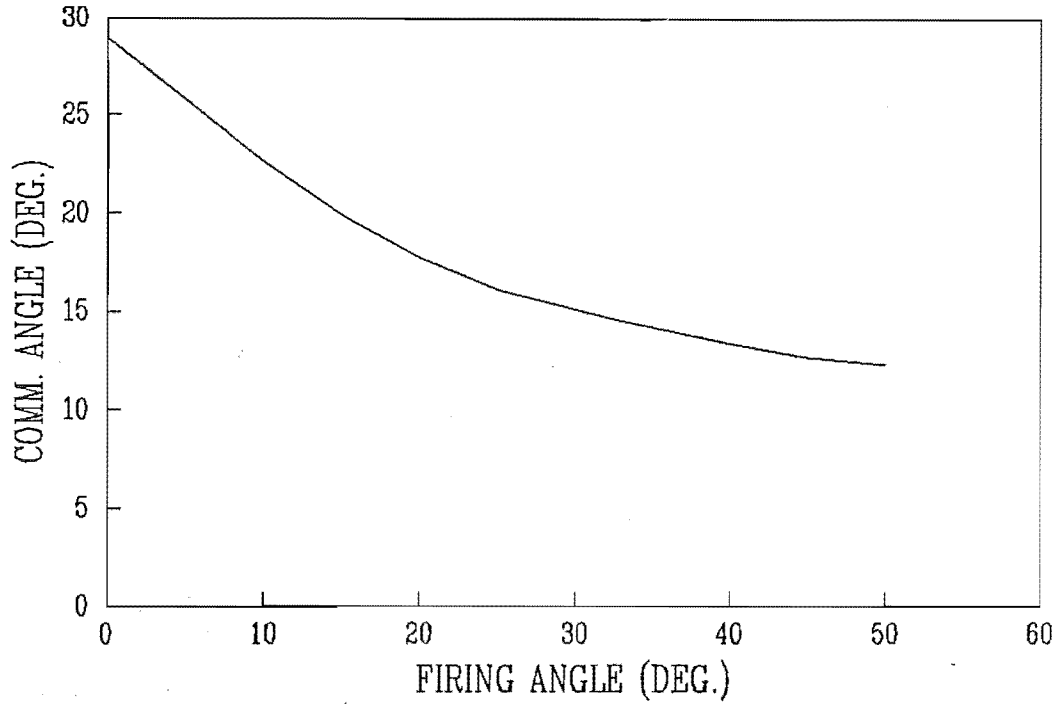

Figure 6.3: Variation of commutation angle obtained from TCS

6.4 Designing with Higher Nominal Firing Angle

In the previous section, the maximum operating capability of unit connected scheme was discussed with reference to the minimum firing angle and the maximum excitation. While the unit connection can be designed to provide a specified nominal power, the absence of filters limits the operational capability at larger current levels and thus reduces the ability of HVdc link to provide temporary power increases. This reduction in operational capability imposes transient stability restrictions. One way of increasing the transient stability margin is to design the unit connected system with a slightly higher nominal firing angle.

Figure 6.3 shows the variation of commutation angle for various firing angles with the constant field excitation, obtained from TCS. It can be seen from the figure that the commutation angle reduces from 28.9 degrees at α=α_{min} (zero degrees for the test system) to 17.7 degrees at α=20 degrees. Hence if the nominal firing angle is chosen as 20 degrees, that would permit relatively higher current levels before the commutation angle reaches 30 degrees.

Choosing a higher firing angle reduces the dc voltage and hence the trans-

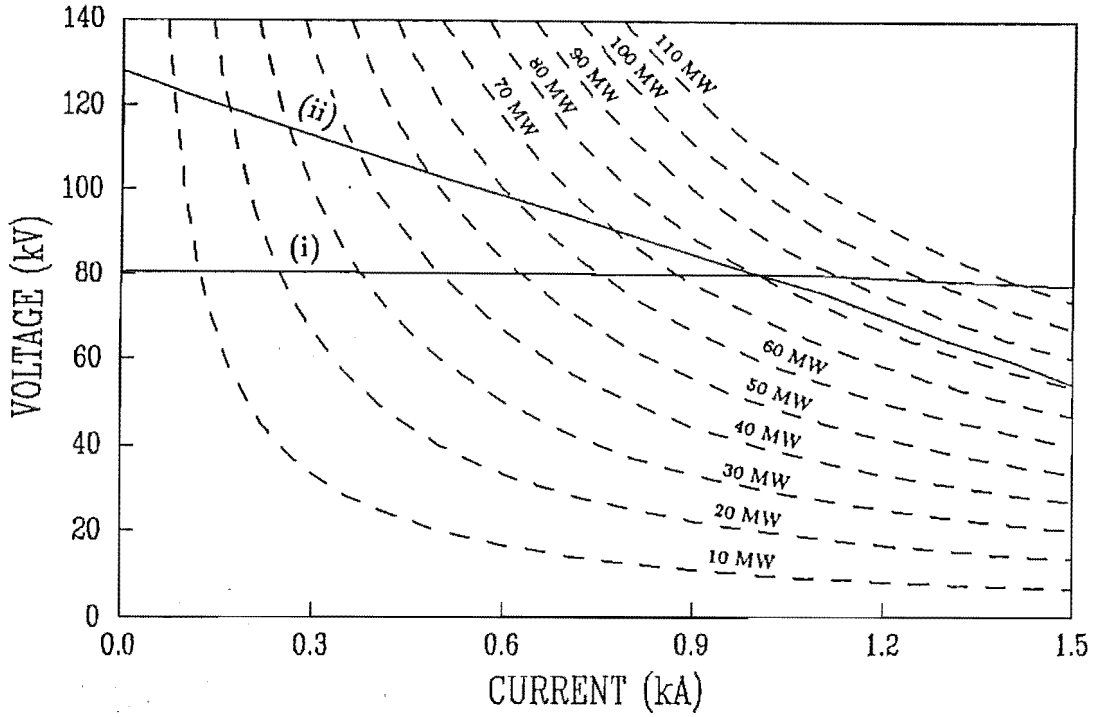

Figure 6.4: Operational capability charts with α_{nom}=20 deg. (i) Conventional (ii) Unit connection

mission efficiency. For the unit connected test system, it was found that in order to have the same dc voltage and dc current as in the previous case (i.e point B of Figure 6.2) for a firing angle of 20 degrees, the increase in required field excitation is 8.7%.

Figure 6.4 shows the voltage regulation characteristic for the unit connected test system with a nominal firing angle of 20 degrees. Unlike in the α_{min}-case, the commutation angle is less than 30 degrees for a current level upto 1.5 p.u. But the amount of extra power that can be obtained is increased by only 6.25%.

Operating the unit connected system at a higher firing angle results in more control margin for the rectifier control from the minimum firing angle. Normally the minimum firing angle for rectifier is about 5 degrees. Figure 6.5 shows the voltage regulation characteristics for α=20 degrees and α=5 degrees. It is seen from the figure that by having a firing angle margin of 15 degrees, the power transfer capability has increased by 26.0%. But the higher firing angle would also produce higher current harmonics and hence more rotor losses. For the test system, the total current harmonics increased from 3.55% for α_{nom}=0 degree to 6.93% for α_{nom}=20 degrees.

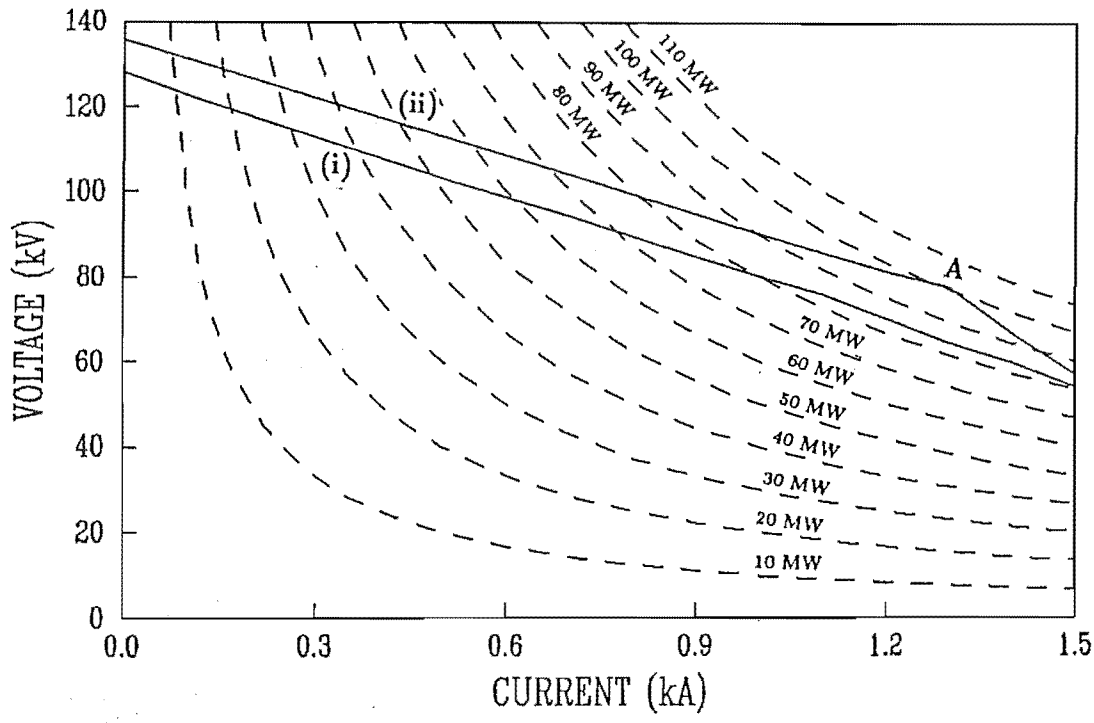

Figure 6.5: Operational capability charts with control margin (i) α_{nom}=20 deg. (ii) α_{min}=5 deg.

6.5 Effect of Field Forcing

In the previous section it was seen that the operating capability could be increased by having some firing angle margin. Referring to the Figure 6.5, the capability of unit connected test system is increased by 26% (point A) when rectifier firing angle is decreased to 5 degrees from the nominal value of 20 degrees, which can be utilised to supply extra power. But, when the system is operated with a low firing angle, the rectifier loses its control margin. Also, at the maximum power (point A in Figure 6.5), the dc voltage is reduced by 4%, which would reduce the transmission efficiency also.

As discussed in section 6.2, the generator excitation control for unit connections could be used to take over the function of On Load Tap Changers to keep the firing angle within the pre-determined range. This excitation control was modelled in TCS to calculate the additional amount of excitation required to keep the dc voltage at 1.0 p.u. Table 6.2 shows the extra excitation requirement to maintain a nominal

Table 6.2: Extra Excitation requirement to increase the capability

D.C. Power (p.u)	Extra Excitation (%)
1.1	3.051
1.2	7.759
1.3	11.511
1.4	19.415

firing angle of 20 degrees.

When the excitation requirement becomes high, extra materials are required to keep temperatures down. Also, when the excitation levels increase, the air-gap flux density tends to increase, resulting in air-gap instability.

6.6 Current Harmonics

In the conventional scheme, the current rating of the generator is practically determined by the fundamental frequency component, as the filters will absorb the steady state harmonic current components. On the other hand, since filter circuits are omitted in the unit connections, the current harmonics generated by the rectifier have to be absorbed by the generator. Their major effect upon the generator is an extra heating of the rotor surface and the damper winding due to the induced harmonic currents in the rotor circuit.

In order to compute the amount of harmonic currents generated by the convertors, a time domain simulation was carried out, from which under steady state condition the current waveform entering the generator was analyzed into fundamental and harmonic currents. This harmonic analysis was performed by varying the firing angle and keeping the same generator excitation.

Figure 6.6 shows the levels of 11^{th} and 13^{th} harmonic currents. For comparison with the conventional scheme, the harmonics were also calculated using the classical analysis with the transformer reactance as the commutation reactance and the convertor terminal ac voltage as the commutating voltage [Kimbark 1971]. The dotted lines in Figure 6.6 show the harmonic current levels for the conventional scheme.

Two different effects are observed. First a considerable reduction in the

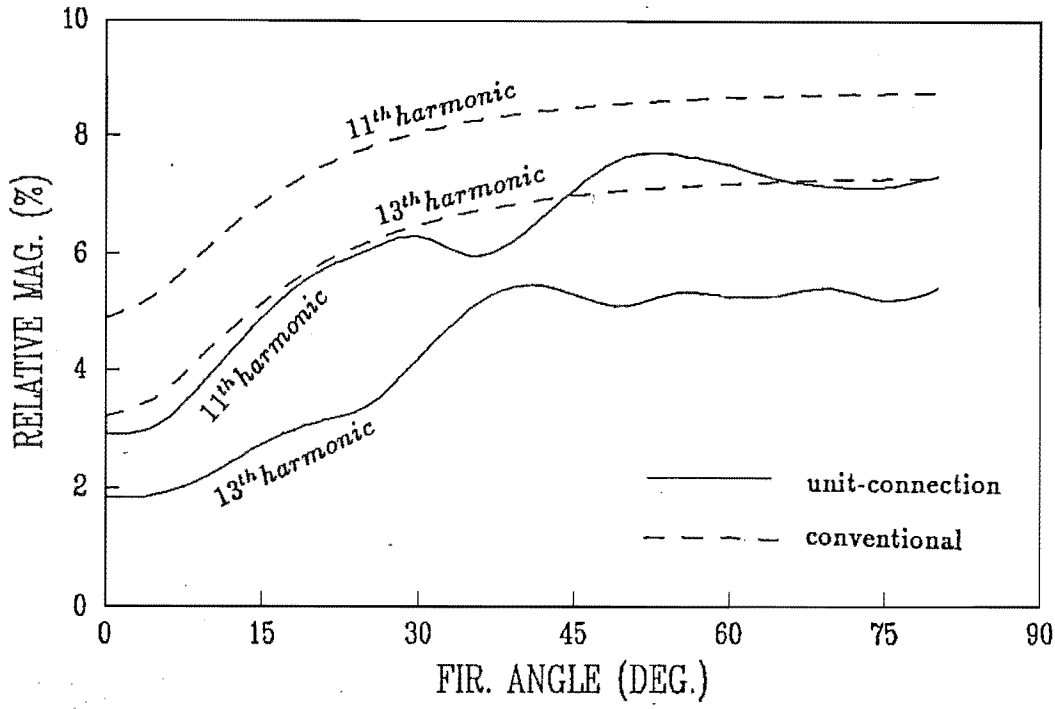

Figure 6.6: Current harmonic content of the 12-pulse convertor

current harmonic levels of the unit connection, which is due to the better shape caused by the increased commutation overlap. The second effect is the oscillatory nature of the harmonic currents with α, in the case of unit connection. This effect is caused by the variation of commutation parameters as explained in chapter 5.

6.7 Generator Rating

The calculation of generator rating for the unit connection should include the total rms current rather than the fundamental frequency component alone. This is to ensure that the extra harmonic loading of the machine does not result in extra temperature rise for the machine as a whole and specifically in the hot spots of the machine. The equivalent continuous negative sequence current is often used as the indicator to find out whether the generator can withstand the extra heating, without any derating.

Normally the generators are provided with a thermal cushion to sustain an equivalent of 10% negative sequence current loading [IEEE 1973]. The negative sequence current loading is a rough indicator of the permissible extra losses due to unbalanced operation. The diode-rectifier as well as the controlled rectifier with

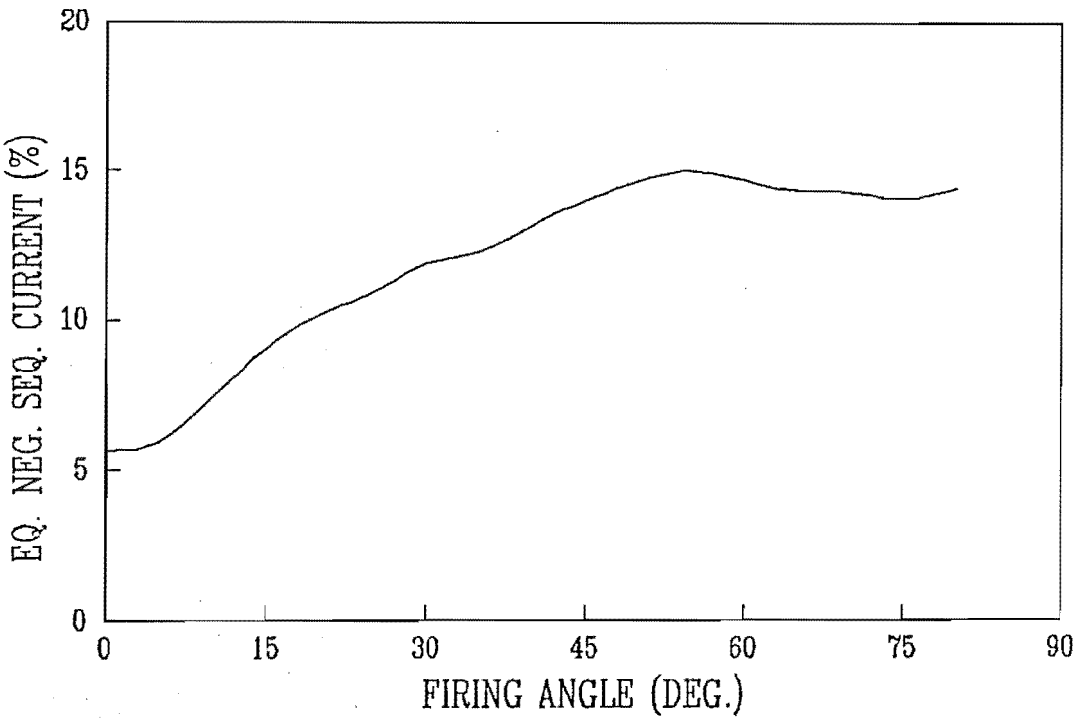

Figure 6.7: Equivalent Negative Sequence current derived from TCS

equidistant pulse firing devices represent an almost ideal symmetrical load. The remaining unsymmetries are due to differences in transformer or generator phase reactances as well as in differences in the firing angles. It has been shown [Reeve 1969] that these effects are negligible in terms of negative sequence load. Hence it is possible to utilise the generator's extra margin for the additional harmonic losses.

To facilitate comparison of the rotor heating effect of the convertor loads with standard specification ratings of generators, an equivalent continuous negative sequence current I_{en} is defined as that which causes equal rotor heating as the convertor load it specifies. The equivalent negative sequence current of the generator due to harmonic currents is given by [Krishnayya 1973]:

$$I_{en} = \sqrt{(\sum \sqrt{h}(I_{h-1}^2 + I_{h+1}^2))/\sqrt{2}} \tag{6.1}$$

The variation of equivalent negative sequence current with varying delay angle for the unit connected test system is shown in Figure 6.7. The results show that for a 12-pulse convertor, the total harmonic losses represent less than 16% of the losses caused by the permissible continuous negative sequence load. At the normal firing angle range (in the vicinity of 15 degrees), the harmonic losses represent less than 10% for the unit connected test system.

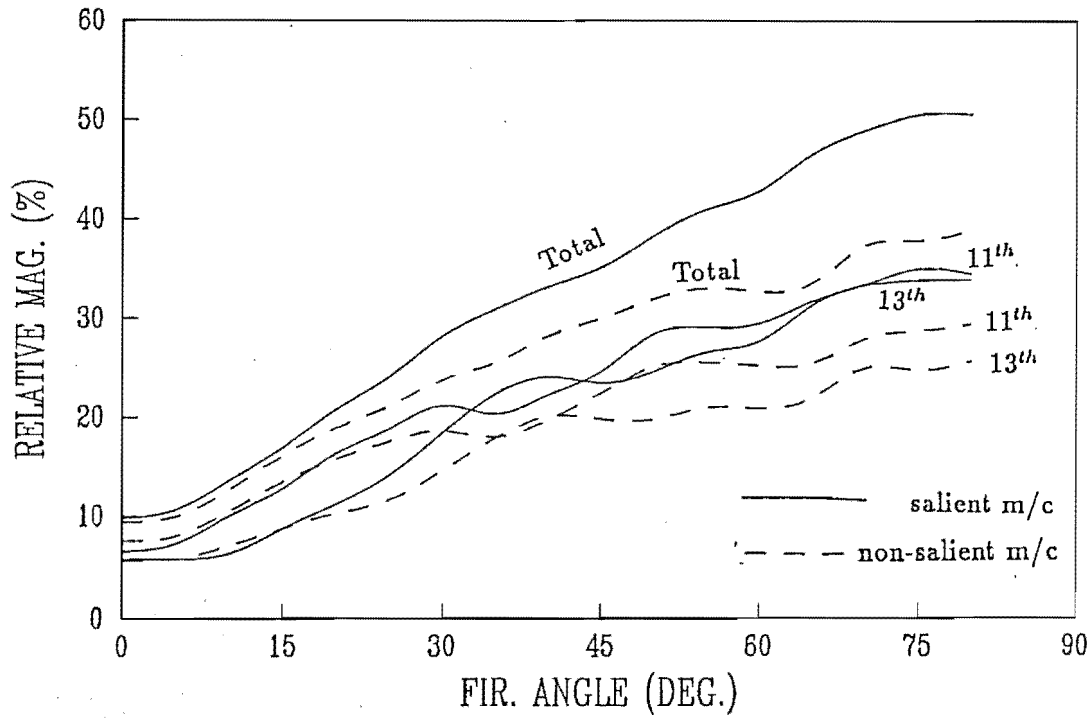

Figure 6.8: Effect of rotor saliency on voltage harmonic distortion

6.8 AC Voltage Harmonics

In the absence of filters, ac voltage waveform would be considerably distorted. Moreover, the synchronous machine acts like a frequency convertor in the presence of harmonic currents and creates additional voltage harmonics.

In unit connected HVdc systems, ac voltage harmonics are important in assessing the quality of ac voltage waveforms and the insulation strength of stator windings. The operation of convertor firing controllers are dependent on the quality of ac voltage waveform. The voltage distortion at the generator terminal of an unit connection can be assessed by using either a time domain simulation program like TCS or the iterative analysis in harmonic domain [Eggleston 1985].

In order to assess the amount of voltage distortion at the generator terminal of the unit connected test system (including a salient machine), the dynamic simulation program TCS was carried out for various firing angles with constant generator excitation. Under steady state conditions, the terminal ac voltage at the generator was analysed into fundamental and harmonic components. The continuous lines in Figure 6.8 show the voltage harmonic levels with respect to firing angles.

In order to show the effect of rotor saliency on voltage harmonic distor-

tion, the voltage harmonics were also calculated by injecting the calculated harmonic currents into a non-salient model, i.e.,

$$V_n = hI_hX'' \tag{6.2}$$

where n is the harmonic order and

$$X'' = \frac{X''_d + X''_q}{2}$$

The dotted lines in Figure 6.8 show the voltage harmonic levels calculated without rotor saliency. Comparing the continuous and dotted lines shows that the distorted emf due to rotor saliency increases the levels of terminal voltage distortion with respect to those to be expected purely from the injection of the convertor harmonic currents. It can also be seen in Figure 6.8 that the effect of saliency is greater at higher firing angles for which the current harmonics are higher.

6.9 DC Harmonics

Even though the unit connected dc schemes do not have ac harmonic filters, dc harmonic filters may have to be provided in order to avoid communication interference due to voltage harmonics present on the dc line [Arrillaga 1985].

At present the dc harmonics of conventional schemes are analysed by a 'three pulse model' [Shore 1989, Dickmander 1989]. This technique takes into account the stray convertor capacitances and various non-ideal convertor parameters such as transformer reactance variations, turns ratio variations, variations in the firing instants and ac system unbalances. However the 'three pulse' model uses classical analysis, in which the commutation voltage and reactance are specified. On the other hand, in the case of unit connection, particularly with salient machine, the commutating voltage and reactance are not known explicitly. So the dc voltage harmonics at the convertor terminal have to be analysed with the help of dynamic simulation rather than the classical analysis.

Figure 6.9 shows the relative magnitudes of 12^{th} and 24^{th} harmonics of the unit connected test system with varying firing angles at the convertor terminals before the smoothing reactor. For comparison, the dc voltage harmonics were also calculated using classical analysis [Kimbark 1971] with the transformer reactance and the

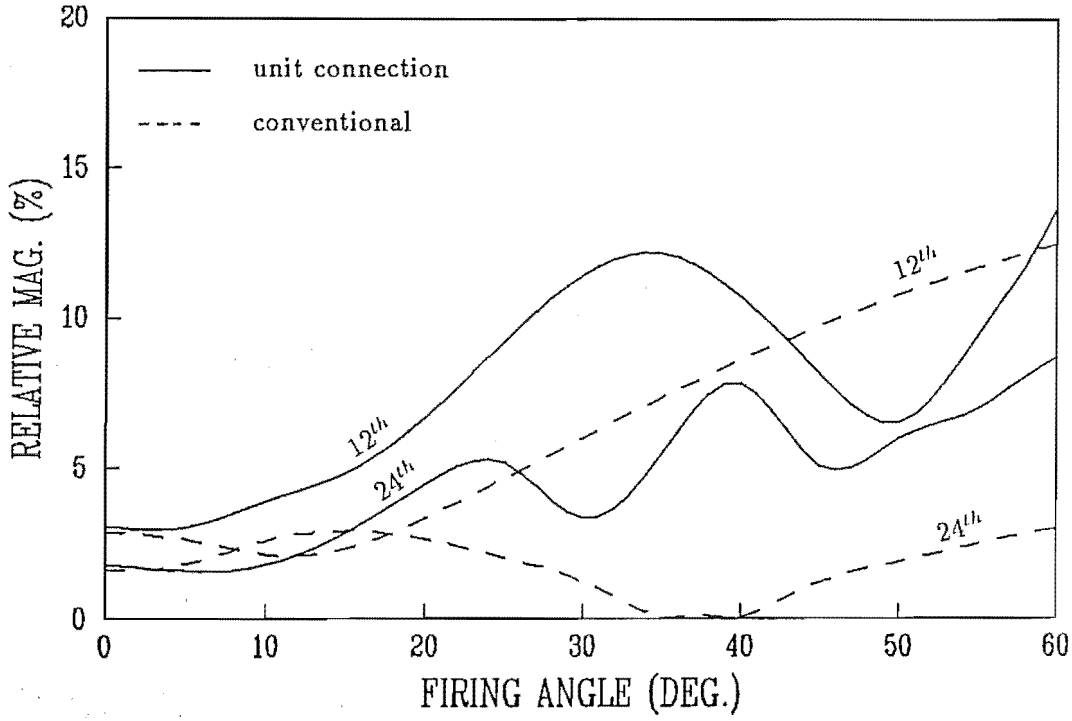

Figure 6.9: DC voltage harmonics derived from TCS

terminal voltage as the commutation reactance and voltage respectively. These are shown in dotted line. Figure 6.9 shows that the relative magnitudes of dc voltage harmonics are higher than those of the conventional scheme.

6.10 Conclusion

The absence of simple equations capable of establishing general relationships in terms of commutating voltage and commutating reactance makes it impossible to provide charts of general applicability. Each individual scheme needs to be modelled to derive operating capability charts and also to determine the harmonic ratings.

While the unit connection can be designed to provide any specified nominal power, the absence of filters limits the operational capability at larger current levels and thus reduces the ability of the HVdc link to provide temporary power increases. This reduction in operational capability imposes transient stability restrictions that must be taken into account in economic comparisons and its conventional alternative.

It is possible to increase the operational capability of unit connections by providing control margin and also by field forcing during the overload condition. But this alternatives would result in extra cost.

Harmonic spectra has been derived for a typical test case with the aid of dynamic simulation. The results show as expected, a reduction in harmonic current levels caused by the increased commutation overlaps. However the generator harmonic voltages in the presence of rotor saliency are considerably higher. The dc voltage harmonics show higher values than in the conventional scheme.

Chapter 7

CHARACTERISTICS OF VARIABLE SPEED OPERATION OF UNIT CONNECTIONS

7.1 Introduction

The synchronous nature of a conventional power system requires the generation of a common frequency at all the interconnecting power stations. Apart from the need for a complex frequency control, the common frequency restriction prevents the individual generating units from operating at their optimal efficiencies.

In the absence of local load, the unit connection concept can be extended to generate power at varying frequencies to suit the optimal operation of the turbines. Examples of possible application for such schemes are remote hydro stations, wind farms and tidal power stations.

The existing information available on the variable speed operation of unit connections have only highlighted the economic advantages [Ingram 1988, Naidu 1989]. Very little is known about their operating characteristics.

The main characteristics of constant frequency unit connected schemes were discussed in the previous chapter. In this chapter, the main factors affecting the operating characteristics of a 12-pulse unit connected generator-convertor system to

match the optimal power-frequency characteristics of hydro electric turbine are examined using TCS.

7.2 Variable Speed Operation of Hydraulic Turbines

Normally hydraulic turbines are designed in such a manner that at nominal water head and at rated power or near it, the operating speed which remains fixed thereafter, is chosen to ensure the highest operating efficiency. The exact value of the operating speed is fixed taking into account the number of poles provided on the generator and the required frequency and is given by:

$$N = \frac{120f}{p} \tag{7.1}$$

where,

N - speed in rpm

f - frequency in Hz

p - number of poles in the generator

Under actual conditions, deviations from nominal conditions occur, e.g., due to seasonal variations the water head may change. Such variations result in the loss of turbine operating efficiency. In the conventional schemes, this reduced efficiency has to be accepted since the turbines have to operate at a fixed speed.

In the case of unit connections, the variable frequency and hence the variable speed operation of hydraulic turbines can be accepted as long as an alternative source for station auxiliaries is arranged. This property can be utilised to operate the turbines at optimal efficiency.

The optimal power of a turbine changes strongly with the water head and there is one optimal speed pertaining to each optimal power [Jaquet 1986]. Hence, there is only one power value for a given water head at which the optimal turbine efficiency is achieved and this only if the optimum speed for this operating point is maintained.

Improvements in turbine efficiency amounts to pondage of water. This water can be used to generate extra energy and hence higher revenue. It has been estimated using Manitoba Hydro's data for the 10 x 100 MW Longspruce generating station that

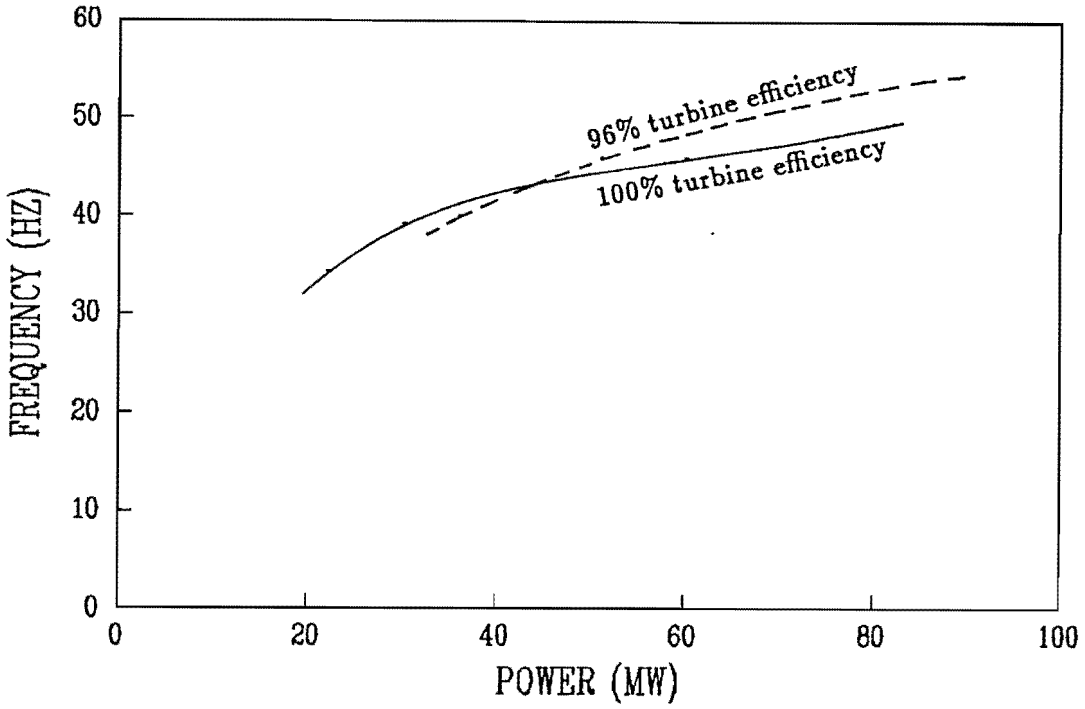

Figure 7.1: Power-frequency characteristics of the turbine

the annual savings due to variable speed operation would be of the order of US$1.24M [Naidu 1989].

7.3 Test System

Some information has recently become available on the efficiency of hydro turbines operating at varying speeds [Jaquet 1986, Vogele 1986]. In the Pan Jia Kou scheme, China, consideration has been given to variable speed operation because of the large differences in water head expected (between 36 and 86 metres). Figure 7.1 shows a range of power-frequency characteristics relating to this scheme for an acceptable range of turbine efficiencies. Table 7.1 shows the discrete values of power and frequency values for 100% and 96% efficiencies.

The generator, transformer and convertor plant will have to be rated for the power generated at the maximum frequency.

In the absence of detailed information of the Pan Jia Kou generator characteristics, the data selected has been taken from a typical hydro machine of similar

Table 7.1: Turbine Power/Speed Characteristics

100% turbine efficiency		96% turbine efficiency	
Power (MW)	Frequency (Hz)	Power (MW)	Frequency (Hz)
82	49.6	85	54.0
60	46.0	51	46.0
36	40.0	30	39.2
22	34.4		

power rating and is given in Appendix E. Also to try and keep the commutation reactance within reasonable limits, the transformer leakage reactance has been reduced to a low but realizable 5% value.

The dc system considered is a back-to-back system in which the rectifier is at constant firing angle and the invertor controls the power. The rectifier firing angle is chosen as zero degrees. The controllers were modelled in TCS using modular controller models described in chapter 2 and typical d.c voltage and current waveforms derived with the TCS algorithm are shown in Figure 7.2.

All the waveforms are processed by the Fast Fourier Transform to obtain information of V_{dc} and I_{dc} (averaged), as well as the harmonic content of the voltage and currents on both sides of the convertor. To reduce sampling errors at points of discontinuity, a high number of samples is recommended for the FFT processing (1024 samples per cycle are used in the present work). But, the variable frequency introduces small errors in the FFT processing due to spectral leakage [Arrillaga 1985] caused by the presence of non-harmonic frequency modulation between the two terminals.

7.4 Operating Characteristics

It is a general requirement in ac systems as well as in dc systems that a generator maintains an almost constant voltage over the full power range. However the generator no-load voltage should vary when operated over a wide range of speed

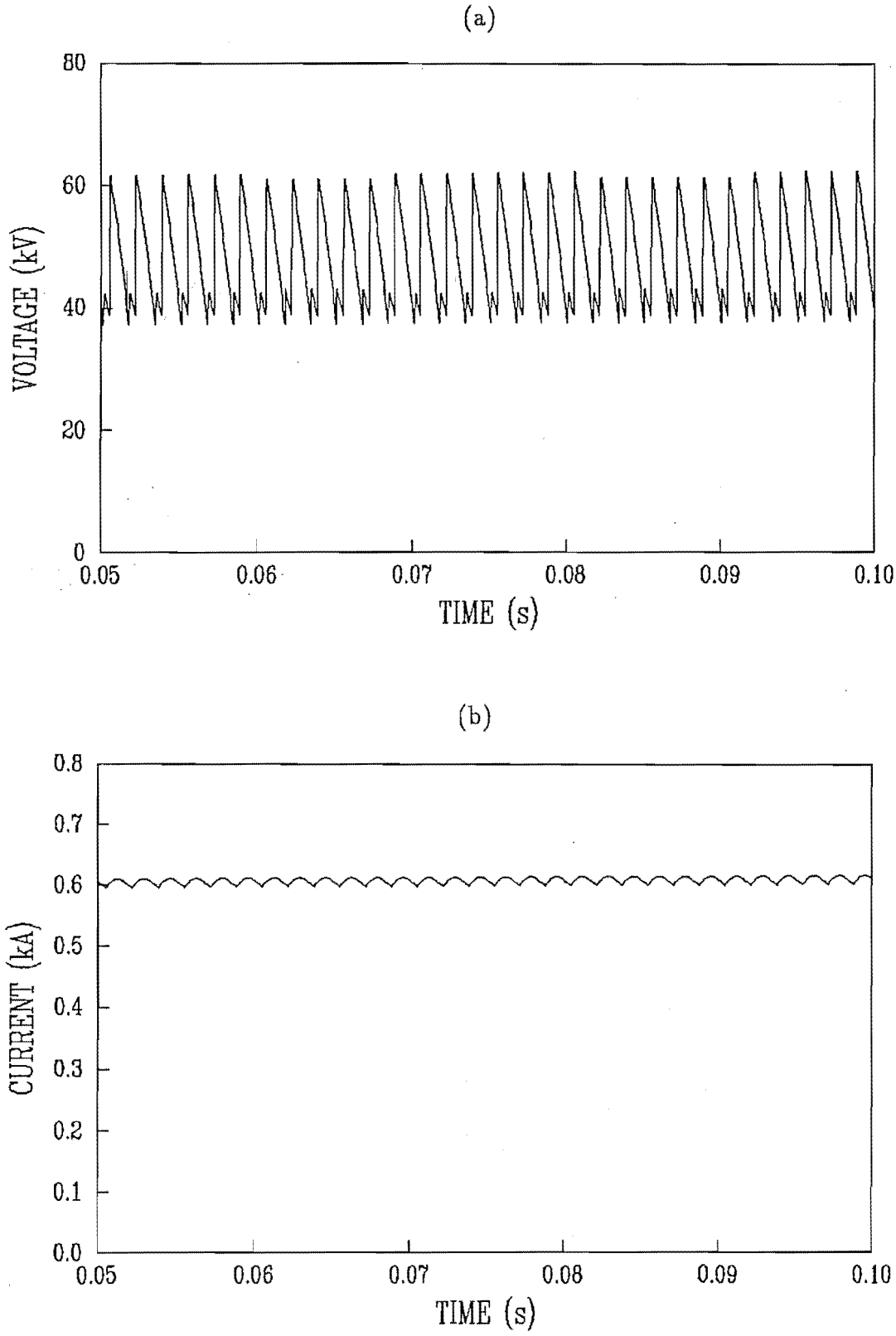

Figure 7.2: DC side waveforms derived from TCS (a) voltage (b) current

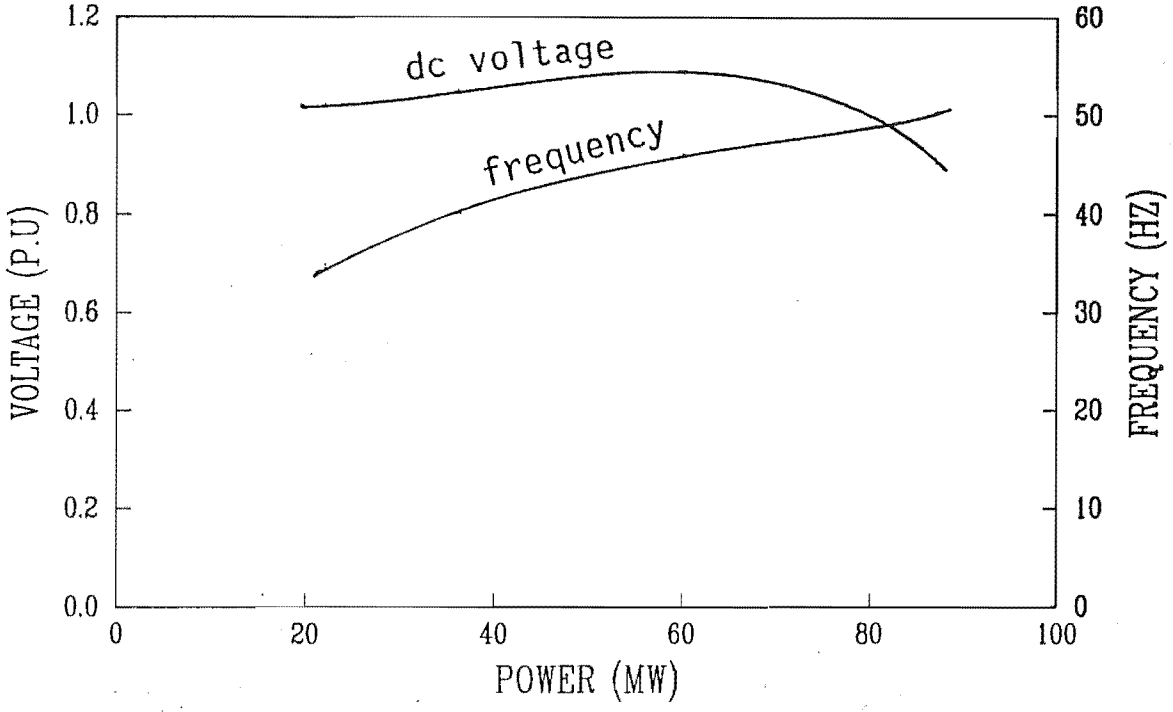

Figure 7.3: Variable frequency operating characteristic at 100% turbine efficiency

according to:

$$\frac{E}{E_n} = \frac{f}{f_n} K_f \tag{7.2}$$

where E is the generator no-load voltage, f is the frequency and the subscript n represents the nominal value. The factor K_f due to induction is frequency dependent and increases from 1 to 1.1 p.u when the frequency drops from 50 to 34 Hz.

In order to assess the voltage regulation during the variable speed operation of unit connections, the dynamic simulations were carried out for 100% and 96% efficiency cases shown in Figure 7.1. The results of the simulation are illustrated in Figures 7.3 and 7.4.

Figure 7.3 shows some important results for the case of 100% efficiency. As the frequency is reduced from 50 Hz, the d.c voltage increases from 1 p.u to a maximum of 1.085 p.u (corresponding to a frequency of 46 Hz). However the voltage increase (8.5%) can be compensated by firing angle or excitation control. Further reductions in frequency appear to have very little effect on the d.c voltage down to the minimum 34.4 Hz specified for maximum efficiencies.

For the reduced efficiency case (96%), Figure 7.4 shows a larger d.c voltage regulation (from 0.99 to 1.09 p.u), that is a 9% overvoltage, which again can be maintained constant by firing angle or excitation control. The larger firing angle will

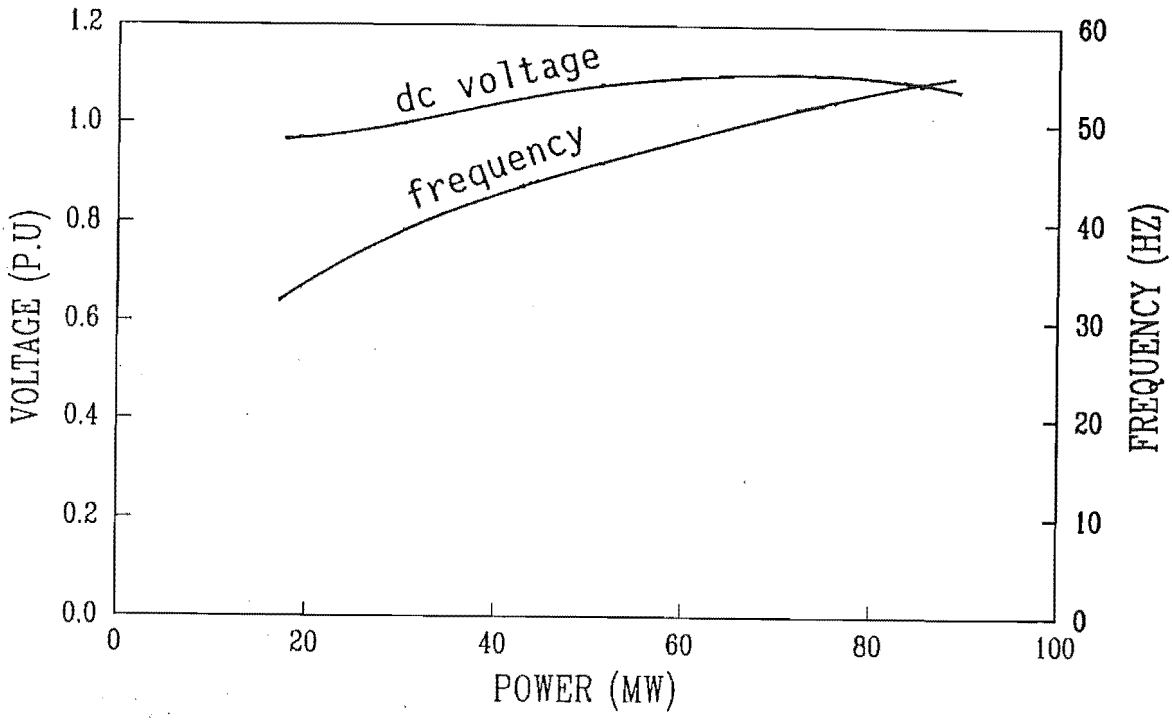

Figure 7.4: Variable frequency operating characteristic at 96% turbine efficiency

Table 7.2: Effect of firing angle control on generator

f (Hz)	P_{dc} (MW)	α (deg.)	V_d/V_{dn}	V_g/V_{gn}	I_g (kA)
54	85	0	1.086	1.066	3.409
54	85	11	1.0	1.005	3.616
50	80	0	1.0	1.0	3.434
39.2	30	0	0.997	0.9738	1.325

increase the reactive power absorbed by the convertor, which will in turn reduce the generator terminal voltage to the required level.

For the test system under consideration, the maximum firing angle variation required to keep the d.c voltage constant (between 39.2 and 54 Hz) is 11 degrees and the maximum generator terminal voltage in that region is 1.005 p.u. The effect of increased firing angle control on the generator voltage (fundamental rms) and current (total rms) rating is illustrated in Table 7.2. The generator current has increased by 6% but the generator terminal voltage remains almost constant.

7.5 Evaluation of the Need for an OLTC

For a unit connection operating under constant speed, On Load Tap Changers (OLTC) are not required at the rectifier transformer. Generator excitation control can take over the task of OLTC, as illustrated in the previous chapter. This further reduces the capital cost and improves the reliability. However, since the generator emf varies due to a wide variation of turbine speed, the need for OLTC have to be evaluated for unit connections during the variable speed operation.

Figures 7.3 and 7.4 show different dc voltage responses to the variable frequency unit connection systems at 100% and 96% efficiencies.

With reference to Figure 7.3 (100% turbine efficiency operation), an increase of frequency from 49.6 to 51 Hz would extend the operating region from 80 to 85 MW. However the machine internal emf only increases by about 2% and the extra power demands a substantial increase in dc current. As a result, the dc voltage is depressed to 0.9 p.u. The use of a 10% range of OLTC makes it possible to provide the extra power with nominal dc voltage. However further increases of frequency and power would require unrealistically high tap change control.

In contrast, Figure 7.4 (96% turbine efficiency) shows good controllability at the upper end of the frequency range, but some dc voltage reductions for frequencies below 34 Hz. However the voltage reduction at low frequency (0.03 p.u at 33.3 Hz) is of little significance.

Considering the limited effectiveness of the OLTC, it would be difficult to justify the extra cost. Instead, a slightly reduced turbine efficiency (96% in the test case) is an acceptable alternative for power generation beyond the nominal frequency.

7.6 Harmonic Effects

The total generator harmonic distortion in the variable frequency application is determined, as in the constant frequency case, by maximum power rating. Although there will be a reduction in the generator cooling capability at the lower speeds, the power and current levels will also be reduced.

There are two problems specific to variable frequency operation in need of

examination, i.e. reductions in harmonic frequencies at low speeds and frequency interactions between the two ends of the HVdc link.

7.6.1 Reduction of the Effective Pulse Number

The frequencies of the harmonic components on the dc side of the convertor will reduce in proportion to the generated frequency. For the test case under consideration, the lowest frequency of the dominant harmonic will be 400 Hz (i.e. 33.33 x 12). This is an effective reduction in the pulse number from 12 to 8, with reference to 50 Hz. Moreover the dc current harmonic levels do not decrease with power because these are caused by the dc voltage ripple, which is kept practically constant.

Harmonic elimination by filters is impractical with variable frequency and the only way to meet the Equivalent Disturbing Current levels [NZED 1983], if required by legislation, will be to reduce the dc voltage at lower frequencies. However this solution would destroy the benefit of variable frequency.

Dynamic simulation studies for varying firing angles indicate that the 400 Hz content is in the order of 1% of the dc operating current, which may be sufficient to cause electromagnetic interference [Arrillaga 1985].

7.6.2 Interaction Between Terminals

The lowest dominant frequency of the rectifier (i.e 400 Hz for the test case) corresponds to the 8^{th} harmonic of 50 Hz and will cause some 7^{th} and 9^{th} harmonic currents at the invertor end.

Similarly the dominant frequency of the invertor end (i.e 600 Hz) corresponds to the 18^{th} harmonic of the lowest generated frequency of the test system (33.33Hz). Simulation results for optimum efficiency power generation at that frequency with a 20 degrees firing angle show the appearance of up to 1 and 0.5% content of 17^{th} and 19^{th} harmonics respectively in the generator currents.

As the generated frequency increases above 33.33 Hz, both the rectifier and invertor ac current waveforms will contain small amounts of variable frequency components (not necessarily harmonic related).

There are also small amounts of intermodulated frequencies (the sum and

difference of the characteristic frequencies produced by the two convertors). As the generated frequency goes through the full range, the differences between dc ripple harmonics will produce all frequencies, including the natural frequency of the dc transmission system.

For the unit connected test system, the intermodulated frequencies which are small amounts of non-characteristic harmonics could not be quantified, due to the presence of dc component in the machine stator currents explained in chapter 4.

The harmonic distortion of the generator currents increases as the frequency reduces. Comparative values of Total Harmonic Distortion Factor $((\sqrt{\Sigma I_h^2})/I_1)$ corresponding to 33.33 and 50 Hz are 0.155 and 0.035 respectively.

However the generator currents at low frequencies are only a fraction of the nominal levels and the increased waveform distortion is not a problem.

7.7 Conclusion

The characteristics of variable speed unit connected generator-convertor plant have been derived using dynamic simulation algorithm.

Dynamic simulation results have shown the capability of a unit connected hydro system to provide controllable dc voltage for frequencies in the range of 33.33 to 50 Hz. At the upper end of the frequency, power increases beyond the nominal level cannot be achieved at the full efficiency without extra excitation or On Load Tap Changers. However considering the limited effectiveness of the On Load Tap Changer, it is unlikely that their presence will be justified; instead, excursions of frequency (and power) beyond the nominal levels can still be achieved at full dc voltage, if a small (about 4%) reduction in turbine efficiency can be accepted.

The use of lower frequencies has been shown to cause two special problems. One is a reduction in the dominant harmonic frequency of the dc line which may cause electromagnetic interference. The second problem is the appearance of relatively small values of many non-characteristic frequency components in the dc line and ac phase currents, which must be taken into consideration when designing unit connected schemes.

Chapter 8

CONCLUSIONS

A critical factor so far ignored in the comparison between conventional and unit connected schemes is the maximum operational capability of the system rather than the rating capability of the individual plant components. The operating characteristics of the unit connection are normally discussed with reference to the conventional steady state formulation. However, in the absence of harmonic filters, the use of such formulation must be reconsidered. The main objective of this thesis has been to assess the validity of conventional steady state formulation and show the need for dynamic simulation to derive the steady state characteristics of unit connected HVdc systems.

Dynamic simulation programs are being used as an alternative to physical simulators in assessing the performance of ac/dc systems. Two basically different approaches are currently used in HVdc dynamic simulation, i.e., the Electromagnetic Transient Program (EMTP) and state variable technique. Transient Convertor Simulation (TCS) program based on the state variable algorithm , which has the ability to predict exact voltage crossings, firing instants and commutation intervals, has been used in this thesis to derive unit connection characteristics.

The TCS program, developed at the University of Canterbury, contains models such as time varying ac system equivalents, frequency dependent equivalents and convertor transformer magnetic history to represent an ac/dc system. The main criticism made against this program has been the lack of realistic controller models. Work has been carried out to provide more realistic and flexible controller models, which have been incorporated in TCS program.

Ideally, the digital programs should be validated by comparison with system recordings. However, such comparisons are unrealistic because of the difficulties involved in setting up identical test system conditions in each model. Thus the only other realistic comparison is between two digital programs, based on fundamentally different algorithms. In this thesis, TCS has been compared with another dynamic simulation program, EMTDC which is based on EMTP algorithm. The comparison has concentrated on the convertor algorithms and has shown that the two algorithms predict the same convertor responses following large disturbances. Hence, both EMTDC and TCS algorithms can be used with confidence to simulate the transient response of ac/dc convertors.

The comparison of TCS and EMTDC has not included ac system components such as generators. Since both TCS and EMTDC contain similar machine models, the dynamic simulation of generator-HVdc convertor units needs to be compared with a different model simulation. This comparison is necessary to validate the dynamic simulation of unit connected systems. As the continuation of this work, TCS must be compared with Finite Element program used by GEC, UK which contains a comprehensive machine model.

The commutation process in unit connected HVdc systems has been analysed using TCS. It has been shown that the conventional steady state formulation based on the use of specified commutating voltage and reactance is not applicable to the unit connection. A modified steady state formulation, which does not require the specification of commutating voltage and reactance, has been proposed. However, in the presence of machine rotor saliency, even this formulation is not applicable for unit connection and so dynamic simulation must be used to derive the unit connected HVdc system steady state characteristics.

Each individual unit connected HVdc scheme requires extensive dynamic analysis to determine its characteristics. With reference to a typical unit connected system, the operating capability charts have been derived using TCS and compared with a corresponding conventional scheme. The results have shown that the unit connections have limitations in their operational capability and additional costs are involved to increase their capability to that of conventional schemes. This factor, which has so far been neglected, must be taken into consideration while comparing unit connections with conventional schemes.

The steady state analyses of unit connections have further been extended to include variable frequency operation so as to match the optimal turbine efficiency. In constant frequency operation, the On Load Tap Changers (OLTC) would not be needed, whereas their need must be evaluated during variable speed operation, due to a wide variation of generator internal emf. Again, dynamic simulation is necessary for such an evaluation. It has been shown, with reference to the test system, that it is possible to operate the turbine-generator units without an OLTC within a wide range of frequencies, at high efficiencies and with good voltage controllability.

In the conventional scheme, the current rating of the generator is determined by the fundamental frequency component, as the filters absorb the steady state harmonic current components. On the other hand, the unit connected generator must be rated for total rms current. Derivation of harmonic spectra using conventional formulation cannot be used for unit connected systems and must be derived from dynamic simulation. Moreover, under variable speed operation, the interactions between the terminals produce non-characteristic harmonic and non-harmonic frequencies which cannot be analysed using conventional formulation. Dynamic simulation and FFT have been combined to derive the harmonic spectra for the unit connected test system under constant and variable speed operation. However, the use of variable frequency introduces small errors in the FFT processing due to spectral leakage caused by the presence of non-harmonic frequency modulation between the two terminals.

The FFT analyses of machine stator currents derived from TCS have shown the presence of small amounts of dc component, which otherwise should not be present. By adopting various numerical techniques, the magnitude of this dc component has been reduced considerably. However, it has been difficult to quantify the expected uncharacteristic harmonics during variable speed operation due to the presence of this dc component in the stator currents. Hence, further work is still required to eliminate this dc component.

Dynamic simulation of generator-HVdc convertor units is extremely demanding computationally and the initial values for the simulation are estimated from the single-phase simplified analysis. It should be possible to reduce the computation time by starting the dynamic simulation from better initial values. Work is currently underway at the University of Canterbury to model the generator, convertor and transformer in harmonic domain, which would be computationally more efficient for

steady state analysis of unit connections. Better initial values for dynamic analysis can also be obtained from such programs.

The conventional ac/dc load flow and transient stability programs cannot be used for systems involving unit connections, since they are based on the steady state formulation. Instead, the characteristics derived from dynamic simulation can be used in such programs to represent unit connected systems and this work is also currently underway at the University of Canterbury.

References

[Ainsworth 1967] Ainsworth, J.D. "Harmonic instability between controlled static convertors and a.c networks", Proc. IEE, Vol. 114, No.7, pp 949-957.

[Ainsworth 1968] Ainsworth, J.D. "The phase-locked oscillator-a new control system for controlled static convertors", IEEE Trans., PAS-87, pp 859-864.

[Al-Khasali 1976] Al-Khasali, H.J. "Generalised dynamic modelling of high voltage dc-ac transmission systems", Ph.D Thesis, University of Manchester Institute of Science and Technology, UK, 1976.

[Arrillaga 1970] Arrillaga, J., Galanos, G., and Powner. E.T. "Direct digital control of h.v.d.c convertors", IEEE Trans., PAS-89, No.8, pp 2056-2065.

[Arrillaga 1983a] Arrillaga, J. "High voltage direct current transmission", Peter Peregrinus Ltd., London, 1983.

[Arrillaga 1983b] Arrillaga, J., Arnold, C.P. and Harker, B.J "Computer modelling of electrical power systems", John Wiley & Sons Ltd., 1983.

[Arrillaga 1985] Arrillaga, J., Bradley, D.A. and Bodger, P.S."Power system harmonics", John Wiley & Sons, 1985.

[Bowles 1970] Bowles, J., "A.C system and transformer representation for HVdc transmission studies", IEEE Trans., PAS-88, No. 7, pp 1603-1609.

[Bowles 1989] Bowles, J., "HVdc unit connected generators- receiving end control", paper no. IV-07, International colloquium on HVdc power transmission, 13-15 August 1989, Recife, Brazil.

[Calverley 1973] Calverley, T.E., Ottaway, C.H. and Tufnell, D.H.A., "Concepts of a unit generator convertor transmission system", IEE Conference on High Voltage DC and AC Transmission, London, 1973.

[Campos Barros 1976] Campos Barros, J.G., "Dynamic modelling of synchronous machines connected to HVdc transmission systems", Ph.d Thesis, University of Manchester Institute of Science and Technology, UK, 1976.

[Campos Barros 1977] Campos Barros, J.G., "Stability of isolated generator-HVdc convertor units", IEEE Summer Power Meeting, 1977, paper no. A-77508-5.

[Campos Barros 1989] Campos Barros, J.G., "Direct connection of generators to HVdc convertors: main characteristics, comparative advantages and prospectives in Brazil", paper no. IP-17, presented at II Symposium of specialists in 'electric operation and expansion planning', 21-25 August 1989, Sao Paulo, Brazil.

[Cazzani 1988] Cazzani, M., Schiappacasse, A., Testi, G., Pincella, C., and Valfre, L., "HVdc simulator versus computer modelling for SACOI 2 HVdc link insulation co-ordination studies", paper no. 14-11, International conference on Large High Voltage Electric Systems (CIGRE), 28 Aug. - 3 Sep., 1988, Paris.

[Chen 1962] Chen, W.Y., "An investigation of commutation problems in a static power convertor", Ph.d Thesis, University of Manchester Institute of Science and Technology, UK, 1962.

[CIGRE 1988] "Records of meetings of SC-11 and SC-14, CIGRE, Paris, France, 1988.

[Concordia 1951] Concordia, C., "Synchronous Machines - Theory and Performance", John Wiley & Sons, 1951.

[de Silva 1987] de Silva, J.R., "Capability charts for power systems", Ph.D Thesis, University of Canterbury, New Zealand, 1987.

[Dickmander 1989] Dickmander, D.L. and Peterson, K.J., "Analysis of dc harmonics using the three-pulse model for the Intermountain power project HVdc transmission", IEEE Trans., Power Delivery, Vol. 4, No. 2, pp 1195-1204.

[Dommel 1969] Dommel, H.W., "Digital computer solution of electromagnetic transients in single and multiple networks", IEEE Trans., PAS-88, No. 4, pp 388-99.

[Dunfield 1967] Dunfield, J.C. and Barton, T.H., "Effect of m.m.f permeance harmonics in electrical machines (with special reference to a synchronous machine)", Proc. IEE, Vol. 14, No. 10, 1967.

[Eggleston 1985] Eggleston, J.F., "Harmonic modelling of transmission systems containing synchronous machines and static convertors", Ph.D Thesis, University of Canterbury, New Zealand, 1985.

[El-Serafi 1980] El-Serafi, A.M. and Shehata, S.A., "Effect of synchronous machine parameters on its harmonic analysis under thyristor bridge operation", IEEE Trans., PAS-99, No. 1, pp 59-67.

[EPRI 1983] "Methodology for integration of HVdc links in large ac systems - Phase 1: Reference manual", EPRI project report, no. EL-3004, 1983.

[Giesner 1971] Giesner, D.B., "The dynamic behaviour of ac/dc power systems under ac fault conditions", Ph.D Thesis, University of Manchester Institute of Science and Technology, UK, 1971.

[Gleadow 1989] Gleadow, J.C., O'Brien, M.T., Fletcher, D.E. and Bisewski, B.J., "Uprating the HVdc system in New Zealand" paper no. VIII-01, International colloquium on HVdc power transmission, 13-15 August 1989, Recife, Brazil.

[Hausler 1980] Hausler, M. and Kanngiesser, K.W., "Generator- convertor unit connection with thyristor and diode rectifiers", Proc. of Symposium on 'Incorporating power transmission into system planning', sponsored by USDOE, Phoenix, Arizona, USA, March 24-27, 1980, pp 255-271.

[Heffernan 1980] Heffernan, M.D., "Analysis of ac/dc system disturbances", Ph.D Thesis, University of Canterbury, New Zealand, 1980.

[Heffernan 1981] Heffernan, M.D., Arrillaga, J., Turner, K.S. and Arnold, C.P., "Computation of ac/dc system disturbances. Part-1: Interactive co-ordination of generator and convertor transient models", IEEE Trans. PAS-100, No. 11, pp 4341-4348.

[Hungasutra 1989] Hungasutra, S. and Mathur, R.M.," Unit connected generation with diode valve rectifier scheme", IEEE Trans., Power Systems, Vol. 4, No.2, pp 538-543.

[IEEE 1973] IEEE Working Group report, "A standard for generator continuous unbalanced current capability", IEEE Trans., PAS-73, pp 320-329.

[IEEE 1990] IEEE committee report on "Application aspects of multiterminal dc power transmission", IEEE Trans., Power Delivery, Vol. 5, No. 4, Nov. 1990, pp 2084-2098.

[Ingram 1988] Ingram, L., "A practical design for an integrated HVdc unit connected hydro-electric generating station", IEEE Trans., Power Delivery, Vol. 3, No.4, pp 1615-1620.

[Jaquet 1986] Jaquet, M., "The Pan Jia Kou pumped storage station, part I: Hydraulic equipment", Fourth ASME International Hydro power Fluid Machinery Symposium, Anaheim, Decmeber 1986.

[Jones 1967] Jones, C.V., "The unified theory of electrical machines", Butterworths, 1967.

[Joosten 1989] Joosten, A.P.B., Arrillaga, J., Arnold, C.P. and Watson, N.R., "Simulation of HVdc system disturbances with reference to the magnetising history of the convertor transformers", IEEE PES summer meeting, Long Beach, California, July 9-14, 1989.

[Kanngiesser 1983] Kanngiesser, K.W., "Unit connection of generator and convertor to be integrated in HVdc or HVac energy transmission", International symposium on HVdc technology, Rio de Janeiro, Brazil, 1983.

[Kanngiesser 1989] Kanngiesser, K.W., "Control functions and their allocation within an unit connection", paper no. IV-01, International colloquium on HVdc power transmission, 13-15 August 1989, Recife, Brazil.

[Kimbark 1968] Kimbark, E.W., "Power system stability: Synchronous machines", Dover publications, New York, 1968.

[Kimbark 1971] Kimbark, E.W., "Direct current transmission, vol. 1", Wiley Interscience, 1971.

[Krishnayya 1973] Krishnayya, P.C.S., "Stresses on generators and transformers of block and double-block connections proposed for HVdc power station infeed", IEE conf. on 'High voltage dc and/or ac power transmission', Publication No. 107, pp 279-286.

[Krishnayya 1987] Krishnayya, P.C.S., "A review of unit connected generator-convertor connections for HVdc transmission", IEEE/CSEE Joint conference on 'High voltage transmission systems", Beijing, China, 1987.

[Manitoba 1988] EMTDC users manual prepared by Manitoba HVdc centre, Canada.

[Mattensson 1986] Mattensson, H., Bahrman, M., Eitzmann, M., Osborn, D. and Wong, W. "Digital programs and simulators as tools for studying HVdc systems - validation considerations", IEEE Montech'86 conference on 'HVdc power transmission', 29 Sept.-1 Oct. 1986.

[Naidu 1989] Naidu, M. and Mathur, R.M.," Evaluation of unit connected variable speed hydro-power station for HVdc power transmission", IEEE Trans., Power Systems, Vol. 4, No. 2, pp 668-676.

[NZED 1983] "Limitations of harmonic levels", notice issued by Electricity Division, Ministry of Energy, NZ.

[Preston 1990] Private communication with Dr.T.E.Preston of Large Machines Department, GEC, UK.

[Rangel 1989] Rangel, R.D., Pedroso, A.S. and Campos Barros, J.G.," Dynamic performance of salient-pole unit connected generators", paper no. IV-03, International colloquium on HVdc power transmission, 13-15 August 1989, Recife, Brazil.

[Reeve 1969] Reeve, J., Baron, J.A and Krishnayya, P.C.S., " A general approach to harmonic current generation by HVDC convertors", IEEE Trans., PAS-88, No.7, pp 989-995.

[Reeve 1988] Reeve, J. and Adapa, R., "A new approach to dynamic analysis of ac networks incorporating detailed modelling of dc systems. Part 1: Principles and Implementation & Part 2: Application to interaction of dc and weak ac systems", IEEE Trans., Power Delivery, Vol. 3, No. 4, pp 2005-2019.

[Shore 1989] Shore, N.L., Anderson, G., Canelhas, A.P. and Asplund, G., "A three-pulse model of dc side harmonic flow in HVdc systems", IEEE Trans., Power Delivery, Vol. 4, No. 3, pp 1945-1953.

[Turner 1980] Turner, K.S.,"Transient stability analysis of integrated ac and dc power systems", Ph.D Thesis, University of Canterbury, New Zealand, 1980.

[Turner 1981] Turner, K.S., Heffernan, M.D., Arnold, C.P. and Arrillaga, J., "Computation of ac/dc system disturbances. Part-2: Derivation of power frequency variables from convertor transient response", IEEE Trans. PAS-100, No. 11, pp 4349-4355.

[Vogele 1986] Vogele, J. and Weber, K., "The Pan Jia Kou pumped storage station, part II: Electrical equipment", Fourth ASME International Hydro power Fluid Machinery Symposium, Anaheim, Decmeber 1986.

[Walker 1953] Walker, J.H., "Operating characteristics of salient-pole machines", Proc. IEE, Vol. 100, Pt. 2, pp 13-24.

[Watson 1987] Watson, N.R., "Frequency-dependent ac system equivalents for harmonic studies & transient convertor simulation", Ph.D Thesis, University of Canterbury, New Zealand, 1987.

[Watson 1988] Watson, N.R. and Arrillaga, J.,"Frequency dependent ac system equivalents for harmonic studies and transient convertor simulation", IEEE Trans., Power Delivery, Vol. 3, No. 3, pp 1196-2003.

[Williams 1986] Williams, B., "Transient stability studies of large power systems with multiterminal HVdc links", M.E Thesis, University of Canterbury, New Zealand, 1986.

[Woodford 1983] Woodford, D.A., Gole. A. and Menzies, R.W., "Digital simulation of dc links and ac machines", IEEE Trans., PAS-102, No. 6, pp 1616-1623.

[Woodford 1985] Woodford, D.A., "Validation of digital simulation of dc links", IEEE Trans., No. 9, pp 2588-2595.

Appendix A

TCS Controller Modules

This appendix contains the basic controller modules available in TCS to build any user defined controller. Apart from these modules, any other required module can be easily incorporated into the program without knowing the structure of TCS, by adding the required function sub-program.

Function	*Control block*	*Description*
COSI	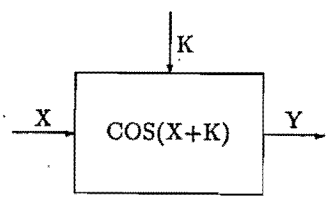	Input : X Output : Y Constants : K
TANI	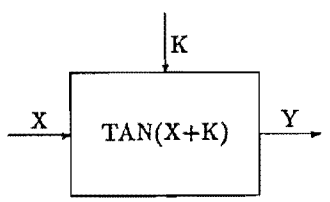	Input : X Output : Y Constants : K

Function	*Control block*	*Description*
ABCD	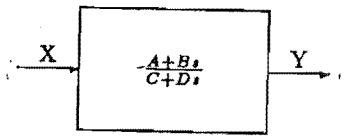	Input : X Output : Y Constants : A,B,C,D
TRAP	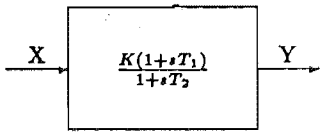	Input : X Output : Y Constants : K,T_1, T_2
INTG	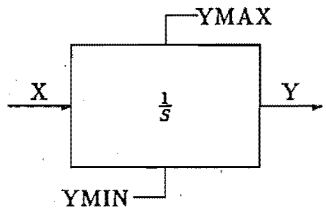	Input : X Output : Y Constants : YMIN,YMAX
LIMS	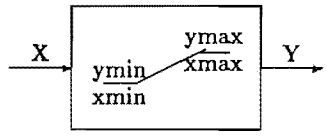	Input : X Output : Y Constants : XMIN,XMAX,YMIN,YMAX
ADDI	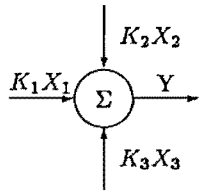	Input :X_1, X_2, X_3 Output : Y Constants : K_1, K_2, K_3
MULT	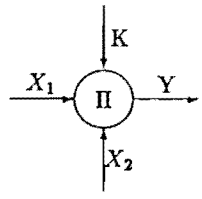	Input : X_1, X_2 Output : Y=KX_1X_2 Constants : K
DIVD	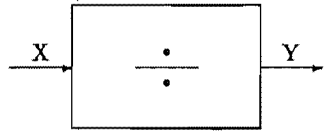	Input : X_1, X_2 Output : Y = $\frac{X_1}{X_2}$

Function	*Control block*	*Description*
LIMC	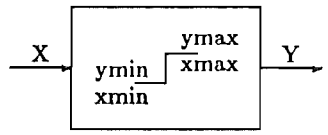	Input : X Output : Y Constants : XMIN,XMAX,YMIN,YMAX
LIMV	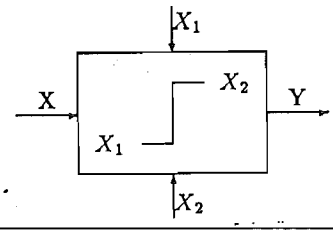	Input : X,X_1, X_2 Output : Y
EQUA	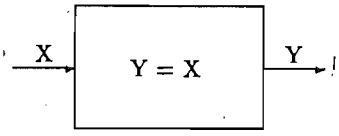	Input : X Output : Y
MAXI	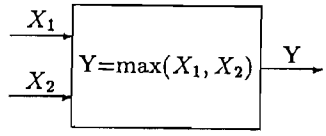	Input : X_1, X_2 Output : Y
MINI	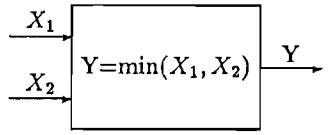	Input : X_1, X_2 Output : Y
INIT	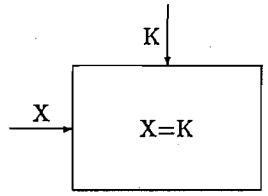	Input : X Initialisation Constants : K
SINI	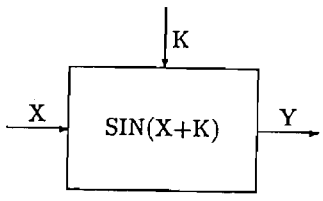	Input : X Output : Y Constants : K

Appendix B

Test System Data for TCS and EMTDC Comparison

The data, pertaining to the test system of Figure 3.1 are given in this appendix.

B.1 AC System

The ac system has been represented by a modified Thevenin Equivalent, consisting of a parallel combination of resistance R_1 and inductor L_1, in series with another inductor L_2. Table B.1 shows the ac system data for the sending end and receiving end systems.

Table B.1: AC System data

item	*AC System - 1*	*AC System - 2*
system capacity	3240 MVA	2200 MVA
impedance angle	85 deg.	78 deg.
voltage (l-l rms)	133 kV	127 kV
frequency	60 Hz	60 Hz
R_1	1.1261Ω	3.7732Ω
L_1	0.002431 H	0.00728 H
L_2	0.006817 H	0.01165 H

B.2 AC Filters

Tuned filters of $5^{th}, 7^{th}, 11^{th}$ and 13^{th} harmonic are used along with a high-pass filter, on both rectifier and invertor ac buses. The total filter capacity is of 178 MVA each. Tables B.2 and B.3 show the filter data for sending end and receiving end systems respectively. Table B.4 shows high-pass filter data, in which the parallel combination of R and L is in series with C.

Table B.2: Sending end tuned filters

Element	*Unit*	*Filter order*			
		5	7	11	13
C	μF	5.153	2.6294	4.3204	3.0929
L	H	0.05457	0.05457	0.01351	0.01351
R	Ω	1.7776	2.6664	1.776	1.776

Table B.3: Receiving end tuned filters

Element	*Unit*	*Filter order*			
		5	7	11	13
C	μF	6.3522	3.2408	4.9828	3.5678
L	H	0.0442	0.0442	0.01167	0.01167
R	Ω	2.1032	2.1032	0.7887	0.7887

Table B.4: High-pass filters

Element	*Unit*	*Sending end*	*Receiving end*
C	μF	12.373	15.367
L	H	0.0012887	0.00107
R	Ω	18.6648	11.0418

B.3 DC Filters

6^{th} harmonic tuned filters are used on both Rectifier and Invertor dc buses. Table B.5 shows the dc filter data.

Table B.5: DC filters

Element	*Unit*	*Rectifier*	*Invertor*
C	μF	0.8	0.8
L	H	0.2444	0.2444
R	Ω	12	12

B.4 DC Line

The dc transmission line has been represented as the cascade of 12-pi sections.

Length	: 556 km
Resistance	: 0.025 ohms/km
Inductance	: 1.63866 mH/km
Capacitance	: 0.0182073 μF

B.5 DC Convertor

B.5.1 Rectifier

Type	: 6-pulse
Minimum firing angle	: 5 deg.
Maximum firing angle	: 155 deg.
Transformer impedance	: 0.2 p.u
Transformer rating	: 341 MVA
Transformer voltage	: 134/134 kV
Smoothing inductor	: 0.75 H

Current reference : 1.45 kA

B.5.2 Invertor

Type : 6-pulse
Minimum firing angle : 108 deg.
Maximum firing angle : 180 deg.
Transformer impedance : 0.2 p.u
Transformer rating : 323 MVA
Transformer voltage : 127/127 kV
Smoothing inductor : 0.75 H
Extinction angle reference 18 deg.
Current margin : 180 A

B.6 Controllers

The following constants are used by the current and extinction angle controllers of Figure 3.2.

B.6.1 Current Control

Proportional gain , K_p : 0.07997 deg/amp
Integral gain , K_i : 5.88 deg/amp - sec

B.6.2 Extinction Angle Control

Proportional gain , K_p : 0.27 rad/rad
Integral gain , K_i : 14.754 /sec

B.6.3 Transducer Delays

Rectifier : 5 ms

Invertor : 18 ms

Appendix C

TCS Controller Data File

This appendix gives the TCS controller data file of the test system, used for the comparison with EMTDC. Since TCS works on per-unit quantities, the controller constants given in Appendix B have to be converted accordingly.

If I_0 and f are the base current and frequency respectively, then the proportional and integral constants for the current controllers must be converted according to the following:

$$K_{p(tcs)} = 17.453 I_0 K_p \text{ rad/pu}$$
$$K_{i(tcs)} = \frac{2.77 I_0 K_i}{f} \text{ rad/rad}$$

Similarly, the extinction angle controllers are converted according to the following:

$$K_{p(tcs)} = K_p \text{ rad/rad}$$
$$K_{i(tcs)} = \frac{0.159 K_i}{f} \text{ /rad}$$

```
\                    CONTROLLER DATA FOR COMPARISON WITH EMTDC
\                    ----------------------------------------
\FN   INP1  INP2  INP3  OUT   CON1    CON2     CON3   CON4
\--   ----  ----  ----  ---   ----    ----     ----   ----
\
\ ***** RECTIFIER CURRENT CONTROLLER ******
\
TRAP  DIO4              IO    1.0     0.0      1.885
ADDI  IDR1  IO          I1    -1.0    1.0
MULT  I1    PONE        I11   0.8821
MULT  I1    PONE        I22   0.1720
INTG  I22               I23   0.0873  2.7
ADDI  I11   I23         I2    1.0     1.0
LIMC  I2                AO04  0.0873  2.7
INIT  IO                      1.0
INIT  IDR1                    2.27
INIT  PONE                    1.0
\
\ ***** INVERTOR CURRENT CONTROLLER ******
\
TRAP  DIO5              IOO   1.0     0.0      6.885
ADDI  IDR2  IOO         I3    -1.0    1.0
MULT  I3    PONE        I31   0.8821
MULT  I3    PONE        I32   0.1720
INTG  I32               I33   1.9     3.14
ADDI  I31   I33         I4    1.0     1.0
LIMC  I4                ALCC  1.9     3.14
INIT  IDR2                    2.00
INIT  IOO                     1.0
\
\ ***** INVERTOR EXTINCTION ANG. CONTROLLER ******
\
ADDI  AREF  EA05        A2    -1.0    1.0
```

```
MULT  A2    PONE        A31   0.27
MULT  A2    PONE        A32   0.0391
INTG  A32               A33   1.9     3.14
ADDI  A31   A33         A3    1.0     1.0
LIMC  A3                ALEX  1.9     3.14
MINI  ALCC  ALEX        A005
INIT  AREF                    0.314
END
```

Appendix D

Transformations: d,q,0 to a,b,c

Under ideal conditions of sinusoidally distributed stator windings and internal symmetry, there is a mathematical equivalence between the a,b,c and d,q,0 frame of references for stator circuits. The transformation is non-singular and may be defined as [Concordia 1951, Kimbark 1968] :

$$\begin{bmatrix} L_d \\ L_q \\ L_0 \end{bmatrix} = \begin{bmatrix} 1 & 1 & 3/2 \\ 1 & 1 & -3/2 \\ 1 & -2 & 0 \end{bmatrix} \begin{bmatrix} L_{aa} \\ L_{ab} \\ L_{a2} \end{bmatrix} \tag{D.1}$$

Under idealised conditions, $L_{a2} = L_{ab2}$, i.e the second harmonic variation of the stator interphase mutual inductance is equal in magnitude to the variation of the phase self inductance. This formulation, together with the absence of fourth harmonic terms is considered to be approximate [Dunfield 1967, Jones 1967].

The a,b,c quantities are derived from the inverse transform of equation as :

$$\begin{bmatrix} L_{aa} \\ L_{ab} \\ L_{a2} \end{bmatrix} = \begin{bmatrix} 1/3 & 1/3 & 1/3 \\ 1/6 & 1/6 & -2/6 \\ 1/3 & -1/3 & 0 \end{bmatrix} \begin{bmatrix} L_d \\ L_q \\ L_0 \end{bmatrix} \tag{D.2}$$

and also,

$L_{a2} = L_{ab2}$

$L_{a4} = L_{ab4} = 0$

The rotor quantities are kept as direct and quadrature axis parameters, when transforming to the a,b,c frame of reference. This is convenient because of the

actual winding arrangement. However, the rotor resistances and inductances must be scaled down by 2/3, in order to compensate for the rationalisation done to the d,q,0 equations.

Appendix E

Unit Connected Test System Data

The machine (both non-salient and salient type) parameters and the dc system data used in this thesis are given in this appendix. The machine resistances and reactances are in per-unit.

E.1 Non-Salient Machine

Rating	: 100 MVA
Terminal Voltage	: 13.8 kV
Direct-axis reactance	: 1.18
Direct-axis damper reactance	: 1.24
Quadrature-axis reactance	: 1.05
Quadrature-axis damper reactance	: 1.05
Field reactance	: 1.27
Direct axis damper resistance	: 0.021
Direct axis sub-transient reactance	: 0.145
Quadrature axis damper resistance	: 0.036
Quadrature axis sub-transient reactance	: 0.145
Field resistance	: 0.00068
Leakage reactance	: 0.075
Armature resistance	: 0.0035
Direct axis open circuit time constant	: 0.042 s

E.2 Salient Machine

Rating	: 100 MVA
Terminal Voltage	: 13.8 kV
Direct-axis reactance	: 1.2
Direct-axis damper reactance	: 1.0
Quadrature-axis reactance	: 0.8
Quadrature-axis damper reactance	: 0.831
Field reactance	: 1.2
Direct axis damper resistance	: 0.02
Direct axis sub-transient reactance	: 0.2
Quadrature axis damper resistance	: 0.02
Quadrature axis sub-transient reactance	: 0.367
Field resistance	: 0.0005
Leakage reactance	: 0.2
Armature resistance	: 0.005

E.3 DC System

E.3.1 Convertor

Type	: 12-pulse
Nominal current	: 1 kA
Nominal voltage	: 80 kV
Smoothing reactor	: 0.4 H

E.3.2 Convertor Transformer

Rating	: 50 MVA
Reactance	: 5%
Voltage	: 13.8/30.36 kV